WDL-TR2366
2 January 1965

SUMMARY REPORT

COMET AND CLOSE-APPROACH ASTEROID MISSION STUDY

FINAL REPORT

VOL. 1

This work was performed for the Jet Propulsion Laboratory, California Institute of Technology, sponsored by the National Aeronautics and Space Administration under Contract NAS7-100.

Prepared for
Jet Propulsion Laboratory
Pasadena, California

WDL-TR2366
2 January 1965

SUMMARY REPORT

COMET AND CLOSE-APPROACH ASTEROID MISSION STUDY

FINAL REPORT

VOLUME 1

CONTRACT JPL 950870

Prepared by
PHILCO CORPORATION
A Subsidiary of Ford Motor Company
WDL Division
Palo Alto, California

Prepared for
Jet Propulsion Laboratory
Pasadena, California

FOREWORD

This summary report is one of eight volumes covering work performed by the WDL Division of the Philco Corporation during the Comet and Close-Approach Asteroid Mission Study for the Jet Propulsion Laboratory under Contract JPL 950870. This document outlines the objectives of the study and summarizes the significant results of work performed during the period 2 July to 2 January 1965.

ACKNOWLEDGMENT

The summary report has been prepared by A. Giddis (Systems and Science) with the help of R. Jensen (Trajectory and Guidance Analysis), M. Fluck (Guidance and Control), H. Bustamante (Telecommunication), J. Fairbanks (Photovoltaic Power), J. Kayne (Thermal Control), R. Walton (Spacecraft Configurations), and J. Gibson (Mission Cost and Schedule).

TABLE OF CONTENTS

LIST OF ILLUSTRATIONS

LIST OF TABLES

SECTION 1

INTRODUCTION

1.1 TECHNICAL REQUIREMENTS

The purposes of the Comet and Close-Approach Asteroid Mission Study (hereafter referred to as the Comet Mission Study) can be summarized as follows:

a. Develop conceptual spacecraft designs for missions to selected comets and close-approach asteroids during the mission period of interest, 1967-1975.

b. Determine tradeoffs among mission parameters, instrument requirements, and subsystem performance.

c. Forecast the state-of-the-art and apply the new technology to conceptual designs of comet/asteroid probes.

d. Specify the feasibility of adaptable spacecraft designs for missions to a number of comets and close-approach asteroids.

e. Compare comet/asteroid spacecraft system concepts with the Mariner Mars 1964 system design.

f. Estimate mission schedule, cost, and probability of success.

1.2 MISSION OBJECTIVES

The primary objective of a comet probe mission is to conduct fly-through scientific observations of a comet and to transmit the results of these observations back to earth. Specific scientific objectives are listed below in order of increasing requirements upon the performance of spacecraft systems designed to support the appropriate scientific instruments:

a. Measure the distribution of matter and of the magnetic field through the coma of selected comets.

b. Observe the nucleus of a comet.

c. Determine the chemical composition of cometary material.

The primary objective of a close-approach asteroid probe mission is to conduct fly-by scientific observations of a close-approach asteroid and to transmit the results back to earth. Specific scientific objectives are to measure the physical and chemical properties of an appropriate close-approach asteroid.

A secondary objective of both probe missions is to perform particle and field measurements in the interplanetary medium enroute to the target with some of the instruments to be used during encounter.

SECTION 2

SCIENCE

2.1 SCIENTIFIC OBJECTIVES

Astrophysicists believe that a definitive insight into the origin and formation of comets and planets will be gained by exploring comets and asteroids with space probes. Much data must be collected in order to refine or to reject extant theories about the evolution of the solar system, about the physics of cometary and asteroidal bodies themselves, and about the dynamics of the interplanetary medium. There appears to be agreement within the scientific community that, as with the moon and planets, the true nature of comets can be revealed only by a direct probing of the coma and tail and by observations and eventual sampling of the nucleus by a space probe. In the meantime, photometric and spectroscopic identification of cometary materials in the laboratory and from ground observations will be continued.

High interest exists in the detection of life throughout the solar system. The possibility of exploring comets to determine the presence of organic compounds fundamental to life has been suggested. Spectroscopic observations of comets indicate unequivocally the presence of CN, C_2, C_3, and CH in the comet's atmosphere (coma). The icy core (nucleus) is presumably composed of the frozen gas molecules CH_4, CO, CO_2, and others.

Scientific measurements performed from on-board a spacecraft during its intercept with a comet fulfill two roles in determining the composition of comets. The first function is to complement measurements performed from earth astronomical observatories by direct sampling of the particle, field and molecular composition of a comet, by close-range

observation of its physical features, and by detecting predicted but unobserved spectral emissions. The second function is to supplement measurements performed on the earth by confirming spectral lines previously recorded, especially those that are ambiguously identified. On-board measurements can better serve their complementary and supplementary functions if they are correlated with simultaneous photometric and spectroscopic observations from Earth.

2.1 COMET MODELS

2.1.1 Geometry

The geometry of periodic comets selected for first-generation comet missions can be represented by a star-like spherical nucleus of 1 km diameter or less, surrounded by a bright region referred to as the nuclear condensation of perhaps 10^3 km apparent diameter, imbedded in a spherical coma of 10^5 km apparent diameter near perihelion (intercept) between 1 and 2 A.U. The position of the nucleus is generally off-center along the sun-comet line. A faint, short tail extends along this line away from the sun.

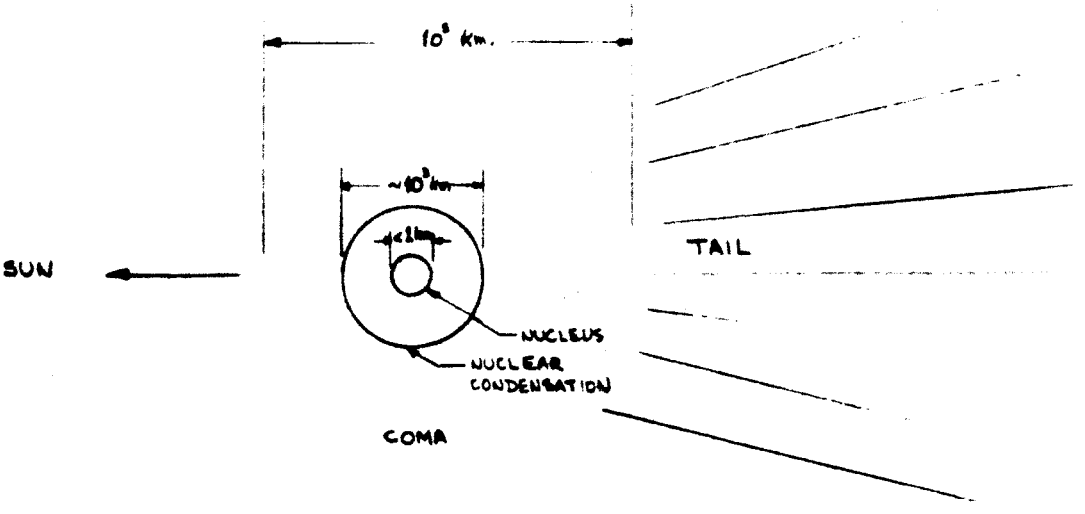

The atoms, molecules, and solid particles in the coma and tail originate in the nucleus. The composition of the nucleus is generally accepted to consist of icy compounds (such as water, ammonia, methane, carbon, etc.) partly in the form of solid hydrates with an admixture of meteoritic dust (e.g., metals and silicates). The observed gases in the coma and tail are atoms and di- or triatomic radicals or molecules resulting from sublimation, photodissociation, ionization, and chemical reactions. Most comae and many tails reveal a solar continuum that is due to the scattering of solar radiation by solid particles. In addition, gases in the coma emit fluorescence spectra as a result of excitation by solar electromagnetic radiation, while gases in the tail show spectra as a result of ionization by solar corpuscular radiation.

The few available data on the composition and physical characteristics of selected periodic comets Tempel (2), Pons-Winnecke, Kopff and Brooks (2) are summarized in Table 2-1.

2.1.2 Particle Distribution

From photometric and spectroscopic observations from Earth, the densities of particles have been estimated. For example, in Brooks (2) the density of the gas molecules CN and C_2 is 10^4 - 10^6/cc near the nucleus and 1-10/cc at 10^5 km from the nucleus, depending upon the heliocentric distance, the particular apparition and the uncertainty in the measurements. No probable distribution of dust has been generated which can be considered useful for estimating the expected change in dust density and velocity as the spacecraft flies through these comets. A gaseous comet like Encke may have an average particle density of 10^{-9}/cc in its coma.

An upper limit to the number of electrons can be obtained by assuming that the number of ions is an order less than the number of the weakest neutral molecule detected, e.g., C_2 or C_3. For 10^{31} molecules, this means 10^{30} electrons. For an equivalent uniform comet diameter of

Table 2-1. Data on Selected Periodic Comets

COMET	NUCLEUS	COMA	TAIL	OBSERVED SPECTRUM	ABSOLUTE MAGNITUDE
Tempel (2) (1873 II)	Stellar at > 2 A.U. Central condensation near perihelion	Diffuse coma of nearly 10^5 km diameter	Some tail near perihelion	CN	13.0
Pons-Winnecke (1819 III)	Stellar Diameter 0.4 - 1 km		Short tail	CN, C_2; continuum	12.5 Total Comet 16.4 nuclear condensation
Kopff (1906 IV)		About 10^5 km diameter at perihelion	No significant tail	CN, C_2, C_3, CH; faint continuum	13.8 16.1 - 17.2 nuclear condensation
Brooks (2)	Stellar at > 2.5 A.U. Diameter 2.4 km max	Small, faint, strongly condensed coma	Faint, short tail	CN, C_2, CO^+; continuum	14.4 Total comet 16.1 - 16.6 nuclear condensation

10^5 km, the maximum average electron density is about 1/cc, a value commensurate with the electron density of the interplanetary medium between 1 and 2 A.U. The distribution of electrons through the coma is unknown.

The proton density in cometary comae is unknown, but not high enough to produce hydrogen in quantities sufficient to generate detectable hydrogen lines. However, 21 - cm emission has been reported.

2.1.3 Radio Emission

The only reported observations of cometary radio emission have been made on Arend-Roland during its perihelion passage in April 1957.

Unequivocal radio emission at 600 Mc is produced by transitions between fine-structure components due to the so-called Λ-type doubling of rotational levels in the fundamental electronic state of the CH molecule. The number of molecules which might explain the observed flux density at the earth of 5.6×10^{-23} watts/m^2/cps is about 10^{30} - 10^{31}, a value compatible with the estimated population of cometary atmospheres. At 1.5 million km away from the comet (near intercept), the flux density should be about 5.6×10^{-17} watts/m^2/cps. With a 4-db spacecraft receiver at 600 Mc and for a desired signal-to-noise ratio of 10, the antenna gain required above isotropic is 13.2 (12 db). A 60-degree corner reflector or a 2.5-foot long Yagi will yield the necessary effective aperture. However, whether radio emission is detectable in the vicinity of the selected periodic comets is debatable.

2.1.4 Magnetic Field Distribution

Robey suggests that the magnetic field distribution in the coma is of the form,

$$B = B_o \left(\frac{d_o}{d} \right)^n , \quad n \leq 1, \qquad (2\text{-}1)$$

for a spherical nucleus of radius d_o surrounded by a concentric spherical coma of radius d, where B_o is the reference magnetic flux density at the surface of the nucleus. The exponent n varies approximately linearly with heliocentric distance from 0.54 to 1.46 A.U. for Encke. Not enough data exists on the selected periodic comets to develop comparable values of n. Therefore, the results for Encke have been used as a model to compute that for a radius of 1 km, the average flux density at the surface of the nucleus decreases logarithmically with decreasing heliocentric distance, i.e., from 0.2 gauss at 1.5 A.U. to 0.0183 gauss at 1.0 A.U. The flux at the outer boundary of the coma varies inversely with heliocentric distance. At 1 A.U., it has been calculated to be 48.3×10^{-15} gauss.

2.1.5 Brightness Distribution

The most reliable estimate of brightness distribution near intercept has been provided by Professor L. Cunningham of the University of California from his observations of Pons-Winnecke during its close approach to the Earth in 1927. In the region of maximum brightness, the brightness distribution of both the coma and the nuclear condensation of faint, periodic comets near perihelion can be described by exponential functions of angle away from the center of the nucleus. That is,

$$B = B_o e^{-KL^2} \qquad (2\text{-}2)$$

where

- B = brightness measured in stellar magnitudes per (minutes of arc)^2
- B_o = brightness at the center
- L = angular distance measured in minutes of arc away from the center by an observer at 1.0 A.U.

The coefficients k and B_o for Pons-Winnecke are as follows:

Region	k	B_o
Coma	8	$4.0^M/(\text{min.})^2$
Nuclear Condensation	2000	$6.0^M/(\text{min.})^2$

The above model can be converted to stellar magnitudes M at 1 A.U.:

$$M = M_o + 2.5\, kL^2 \log e \qquad (2\text{-}3)$$

where M_o is the absolute magnitude.

2.3 COMET EXPERIMENTS

Table 2-2 represents a full complement of scientific instruments for determining the distribution of matter and of the magnetic field through the coma of selected comets (P) for observing the nucleus (O), and for determining the chemical composition of cometary material (C).

Mariner-C Comparison

Referring to Table 2-2, Items 1, 2, 3, 5, 6 and one each of Items 8 and 9 are identical to the Mariner-C science complement. It will be shown in Section 6 that a Mariner-C launched with an Atlas-Agena in 1969 can be modified to include an ion-mass spectrometer (Item 7) and a gimballed comet tracker to direct two UV photometers toward the nucleus (Item 9) in addition to supporting two Lyman-alpha photometers (Item 8). It is also shown that a modified Mariner-C launched with an Atlas-Agena in 1970 can support, in addition, an Advanced Mariner television subsystem (Item 11) to observe the nucleus.

Table 2-2 Atlas-Centaur Comet Probe Science Payload

	Instrument	Weight (lb)	Power (w)	Function
1.	Magnetometer	6.1	7.0	P
2.	Dust Detectors (2)	2.3	0.2	P
3.	Plasma Probe	7.0	3.5	P
4.	Ion-Electron Trap	8.0	2.0	P
5.	Ionization Chamber	2.6	0.5	P
6.	GM Tube	2.1	0.4	P
7.	Ion-Mass Spectrometer*	8.0	8.0	P,C
8.	Lyman-α Photometers (2)	3.0	3.0	P,C,O
9.	UV Photometers (2)	3.0	3.0	C,O
10.	UV Spectrometer	22.0	12.0	C,O
11.	Television	35.0	16.0	O
	Totals	99.1 lbs	55.6	

* Generally speaking, a neutral mass spectrometer could be expected to detect neutral molecules only if the densities were 10^4 to 10^6 per cc. The densities of CN and C_2 molecules in the vicinity of the nucleus of Brooks (2) fall within this range.

Table 2-3 compares the science payloads of the basic Mariner and the near-minimal and maximal modifications discussed in Section 9.

Table 2-3 Mariner-C Comet Probe Science

Instrument	Mariner-C (1964)	Mariner Mod. 1969	Mariner Mod. 1970
Magnetometer	x	x	x
Dust Detectors (2)	x	x	x
Plasma Probe	x	x	x
Ionization Chamber	x	x	x
GM Tube	x	x	x
Ion-Mass Spectrometer		x	x
Lyman-Alpha Photometer	x	x (2)	x (2)
UV Photometer	x	x (2)	x (2)
Television	x		x
UV Spectrometer*			(x)
Ion-Electron Trap*			(x)

* Alternative couple to the television

2.4 ASTEROID MODELS

Significant data on the physical properties of close-approach asteroids are scarce. A digest of their physical properties and composition of close-approach asteroids is given below:

Shape	:	Irregular (Eros	: 22 x 6 km)
Size	:	Icarus	: 1.4 km
		Geographus	: 2.0 km
		Eros	: 22.0 km
Apparent Magnitude	:	Icarus	: 18
		Eros	: 9 to 10.4
Rotation Period	:	Eros	: 5.5 hr
Density, Mass	:	Unknown	
Surface Temperature	:	Icarus	: 800°K
		Eros	: 300°K
Composition	:	Alumino-silicates, silicates, nickel-ferrous compounds	
Atmosphere	:	No atmosphere indicated	
Magnetic Field	:	Unknown	

2.5 ASTEROID EXPERIMENTS

The following experiments in the vicinity of a close-approach asteroid are suggested:

EXPERIMENT	OBJECTIVE	TECHNIQUE
Visual Observation	Ascertain shape, size and rotation	TV with color filters
Infrared Radiometry	Determine surface temperature	IR Radiometer
Ultraviolet Photometry	Determine surface emissions	UV Photometer (e.g., Mariner '64)
Magnetic Field	Measure direction and intensity	Magnetometer (e.g., Mariner '64)

Chemical analysis techniques can be performed only from the asteroid surface and thus require a lander mission. Spectroscopic measurements, however, can provide data from which the surface composition can be estimated. A mission to Eros is described in Section 3 in which a "shotgun" experiment is outlined. Before encounter a spinning payload is separated from the spacecraft, the spacecraft retrofires to slow down, the payload releases a cross-section of particles that impacts on the asteroidal surface and creates a cloud of surface dust, and the trailing spacecraft analyzes the reflected sunlight with a spectrophotometer.

SECTION 3

TRAJECTORY AND GUIDANCE ANALYSIS

3.1 MISSION CONSTRAINTS

To establish boundaries on the analysis, a set of mission constraints was generated to limit the scope of the analysis to comets and launch periods that are commensurate with current vehicle development and existing launch facilities. A list of the imposed trajectory constraints used for selective purposes is as follows:

1.	Launch period:	1967-1975
2.	Booster vehicles available:	a) Atlas/Agena b) Atlas/Centaur
3.	Spacecraft available for Atlas/Agena:	Mariner-C
4.	Launch pad:	AMR
5.	Range safety consideration:	$90^{\circ} < AZ_L < 114^{\circ}$
6.	Hyperbolic excess speed at arrival:	< 15 km/sec.
7.	Time-of-flight limit:	< one year
8.	Communication distances at arrival:	< 2 A.U.
9.	Terminal miss error:	5000 km to 10,000 km

3.2 COMET SURVEY

The preliminary portion of this study was devoted to conducting a general survey of possible comet targets for the time span under consideration, 1967-1975. From results of previous studies [JPL, 1964; STL, 1963], a table of comets to be considered was generated. Using

this table as a starting point, the possibilities occurring each year were analyzed in more detail by using the WDL Quick-Look Program [Philco, 1964]. The results of studying each comet as a potential mission candidate led to evaluating the energy requirements as a function of launch date. Using the energy requirement as a criteria, the comets were segregated into two groups. The first group consisted of comets which were beyond reasonable energies for the given launch vehicles. The second group contained all comets that might make a reasonable mission.

Additional analysis was conducted on the second group to select the strongest possible candidates for comet missions. The results of this analysis are presented in Table 3-1. The realistic comet missions for the time span of interest are shown according to booster requirements, Atlas/Agena and Atlas/Centaur. The five possible missions in the first two rows of the table were those selected for extensive investigation and evaluation. The groups of comets labeled "potential missions requiring additional investigation" contain some relatively high energy missions ($C_3 > 20$ km/sec^2).

3.3 TRAJECTORY CHARACTERISTICS

Each of the five comets selected in Section 3.2 was investigated in detail according to basic trajectory characteristics, guidance sensitivity and comet sighting. The basic trajectory characteristics generated are the following:

a)	Geocentric injection energy v. launch date	: Figs. A-1 to A-5
b)	Hyperbolic approach velocity vs. launch date	: Figs. A-6 to A-16
c)	RT ascension and declination vs. launch date	
d)	Earth-comet-vehicle angle vs. time of flight	: Figs. A-11 to A-15
e)	Heliocentric trajectory profile	: Figs. A-16 to A-20
f)	Encounter trajectory profile	: Figs. A-21 to A-26

These figures appear in Appendis A of Volume 3.

Table 3-1 Comet Survey (52 Opportunities)

		1966	1967	1968	1969	1970	1971	1972	1973	1974	1975
Possible Missions Investigated in Detail	Δ/A					Pons-Winnecke			Tuttle-Giacobini-Kresak		
	Δ/C		Tempel(2)			Kopff				Brooks(2)	
Potential Missions Requiring Additional Investigation			Finlay	Perrine-Mrkos	Honda-Mrkos-Pajdusakova Faye	D'Arrest		Giacobini-Zinner		Finlay Forbes Encke	
Non-Realistic Missions Based on Energy Constraints *		Giacobini-Zinner Neujmin(1)	Arend Borrelly Brooks(2) Encke Forbes Grigg-Skjellerup Harrington Reinmuth Tuttle Tuttle-Giacobini-Kresak Wirtanen Wolf(1)	Schaumasse Schwassman-Wachmann(2)	Coma- Sola Harrington-Abell	Johnson Whipple	Arend-Rigaux Daniel Encke Vaisala Wolf-Harrington Ashbrook-Jackson	Grigg-Skjellerup Neujmin(3) Tempel(2)	Reinmuth (1)	Borrelly Harrington Honda-Mrkos-Pajdusakova Reinmuth(2) Schwassman-Wachmann(1) Schwassman-Wachmann(2)	Perrine-Mrkos Arend

* Poor Earth Position or r_p Too Large

3.4 GUIDANCE PARAMETER

For purposes of guidance calculations, a guidance sensitivity parameter, $\left|\frac{\partial \vec{B}}{\partial \vec{V}}\right|$, was computed along trajectories of different flight times. This guidance parameter may be used to determine the effect of velocity additions at various positions along the trajectory. See Figures A-27 to A-31.

3.5 COMET SIGHTING

To study sighting problems of comets, the ephemeris of comet and earth were generated for one year prior to encounter. A latitude time history of the comet in the vicinity of perihelion also was generated to understand the relation between perihelion and the crossing of the ecliptic plane. See Figures A-32 to A-41.

3.6 COMET ORBIT DETERMINATION

It has been concluded from all studies and investigations conducted to date that a preacquisition phase must be incorporated into a comet probe mission. Basically, a preacquisition phase, hereafter called Phase 0, is a detailed and thorough investigation of all available observational data for the particular comets of interest. A chronological search of all observations and plates, both reduced and unreduced, should be made with consideration to accuracies attained, equipment used, seeing conditions, reliability of the observer, and any other factors affecting the orbital elements of the comet in question. Some of the photographic plates could be re-measured to assure the accuracies necessary for their utilization in calculating orbital elements. Having accumulated all worthwhile data related to the comets of interest, a numerical fitting and weighting process would be used to fit data from apparition to apparition. Orbit fitting would include three and possibly four or five apparitions, if data were available. This type of work can best be

accomplished by an astronomer in the field who is familiar with the data, the observers, and the possible sources of error in the past data.

3.7 JUSTIFICATION FOR PHASE-0 STUDY

The task depicted for Phase 0 is a 6-month to one-year effort conducted at least 1 to 2 years after the last apparition. This time delay allows for collecting and reducing all data taken during the previous apparition.

The question: "Why accomplish a Phase-0 study?" has not been fully answered. Column 1 of Table 3-2 gives some indication of the realistic initial uncertainties that are expected for the comets if no prior orbit fitting work or integration is accomplished. It is true that these uncertainties can be reduced for a particular apparition if sufficient observations are made after acquisition. However, the complications of launching a month or two after acquisition means that the comet uncertainty is still likely to be large and would require large compensating velocity corrections. A more realistic approach is to use existing data which contain sufficient accuracy to produce the predicted acquisition accuracies shown in column 2 of Table 3-2.
As is evident from the remaining columns of the table, the guidance problem due to comet uncertainty is greatly diminished once the preacquisition analysis has been accomplished and incorporated into the mission plan.

Other factors in favor of a Phase 0 study are the following:

a. Reduced reliance on observatories, both before and after launch. (Probably one pair of observations would be made each new moon).

Table 3-2 Predicted Comet Positional Uncertainties at Perihelion

Comet	Initial Acq. Uncertainty W/O Orbit Refinement	Initial Acq. Uncertainty With Orbit Refinement	Comet Uncertainty At Time Of Launch	Comet Uncertainty At Time of 1st Correction		Comet Uncertainty At Time of 2nd Correction *		Uncertainty At The Time of Arrival in KM ($\widehat{4}$ ")*
				30^d After Injection	60^d After Injection	40^d Before Arrival	20^d Before Arrival	
Tempel (2)	1.5^d	1^h	10^m	4^m	3^m	$\widehat{4\text{-}8}$ "	$\widehat{2\text{-}4}$ "	1200
Pons - Winnecke	4^d	3^h	30^m	10^m	7^m	$\widehat{4\text{-}8}$ "	$\widehat{2\text{-}4}$ "	1800
Kopff	1^d	2^h	30^m	10^m	7^m	$\widehat{4\text{-}8}$ "	$\widehat{2\text{-}4}$ "	5300
Brooks (2)	0.5^d	1^h	10^m	4^m	3^m	$\widehat{4\text{-}8}$ "	$\widehat{2\text{-}4}$ "	5800

* As viewed from the Earth.

b. Capability to launch before the comet has been acquired. There is absolutely no reason that a launch could not take place before comet acquisition if a thorough Phase-0 study has been completed.

c. Reduced fuel expenditures due to both the smaller uncertainties of the comet and the possibility of earlier first and second corrections.

d. Possibility of mission failure because of the lack of observational data or because of adverse observational conditions (cloud over, etc.) is greatly reduced. The mission could be a partial success if only 3 or 4 observations were obtained.

3.8 COMET RECOVERY

An analysis of the comet motion before launch was conducted to determine possible recovery times for each comet target. The significant parameters considered in determining recovery times and positions are as follows:

a. Distance of comet from the earth

b. Distance of comet from the sun

c. Earth-sun-comet angle histories

d. Declination of the comet W.R.T. the equator

e. Prior recovery data pertaining to magnitudes and distances at which the comet was recovered

A pre-launch and post-launch ephemeris for each of the possible comet targets and earth are presented in Figures A-32 to A-36.

A summary of comet recovery lead times is shown in Table 3-3

Table 3-3. Comet Recovery Table

COMET	PREDICTED DATE OF RECOVERY	PREDICTED DATE OF LAUNCH	LEAD TIME (MONTHS)
Tempel (2)	Jan. 10, 1967	Apr. 10, 1967	3
Pons-Winnecke	Dec. 1, 1969	Jan. 31, 1970	2
Kopff	Dec. 15, 1969	Feb. 1, 1970	1½
Tuttle-Giacobini-Kresak	Jan. 6, 1973	Oct. 5, 1972	-3
Brooks (2)	May 4, 1973	May 4, 1973	0

3.9 MARINER-C COMET PROBE

Since the mission to Pons-Winnecke in 1969-1970 is the only one found which is suitable for using an Atlas/Agena launch vehicle and for accomplishing the scientific objectives, it was chosen for the comparison. The mission to Tuttle-Giacobini-Kresak in 1973 may be accomplished using an Atlas/Agena combination. However, the comet is faint and not recoverable for at least 3 months after launch (see Table 5-1). No earlier launches to periodic comets were discovered that might use an Atlas-Agena/Mariner-C combination. A mission to the comet Tempel (2) in 1967 looks favorable for an Atlas/Centaur launch. Similarly, missions to the comet Kopff (1970) and Brooks (2) (1973) fall into the Atlas/Centaur class.

Range-safety and energy limitations prohibit using a single time-of-flight curve for more than a few days of launch time. Tables of launch-heliocentric and comet-centered information were compiled for a typical 30-day launch window for two types of trajectory in 1969-1970. For an actual launch table more frequent time-of-flight changes would be utilized to eliminate the large jumps in energy. The net effect would be that of following the envelope of the energy curves instead of individual curves for a number of days.

A Mariner-C mission to Mars and several possible missions to Pons-Winnecke are compared in Table 3-4. The Mariner-C payload capability is based on the actual launch weight of 565 lbs. The midcourse velocity capability of Mariner-C was based on 80 m/s as provided by JPL. In comparing the numbers presented in the table, it is evident that an Atlas/Agena-B/Mariner-C spacecraft combination can be used for a mission to Pons-Winnecke in either late 1969 or early 1970. It seems most likely that both opportunities would be considered (Type I and Type II) and hence improve the overall reliability of mission success by having two launch periods spaced only a month or so apart.

3.10 MISSION TO EROS

It seems logical to justify a mission to an asteroid, sometimes referred to in the literature as a gray rock, that one must set out to accomplish one of the following tasks:

1. Fly by at very close distance and obtain high-resolution TV pictures which could be used to analyze the surface character of the asteroid.

2. Obtain spectrographic information which could result in analysis of the composition of the asteroid.

Table 3-4 Mariner-C Comparison Chart for a Mission to Pons-Winnecke (1970)

COMPARISON QUANTITY	MARINER-C TO MARS	MARINER-C TO COMET PONS-WINNECKE Type I	Type II
Geocentric Injection Energy (C_3) (For 30 Day Launch Window) Km^2/Sec^2	10.2	2.8 - 7.5	4.0 - 8.9
Payload Capability to Achieve Injection Energy Requirements (lbs.)	565	630	578
Range of Flight Times to Encounter (Days)	220-250	200-170	270-240
Earth-Vehicle Communication Distance at Arrival (millions of Km.)	220-250	94-96	92-97
Relative Approach Velocities at Encounter (Km/Sec)	5-6	14.7-15.0	13.6-15.5
Midcourse Velocity Requirements with a Preacqusition Study (m/s)	80	80	120
Minimum Encounter Approach Distance (Km)	10,000-25,000	5,000-10,000	5,000-10,000

Both of the tasks mentioned above seem extremely difficult to achieve due to the small size of the asteroid and the solid character of its mass. However, a solution has been considered for accomplishing the second task. In order to conduct spectroscopic measurements on asteroidal surface material on a fly-by mission, an experiment is proposed which might be called the shotgun method. This experiment is outlined below.

The Shotgun Experiment consists of the following sequence of events:

1. Achieve a distance of closest approach of 100 to 300 km by using a triple-correction guidance scheme. Without a closed-loop guidance system, the minimum error can never be smaller than A.U. uncertainties.

2. At a specified time before arrival from the asteroid, separate a spinning payload from the spacecraft.

3. Re-orient the spacecraft and retro-fire the spacecraft engine ($\Delta V \geq 100$ m/s). The spacecraft will then travel on a slower trajectory than the spinning payload.

4. At fixed-time increments, release rings of particles from the spinning payload. The net effect of the propagation of these particles is to create a cross-sectional area of particles such that at least one and preferably more will impact the asteroid. The size of these particles may be that of a ping-pong ball or smaller and the composition is such that a maximum cloud of asteroid material is created.

5. The spacecraft is equipped with a spectrograph which then analyzes the artificially created cloud of asteroid material. The small gravitational coefficient of the asteroid should allow the cloud to remain dispersed for a relatively long period of time.

No refined estimate of particle sizes, composition, etc., have been made, but a 100-lb. spinning payload should provide ample margin.

The Shotgun mission as briefly described herein seems to be a reasonable approach for obtaining good composition data for the asteroid Eros. A TV system could additionally be used if the total payload weight permitted.

SECTION 4
SYSTEM REQUIREMENTS

4.1 MISSION CONSTRAINTS

Mission constraints for the design of conceptual spacecraft to acomplish the Comet Mission objectives are tabulated below in Table 4-1.

Table 4-1. Mission Constraints

Mission Period	1967-1975
Launch Vehicles	Atlas-Agena Atlas-Centaur
DSIF Capability	1964-1968
Injection Energy (C_3)	7 - 22.2 km^2/sec^2
Flight Time (to intercept)	160 - 300 days
Heliocentric Distance (at intercept)	1.25 - 1.80 A.U.
Geocentric Distance (at intercept)	(92-294) x 10^6 km
Closing Velocity	8 - 15.5 km/sec
Corrected Miss Distance (3σ)	5000 - 10,000 km
Payload Capability	
Atlas-Agena	578 - 630 lbs
Atlas-Centaur	900 - 1400 lbs

4.2 SEQUENCE OF EVENTS

A sequence of events for the photovoltaic-configuration spacecraft is tabulated in Table 4-2, using a mission to Pons-Winnecke to time-key the events. The sequence is the same for the isotopic configuration

Table 4-2 Mission Sequence of Events - Photovoltaic Configuration

PHASE		EVENT	TIME	SOURCE	DESTINATION	COMMENTS
Launch	1	Lift-off (T)	0	Event	---	---
	2	RF Power Up, Cruise Science On	5 min	Centaur timer	Power	At shroud separation
	3	Injection (I)	45 min	Centaur	---	---
Acquisition	4	Separation (S)	48 min	Agena D timer	---	---
		a. RF Power Up, Cruise Science On, Data Mode II	---	Separation connector	Power	Back-up to #2.
		b. Enable CC&S	---	Separation connector	CC&S	---
		c. Arm Pyro-technic	---	Pyro-arming switch	Pyro	Switch parallel with timer.
		d. Attitude Control Subsystem On	---	Pyro-arming switch	A/C	Start sun acquisition.
		e. Timer On	---	---	---	---
	5	Arm Pyrotechnics	48.3 min	Timer	Pyro	See #4c.
	6	Deploy Solar Panels and Solar Vanes, Unlatch Scan Platform	49.6 min	Timer	Pyro	---
		a. Deploy, unlatch	53 min	CC&S	Pyro	Back-up DC Back-up
	7	Deploy Science Boom	54 min	Timer	Pyro	---
		a. Deploy Boom	58 min	CC&S	Pyro	Back-up. DC back-up.
	8	Roll S/C to calibrate magnetometer	---	---	---	---
	9	A/C On	63 min	CC&S	A/C	Back-up to #4d. Direct command back-up (DC).
	10	Sun Acquisition Complete	70 min	---	---	---
	11	Canopus Sensor and Solar Vanes On. Start Roll Search about z-axis.	997 min (16.62 hr)	CC&S	A/C	DC Back-up. Stop Magnetometer calibration roll signal.
	12	Canopus Acquisition complete	1060 min (17.67 hr)	---	---	---

Cruise	13	Set Roll and Pitch Turn Duration and Polarity	25 days	Quantitative Command (QC)	CC&S	---
	14	Set Motor Burn Duration	25 days	QC	CC&S	---
Maneuver	15	Start Maneuver Sequence (M)	30 days	DC	CC&S	---
		a. Gyro Warmup	---	CC&S	A/C	---
		b. Switch to Data Mode I	---	A/C	Data Encoder (D/E)	DC Back-up
	16	Start Maneuver	M + 60 min	CC&S	A/C	First midcourse
		a. S/C to Inertial Control (all axes). Star-Sensor Auto-pilot Off	---	---	---	---
	17	Stop Roll and Pitch Turns.	M + 90 min	CC&S	A/C	---
	18	Ignite Midcourse (M/C) Motor	M + 103 min	CC&S	Pyro	---
	19	Stop M/C Motor	M + 105 min	CC&S	Pyro	---
Acquisition	20	Start Reacquisition of Sun & Canopus	M + 110 min	CC&S	A/C	---
		a. Switch to Data Mode II	---	A/C	D/E	DC Backup.
	21	Sun Reacquisition Complete	M + 120 min	---	---	---
	22	Canopus Reacquisition Complete	M + 180 min	---	---	---
	23	Maneuver Counter Off	M + 199 min	CC&S	CC&S	Permits 2nd maneuver.
Maneuver, Acquisition	24	Arm 2nd Maneuver	---	DC	Pyro	---
	25	Repeat Events 13-23	116 days (E - 40^d)	---	---	Second midcourse
Cruise	26	Update Canopus Sensor Cone Angle	126 days (E - 30^d)	CC&S	A/C	DC Back-up.
	27	Transmit via High Gain, Receive via Omni	136 days (E - 20^d)	CC&S	Radio	DC Back-up.

Encounter	28	Start Encounter Sequence	---	DC	CC&S	---
	29	Start Comet Acquisition	126^d ($E-30^d$)	CC&S	A/C (CT)	DC Back-up.
	30	Comet Acquisition Complete	154^d ($E-2^d$)	Comet Tracker (CT)	Data Automation System (DAS)	---
		a. Switch to Data Mode III or IIIa	---	DAS	D/E	Option depends on data rate capability.
	31	Intercept Science On	154.5^d ($E-1.5^d$)	CC&S	Power	DC Back-up. At 1.3×10^6 km away from comet.
		a. Instrument Cover Off	---	CC&S	Pyro	---
		b. Tape Recorder On	---	Power	Recorder	---
	32	Start Recording	155^d ($E-1^d$)			
		a. Start Tape Recorder	---	DAS	Recorder	Recorder on for either Data Mode III or IIIa.
	33	Closest Approach (E)	156 days	---	---	---
	34	Tape Recorder Stop	157^d ($E+1^d$)	Recorder Recorder	Recorder DAS	Automatic Stop.
		a. Switch to Data Mode II	---	DAS	D/E	DC Back-up.
		b. Inhibit Start Tape Commands	---	DAS	DAS	---
	35	Intercept Science Off	157.5^d ($E+1.5^d$)	CC&S	Power	DC Back-up. At 1.3×10^6 km away from comet.
Playback	36	Tape Playback	158^d ($E+2^d$)	CC&S	D/E	DC Back-up.
		a. Switch to Data Mode V	---	---	---	---
		b. Cruise Science Off	---	D/E	Power	---
		c. Playback Twice	---	---	---	---
Cruise	37	Switch to Data Mode II	186^d ($E+30^d$)	DC	D/E	Optional after all recorded data received and if power and gas permit
		a. Cruise Science On	---	DC	Power	

except for the solar deployment events.

4.2.1 Data Modes

Data modes referred to in Table 4-2 are as follows:

- I: Sampling of only engineering data during maneuvers and during cruise.
- II: Transmission of alternating engineering and science data block during launch, initial acquisition and cruise.
- III: Sampling of only science data during intercept. (No engineering data.)
- IIIa: Transmission of science data during intercept, except TV, at maximum bit rate.
- IV: Transmission of stored science data and of real-time Mode I engineering data during post-intercept.

4.2.2 Events

If the science boom for extending the sensitive magnetometer and ionizatin chamber is obviated by very low residual spacecraft magnetism, the low-gain antenna waveguide can be used to mount these instruments and Event 7, deploy science boom, is deleted.

On a mission to Brooks (2) at 1.8 A.U. heliocentric distance, Event 31, intercept science on, occurs before the scheduled encounter in order to offset the cold temperature of the tracking assembly and science platform at this large distance.

4.2.3 Encounter Sequence of Events

The series of events during the encounter phase is illustrated in Figure 4-1 for an Atlas-Centaur boosted spacecraft from AMR to

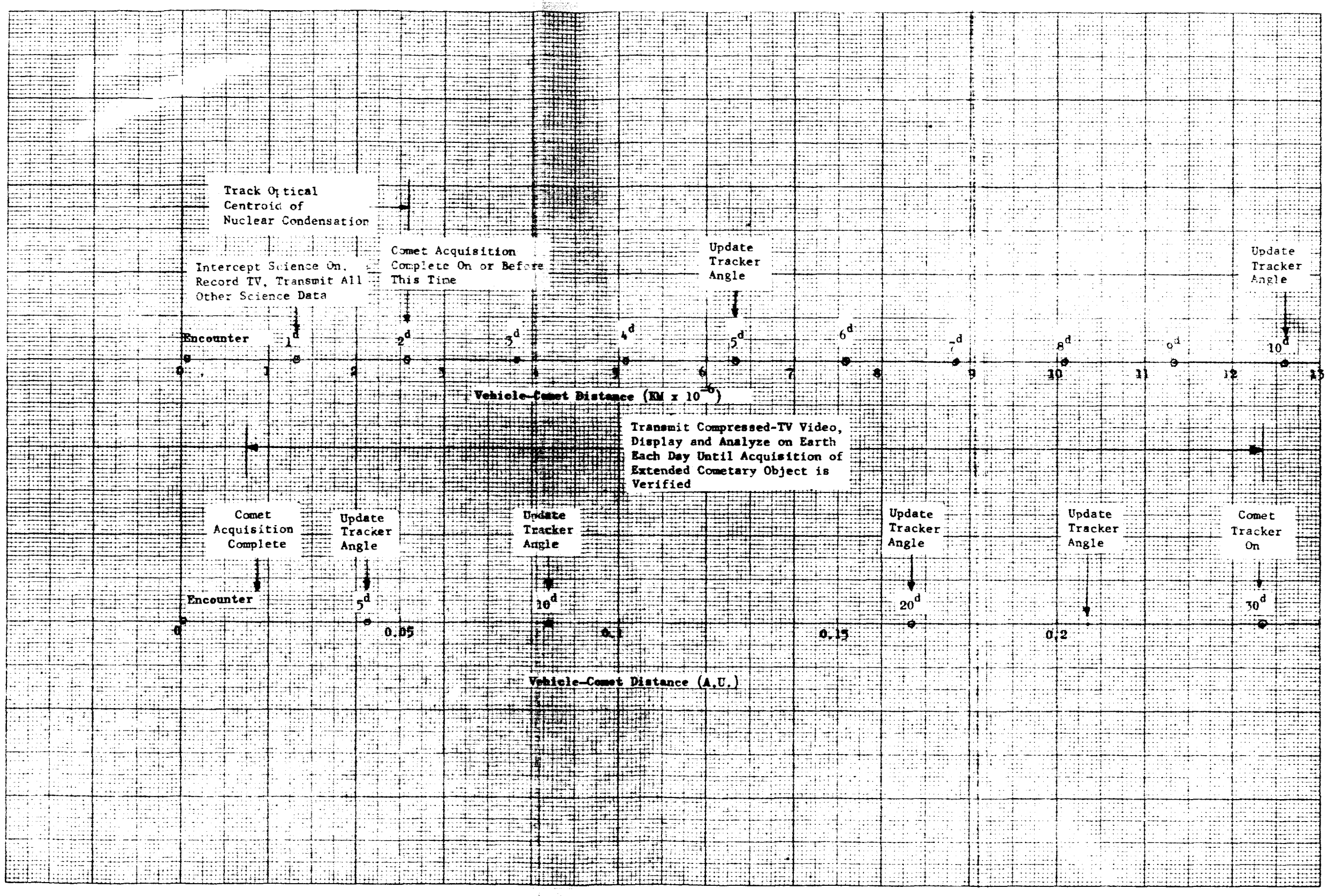

Figure 4-1 Encounter Sequence of Events for Pons-Winnecke 1970

Pons-Winnecke in 1970, and is detailed below:

Event 29: Start Comet Acquisition

(i) The comet tracker, pre-set before launch at an angle determined by the planned approach trajectory, is turned on by direct command 30 days before encounter after the second maneuver has been executed.

(ii) The comet tracker is a TV-tracker whose scanned image is compressed and telemetered through a buffer storage to Earth.

(iii) The received video on the Earth is reconstructed for display and analysis to verify that the target in the field of view is the comet and not bright stars radiating through the coma. The intensity and its time change is also recorded.

(iv) Transmission and analysis of the compressed TV images continue until ground analysis verifies the detection of the comet as an extended object in the star field.

(v) The angular position of the comet tracker is updated every 5 days either by direct command or by a clock-actuated signal (with DC back-up) based upon the planned approach velocity vector. The former option is exercised after acquisition in the field of view has been established. The latter option is excercised only during the period of compressed-TV transmission and analysis.

(vi) Cruise science and engineering data are sequenced for transmission between a series of TV pictures.

Event 30: Comet Acquisition Complete

(i) The auto-track mode is initiated by direct command in order to track the optical centroid of the verified cometary object (nuclear condensation).

(ii) The nucleus-oriented intercept science ("Advanced-Mariner" TV, photometers, and spectrometers) is slaved to the comet tracking assembly.

Event 31: Intercept Science On

All cruise science remains on for measurements of cometary phenomena during the intercept; the ion-mass spectrometer, science TV, etc. are turned on; the tape recorder is turned on.

Event 32: Start Recording

At Pons-Winnecke, the tape recorder records mass-spectrometer and science-TV data, while all other science is transmitted in real time. With an increase in transmitter power from 10 to 25 watts and the use of the 210-foot DSIF receiver, all data but the science TV can be transmitted, as indicated by Event 30a of Table 4-2 (Switch to Data Mode IIIa)

Event 36: Tape Playback

All data is played back twice. With real-time transmission of most of the intercept science data, it is necessary to record and playback only the TV. The option exists for recording and thus playing back all the data up to 30 days after encounter (point of closest approach), as indicated by Event 37 in Table 4-2.

SECTION 5
GUIDANCE AND CONTROL

5.1 OBJECTIVES

The objectives of this study have been the following:

a. Organize and define the operational requirements of the attitude control and midcourse propulsion subsystem.

b. Define preliminary system configurations to meet the operational requirements and to provide a basis for making the final selection of an attitude control system.

c. Identify critical subsystem areas and components and provide a detailed evaluation of available options for missions.

d. Recommend a system and identify the areas requiring further study.

Within the scope of the study, the effort has been based on relevance to the scientific mission objectives and, consequently, on components that limit the performance. System performance is measured by reliability, precision, component weight and power requirements. The subsystem performances required for comet missions do not require any extension of the performance state-of-the-art.

The Mariner-C system has been adopted as the standard system. The study recommends improvements, by either the addition or the exchange of components to the Mariner-C attitude control and propulsion systems. The principal study areas reported are the following:

a. Comet tracking prior to encounter and during the encounter phase.
b. Propulsion system tradeoffs.
c. Improved inertial components.

5.2 SUBSYSTEM REQUIREMENTS

The attitude control and stabilization system (A/C) is required to acquire and maintain three-axis control over the entire mission beginning with an acquisition mode following separation from the third-stage booster. **The A/C system configuration is based on satisfying the following requirements. See Table 5-1 below:**

a. Stabilization during two midcourse guidance corrections.
b. High-gain antenna pointing.
c. Thermal control.
d. Pointing and slewing of scan platform during intercept.

TABLE 5-1
A/C REQUIREMENTS

Subsystem	Requirement	Tradeoffs
Cruise Science	Orient instruments along the S/C velocity vector, S/C x-y-z axes, and toward Sun within $\pm 0.5^{\circ}$.	---
Intercept Science	Orient TV, photometer and spectrometer toward nucleus within $\pm 0.5^{\circ}$ accuracy and at a maximum rate of 1°/sec.	1. Gimballed scan platform vs gimballed S/C. 2. Scientific value vs pointing accuracy.
Guidance	Control midcourse thrust direction.	Attitude accuracy vs terminal aiming error.
Telecommunication	Point high-gain antenna toward earth within $\pm 1^{\circ}$ accuracy at a 1°/sec rate.	---
Power	Orient solar panels toward Sun within $\pm 5^{\circ}$.	---
Thermal	Establish Sun line within $\pm 5^{\circ}$.	---

The requirements in Table 5-1 are compatible with present Mariner-C **capabilities, except for comet pointing which requires adding a mechanically gimballed comet tracker and science package with two degrees of freedom.**

5.3 ATTITUDE CONTROL SUBSYSTEM

Three distinct modes of operation are indicated to accommodate the A/C system requirements:

a. Acquisition and Cruise Mode. When operating in this mode the attitude control subsystem shall be capable of acquiring and maintaining 3-axis stabilization using the Sun and Canopus as reference objects to a nominal accuracy of ±1.0 degrees with respect to each axis. Reacquisition in the event of loss of acquisition for any noncatastrophic reason shall be automatic. The cruise mode permits a bias offset in roll to position the Canopus tracker.

b. Maneuver Mode. In this mode, the attitude control subsystem in response to commands from the CC&S is capable of pointing the propulsion subsystem thrust axis to any arbitrary new orientation to a 3 accuracy of ±2.0 degrees from the nominal reference attitude and with a drift rate of less than 0.5 degrees per hour. This stability will be maintained during motor burning using an autopilot with jet vane actuation.

c. Encounter Mode. Three-axis stabilization as in the cruise mode and operation of a platform-mounted comet tracker. Onboard tracking or pointing toward the Comet is to be accomplished by utilizing a gimballed tracker during the encounter phase of the trajectory. Orientation requirements for the scientific equipment and other spacecraft subsystems form the basis for the design objectives.

5.3.1 Sequence of Events for A/C

The following summarizes the Comet Mission A/C system sequence of events:

Acquisition. Following separation from the upper booster stage, the spacecraft acquires the Sun and Canopus references. The separation interface from the booster upper stage results in an uncertainty in spacecraft attitude and angular rates. Acquisition is accomplished by first stabilizing with respect to the Sun and then searching for the stellar reference by rolling the spacecraft about the Sun-line. The design permits acquisition of the Sun-star references at any time following the initial acquisition and before intercept. Initial acquisition has several requirements which must be allowed for in the formulation of a sequence of events.

These are the following:

a. Initial search of the star field must avoid bright sources of interference to the star tracker; notably spacecraft reflections of earth albedo and comet albedo, and stellar objects having a brightness comparable to the celestial reference.

b. Payload separation rates from the upper stage of the launch vehicle must be within the range of the sensors. The problem of initial acquisition requires that boundary conditions be established regarding maximum separation rates. Inertial rate gyros are capable of sensing rates up to 22,000°/hr; however, separation rates are much less than this (estimated to be less than 0.1°/sec). Initial acquisition can be carried out without the use of gyros for a Centaur separation; however, this has not been verified by simulation, although related experience on similar control systems supports this conclusion.

Cruise. The A/C operates in a combinational mode consisting of derived-rate deadband ($\pm 1.5^{\circ}$) operation about the three reference axes plus the use of a solar vane system for stabilization with respect to the Sun. Following acquisition of the Sun reference and the stellar reference, spacecraft angular rates are reduced to a minimum level. Minimum rates are obtained by limit-cycle operation set by the minimum impulse obtained from the mass expulsion system. Deadband rates of 2.0×10^{-3} degree/second, are practical and within the requirements for the Comet Mission. The use of solar vanes for the pitch and yaw axes further reduce the rates about these axes. The low rates enhance the scientific objectives by reducing the amount of skewing of the optical sensors. This is particularly so if the A/C thrusting subsystem were to use hot-gas propellant expulsion for active control. The system indicates spacecraft attitude to a 3-sigma value of ± 0.1 degrees. Detailed descriptions of this operational mode can be obtained from JPL specifications of the Mariner-C A/C System, and from the Solar Probe Study.

Maneuver. The A/C system accepts maneuver commands via the spacecraft command subsystem. The maneuver sequence consists of a roll turn followed by a pitch (or yaw) turn. The 3-sigma accuracy of orientation at the end of the maneuver does not exceed ± 2.0 degrees and the time required to reach the desired orientation and return does not exceed one hour. The inertial system serves as a reference attitude sensor, provides control signals to the autopilot, and has a 3-sigma drift rate better than 0.5°/hr. Attitude control is accomplished by inserting vanes in the nozzle for thrust-direction control.

Encounter. The encounter mode is initiated approximately 30 days prior to closest approach. Initiation of this mode consists of actuating a gimballed TV/Tracker which records a complete scan frame for purposes of determining the acceptability of the picture to the tracker and of establishing an empirical comet brightness model. The uncertainty in the comet illumination model requires that the tracking illumination pattern be inspected and a decision to track from on-board be made. In the event that tracking is not possible, due either to a bright stellar background or a large anomaly in the predicted illumination model, tracking is carried out with a pre-programmed combination of gimbal angles. This latter case is a precautionary measure to allow for the possibility that the tracker cannot operate on the actual comet illumination pattern.

An inertial system stabilizes the spacecraft during encounter to insure against the possibility of having the sun sensor lose track or the startracker lose Canopus. An interference-free condition cannot be guaranteed although the predicted particle density is extremely low within the coma.

The block diagram of the attitude control system is shown in Figure 5-1 in which the solar vanes, microthruster, telemetry and CCSS interfaces are not shown in order to simplify the diagram.

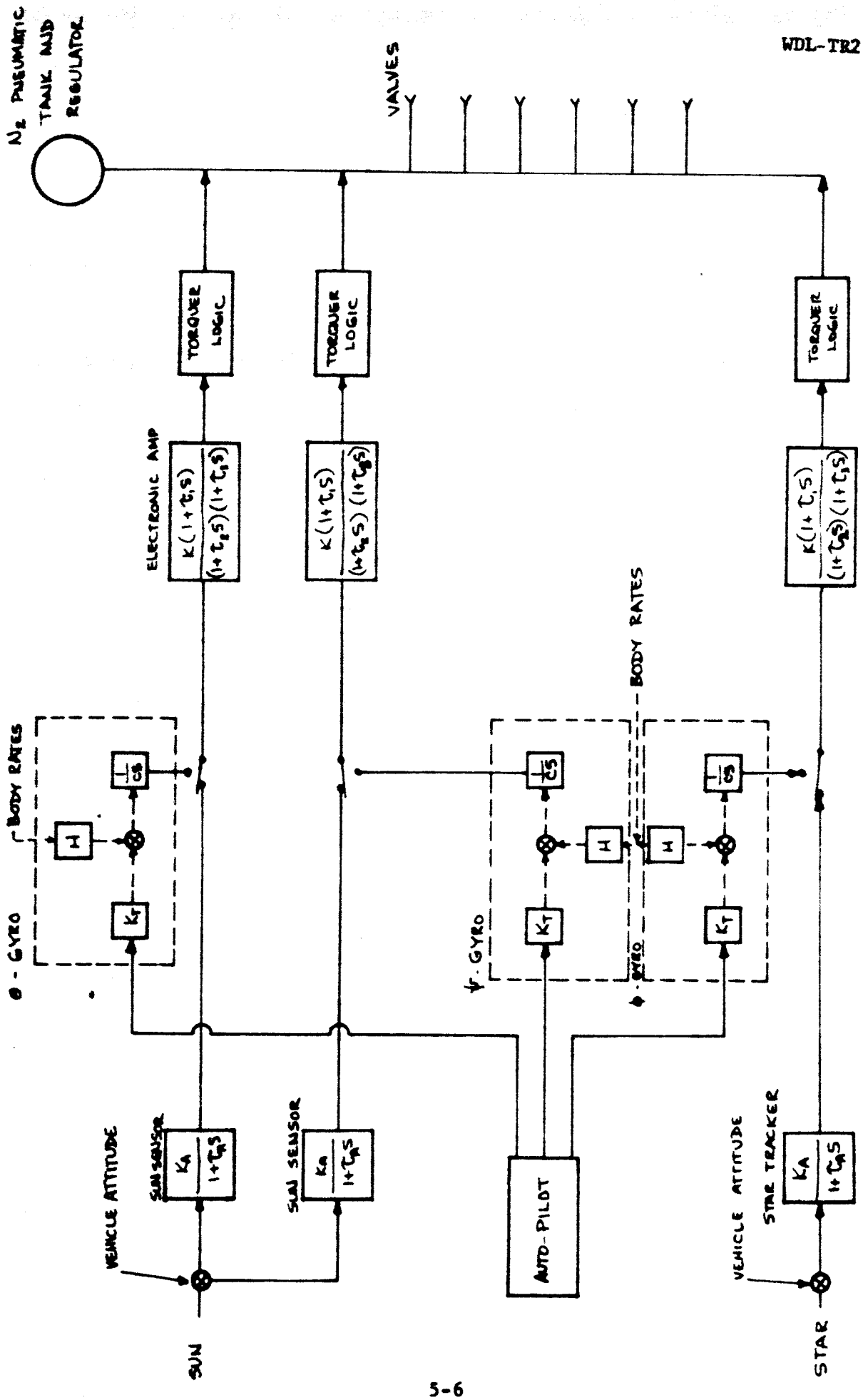

Fig. 5-1 Simplified Attitude Control System

5.4 MIDCOURSE PROPULSION SUBSYSTEM

The torquers for the Mariner C are preumatic; complemented by solar vanes in pitch and yaw in the cruise mode operation. The studies for the Comet Probe have shown that it is possible to use microthrusters for 3-axis solar vanes. Advantages of the microthruster system are manifested in a greater freedom of mounting on the vehicle, ruggedness and in larger torque levels (10^{-5} to 10^{-3} lb ft for the microthruster) and a higher speed of response that for solar vanes. Figure 5-2 is a photo of the microthruster feasibility model.

The system studies of the midcourse propulsion have defined the weight savings for a bipropellant engine to replace the hydrazine monopropellant engine. Several comparisons of systems using the same propellant for attitude control and midcourse velocity corrections and found to be feasible. The use of a bipropellant attitude control system operating with solar vanes or a microthruster to reduce deadband rates have been demonstrated by analog simulation.

5.5 ON-BOARD COMET TRACKING

On-board Tracking for purposes of making guidance computations during the early part of the flight is impractical for the following reasons:

1. Tracking during the early part of the flight following launch, requires unrealistic optical systems to sense comets that are approximately 20th magnitude at that time. The estimated weight of an optical systems required to detect the presence of a comet in a known stellar background is shown in Figure 5-3. If a

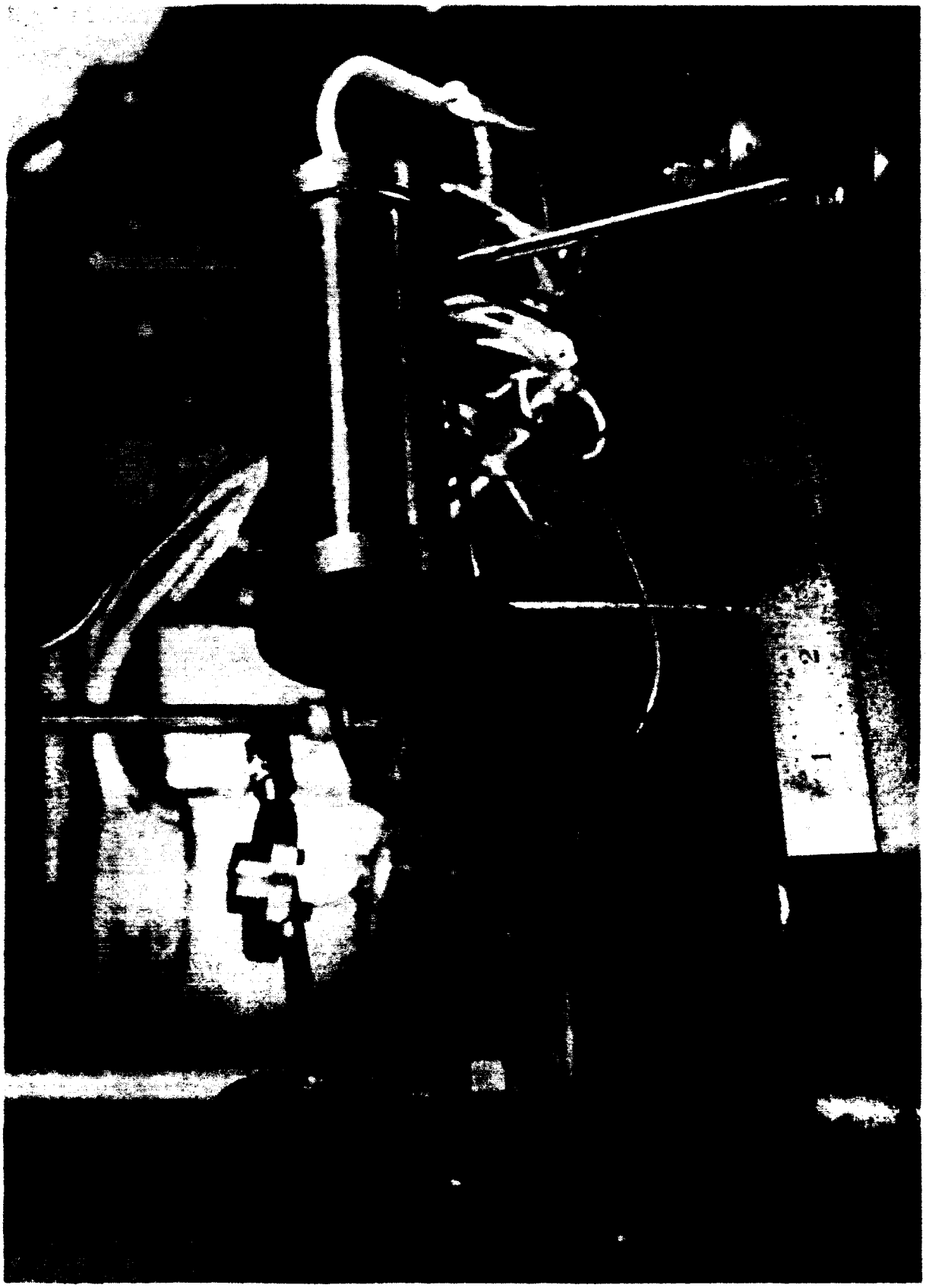

Fig. 5-2 Feasibility Model Hydride Thruster (Deflection Vane Pulled Away)

signal to noise ratio of six is defined as a threshold level for detection, then several detector sensitivities may be compared in terms of weight required from Figure 5-3. The weights required to satisfy the tracking requirement for stars having a magnitude less than 10 is considered prohibitive. In fact an order of magnitude reduction would only render it possible to track at about 30 days prior to closest approach. The uncertainty of $\pm$ 2 magnitudes in the comet brightness model makes this postulatd situation one of chance.

2. Comet brightness does not reach levels that are practical for the purpose of tracking until after a guidance maneuver becomes effective.

3. Tracking for the purpose of guidance computations can be done by Earth observatories. A pre-recovery study of comet orbits is to be completed prior to launch in order to improve the predicted time of their passage through perihelion.

5.6 ENCOUNTER TRACKING

During encounter, which could be as early as 30 days prior to the point of closest approach, the encounter tracking is initiated in the form of an acquisition mode. Since the comet-vehicle-sun angle is nearly constant from 10 to 30 days, the comet appears at a predetermined direction. During that time the comet intensity distribution is viewed continously. The background stellar sources influence the tracker and by monitoring the TV system output this condition can be observed. Due to the possibility of losing lock, a programmed search mode is necessary. During the hour prior to closest approach, the comet brightness becomes so bright that light from the stellar background becomes insignificant.

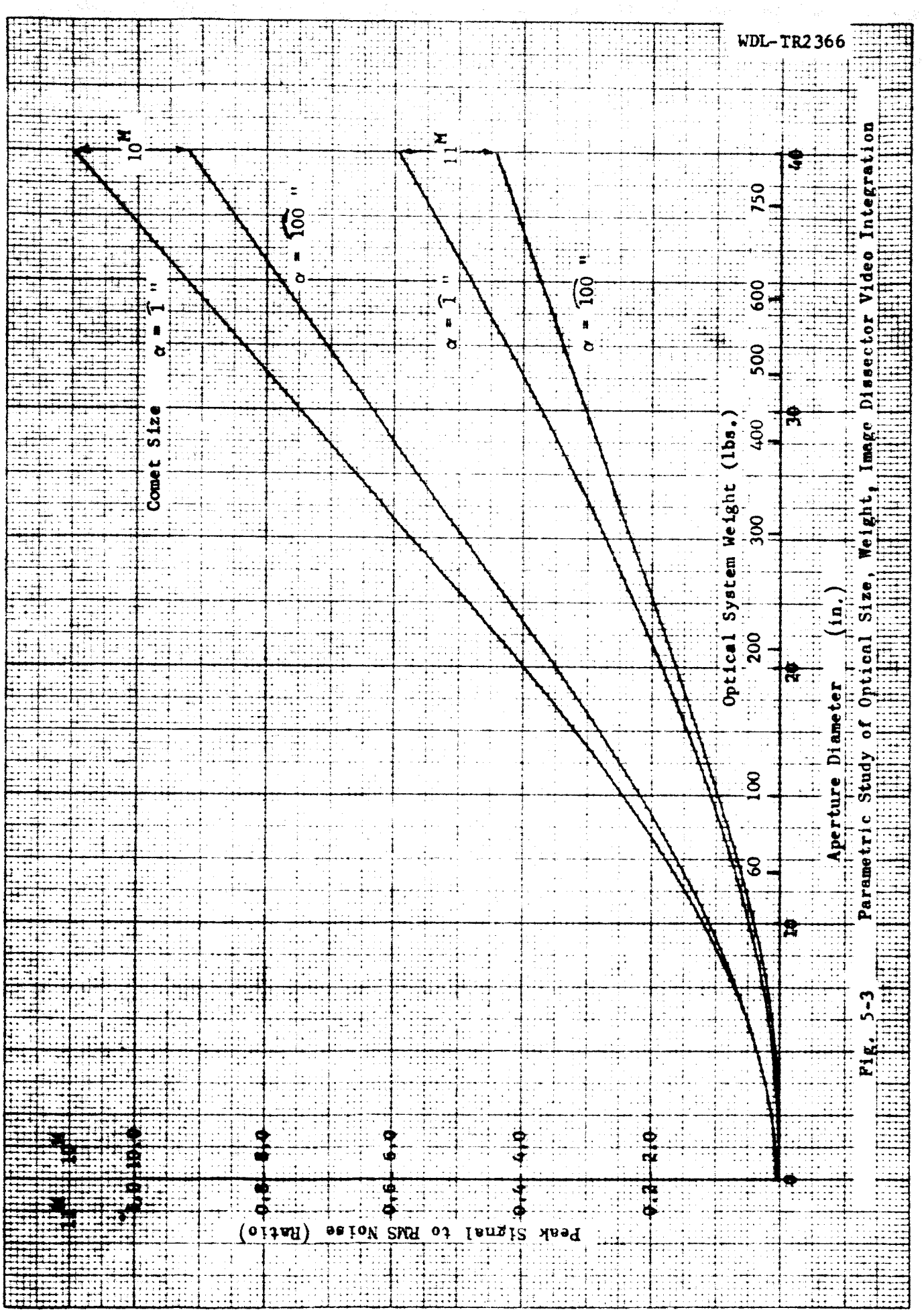

Fig. 5-3 Parametric Study of Optical Size, Weight, Image Dissector Video Integration

Although the sun-vehicle-comet angle is constant prior to closest approach, the gimbal angles required for tracking during closest approach are determined entirely from the geometry of the miss distance. In order to view the comet from the sun side, the trajectory is biased off. The gimbals for the tracker platform require two-degrees of freedom and must cover a full hemisphere.

Since the TV system operates continously with the tracker to observe the comet, an improvement in mission reliability, a reduction in power, and the advantage of a single optical system for both functions can be realized by using the TV scan for tracking. A block diagram of such a system is shown in figure 5-4.

5.7 MARINER-C COMPARISON

A comparison with the Mariner-C attitude control and propulsion system shows two significant deviations; (1) the need to impart larger velocity corrections (i.e. up to 150 meters/sec vs. 80 meters/sec); (2) the range of comet intensity variation and the uncertainty in the levels make the comet tracking problem unique. In addition to these differences, several improvements to the system are possible:

1. Improvement to the already reliable inertial components is possible. The improved versions are reported to use less power, operate more accurately, and have longer life.

2. The higher velocity requirement would be attained more efficiently with a bipropellant system.

3. A microthruster would improve the cruise stabilization mode of

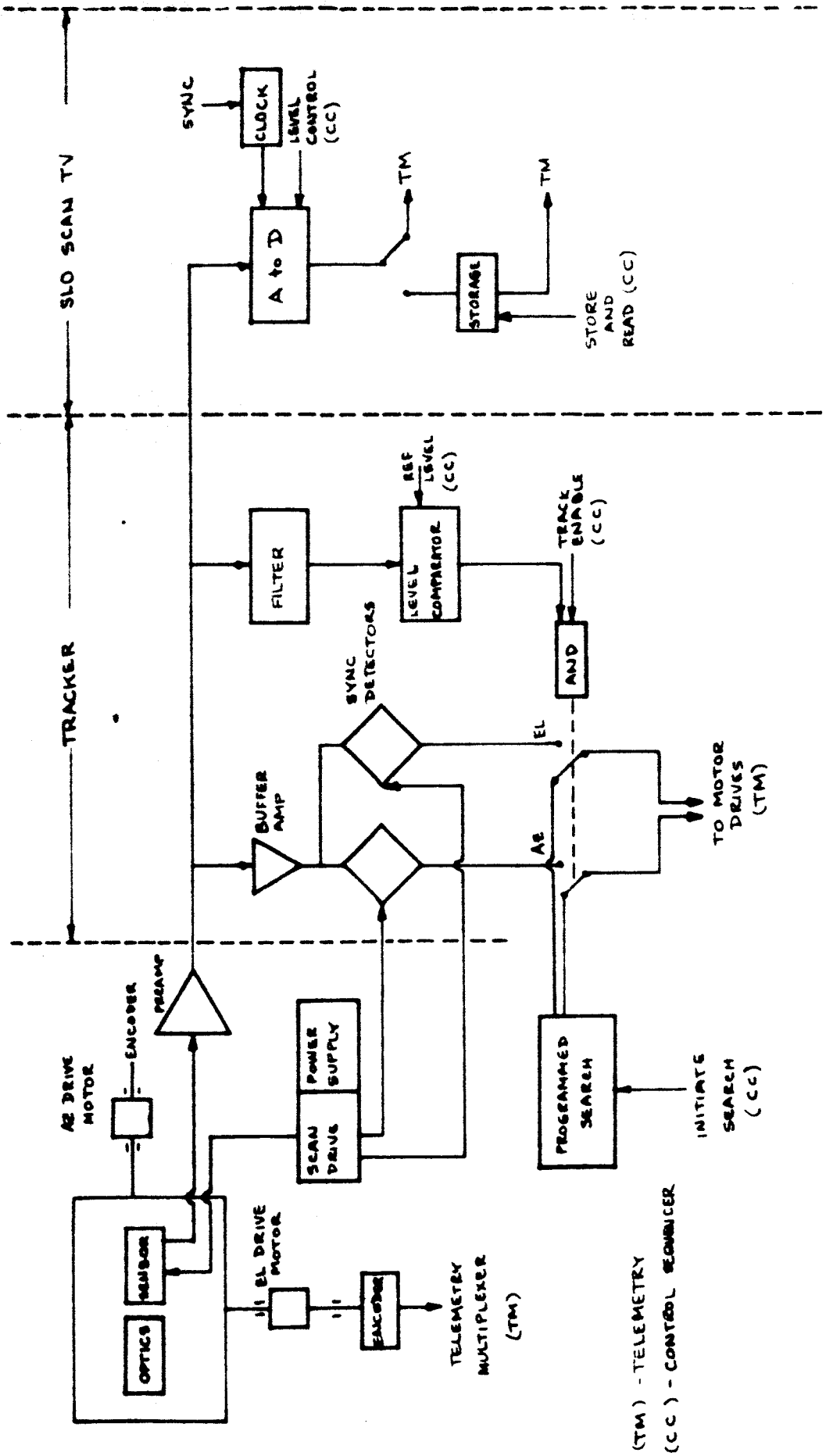

Fig. 5-4 Comet Tracker Functional Diagram

operation in the same way that solar vanes do for the Mariner-C This system would be more rugged and be relatively free of mounting restraints.

The weight and power schedule for the two systems appears in Table 5-2.

TABLE 5-2

GUIDANCE AND CONTROL

Subsystem	Weight (lbs)*		Temperature (°F)**	
	Comet Probe	Mariner-C	Minimum	Maximum
1. Propulsion	75.0	50.22	35	125
2. Comet Tracker & Gimbal	15.0	-	-30	+100
(Planet Scan)	-	18.0	-	-
3. A/C Electronic Assembly 7				
Gyro & Electronics	11.0	11.04	30	131
Electronic Assembly 7 less Gyro & Electronics	27.0	27.0	30	131
4. A/C Gas System				
Pneumatic System	29.0	29.0	40	140
Solar Pressure Vanes	4.0	4.0	-200	+250
5. A/C Sensors				
Sun Sensor	0.93	0.93	30	130
Earth Detector	0.25	0.25	30	130
Canopus Sensor	5.5	5.5	-30	+100
TOTALS - A/C	92.68	95.72		
Propulsion	75.0	50.22		

* Based on the weight profile for Mariner C given in JPL EPD-224
**Based on temperature profiles for Mariner C given in Specification MC-4-120B.

SECTION 6

TELECOMMUNICATION

6.1 TELECOMMUNICATION SYSTEM

The recommended system is described by the block diagram shown in Figure 6-1. PM synchronizing techniques with PSK modulation are used to maximize the total amount of proven hardware and to provide the most efficient modulation technique. Table 6-1 below is a tabulation of major hardware indicating which is Mariner equipment and which is new for a minimum-modification system.

Table 6-1 Communication Hardware for Minimum-Modification System

COMPONENT	SOURCE
Transponder	Mariner
10-watt Power Amplifier	Mariner
25-watt Power Amplifier	New: Raytheon Amplitron Watkins-Johnson TWT
4-foot Antenna	Modified Mariner
6-foot Antenna	New: Hexcel-Honeycomb
Ranging Module	New
Command Detector	Mariner
Command Decoder	Modified Mariner
Data Encoding and Storage	Modified Mariner and New Proven Equipment
Tape Recorder	Possibly Mariner
Pre-Amplifier	New
Omni Antenna	Modified Mariner
Computer Sequencer Programmer	Modified Mariner

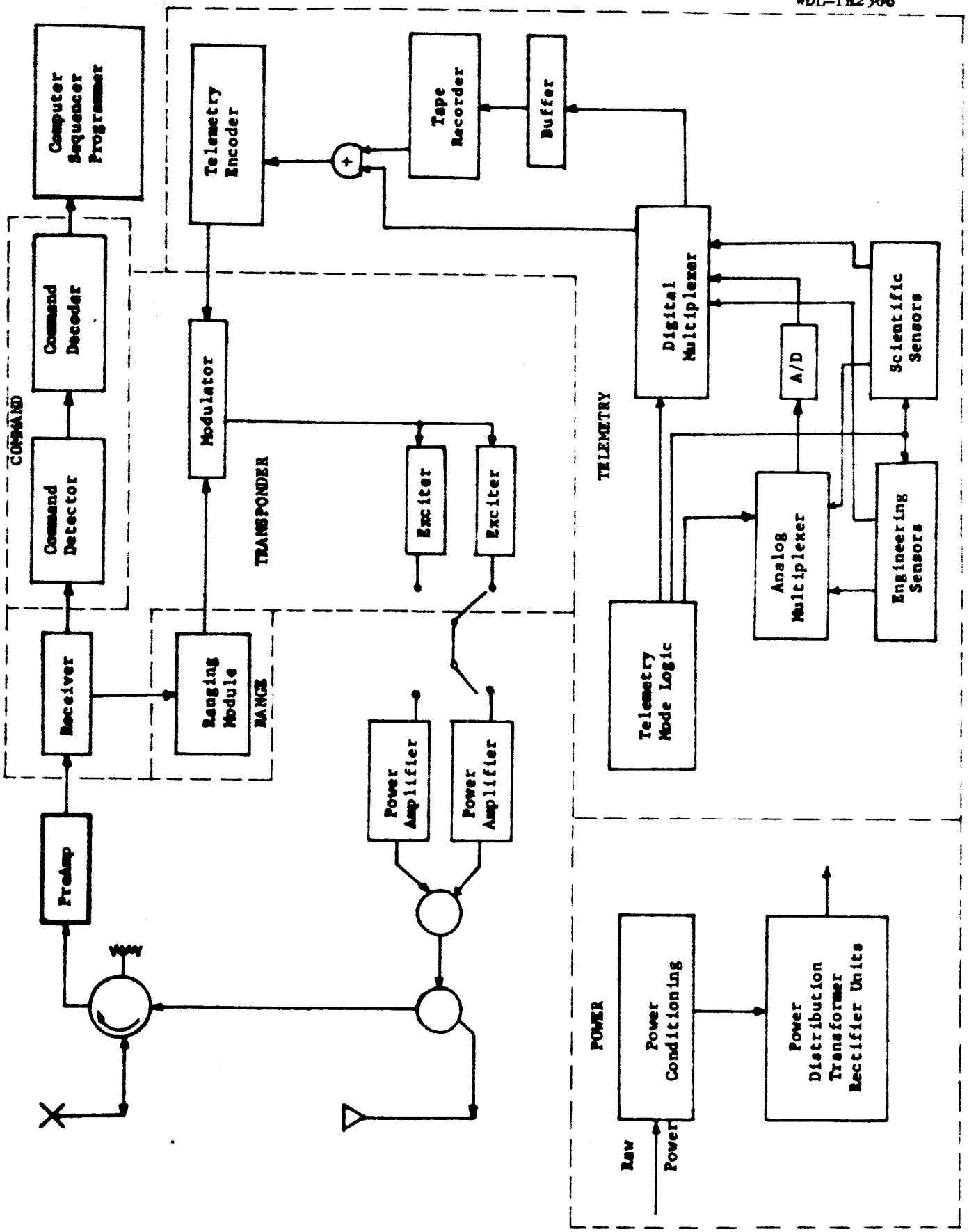

FIG. 6-1 Spacecraft Telecommunication Subsystems

Switching is provided for the telemetry transmitter so that it can feed either the high-gain antenna or the omni. The power amplifier output drives the antenna in all cases. This minimizes coverage requirements for the high-gain antenna by utilizing the wide coverage capability of the omni during the near-earth portion of the flight. Power amplifiers at both 10 watts and 25 watts are indicated. The unit to be used depends on the operating range requirements of the particular comet mission and on the data rate requirements.

Examination of the system diagram indicates only two functional changes in the overall system as compared to the Mariner-C system: (1) a pre-amplifier has been inserted prior to the transponder, and (2) reception of command signals via the high-gain antenna is not provided for. The pre-amplifier provides a decrease in system noise temperature of about 7 db which permits adequate reception out to a range of 100 to 200 million miles (160 to 320 million km). This is sufficient to satisfy all missions and eliminates the need for switching to the high-gain antenna at the extreme ranges. The system is considerably more reliable at a cost of only 1 pound and an insignificant amount of power for the pre-amplifier.

6.2 COMMAND SUBSYSTEM

The JPL PCM/PSK/PM modulation with PN code synchronization is recommended for the command system. The commands required on comet missions are comparable in number and type to those required for the Mariner Mars spacecraft. The number of commands is somewhat larger because of two midcourse corrections and encounter comet acquisition, verification, and tracking functions. These functions make the command system a necessity rather than a backup system during the encounter. Table 6-2 below includes a tabulation of the power requirement and system capability of the command link at intercept and at 30 days

after intercept. All command systems are capable of good operation with at least several db margin at the extreme range and the 50 dbw capability is not required as it is for the Mariner-C. If for any reason the recommended pre-amplifier is not used, the ground transmitter power requirements will exceed 40 dbw in most cases. Should the 50 dbw capability be a requirement, the mission will depend on Goldstone, assuming that the 100 kw transmitter will not be installed elsewhere.

Table 6-2. Command Capability at Encounter

Link Power	Pons-Winnecke	Kopff	Brooks (2)	Tempel (2)
Intercept	30 dbw	37.5	37	24.2
Intercept +30 days	32.5 dbw	38	38	32.5

6.3 TELEMETRY SUBSYSTEM

The telemetry system utilizes PN-PSK/PM, as was recommended for the command link. In this case a complete unit cannot be recommended since the system depends on the specific experiments to be flown and their relative sample rates. The building blocks, however, can be those used on the Mariner-C spacecraft interconnected in a slightly different manner to accommodate the requirements peculiar to a comet probe. Table 6-3 tabulates the telemetry power requirement and data rate capability at and after encounter for a 35-foot receiving antenna equipped with a maser, a 10-watt power amplifier on board, and the gain equivalent to a 4-foot parabola on board.

Table 6-3. Telemetry Power Requirements and Data Rate Capability at Encounter

Comet Mission	T/M at Intercept		T/M at Intercept + 30 days		Comments
	AP_t (dbw)	R_b*	AP_t (dbw)	R_b*	
Pons-Winnecke (1970)	-4	19 db / 80 bps	-1	15 db / 32 bps	10w transmitter provides an excellent system
Kopff (1970)	6.5	8.4 db / 7 bps	7.2	7.0 db / 5 bps	20w transmitter required to provide operation comparable to Mariner-C.
Brooks (2) (1973)	+6	9 db / 8 bps	+6	9 db / 8 bps	10w transmitter provides Mariner-C capability
Tempel (2) (1967)	-7.5	27.5 db / 560 bps	-3	23 db / 200 bps	10w transmitter provides an excellent system

* R_b based on 7 dbw modulation power

The storage capacity needed during intercept and the time needed for playback after intercept can be determined as follows. The relative speed between the spacecraft and comet at intercept is of the order of 10 km/sec. Beginning intercept at 10^6 km away from the point of closest approach defines the intercept period as being 2×10^5 seconds long, or 53.3 hours. Except for TV, encounter science requires about a 300-bps transmission rate is required of the telemetry subsystem. This represents

6×10^7 bits for the entire intercept period. If it is further assumed that 20 TV pictures (10 pictures with two color filters) are adequate for the mission, a total of 6.3×10^7 bits of data are accumulated during each encounter. Finally, it is assumed that this data is to be played back twice to the DSIF. This establishes a 6.3×10^7 bit requirement on the intercept data storage and 1.3×10^8 bits to be played back during the post-intercept period.

6.4 SPACECRAFT ANTENNAS

6.4.1 Low-Gain Antenna

The omni antenna is a body-fixed structure. If its axis points at the sun, clock angle plots indicate that, in order to satisfy all comet requirements, at least 110° coverage away from the sun line is required. The Mariner-C antenna satisfies both of these requirements. The present parasitic array should be fed with a smaller diameter waveguide to preclude higher-mode propagation. A simpler quarter-wave plate should replace the conical spiral in providing circular polarization.

6.4.2 High-Gain Antenna

The high-gain antenna is a body-fixed elliptical parabola generating a fan beam. Antenna pointing angles are defined by the cone angle and the angle away from a plane containing the probe-Sun line and the 90° clock angle line and in a direction perpendicular to it. This angle calculated as shown in Figure 6-2. The clock angle minus 90° is shown as angle a. Both of the lines ℓ_1 and ℓ_2 defining angle a are perpendicular to the probe-Sun line. Line ℓ_1 defines the 90° clock angle. Angle b represents the clock angle motion of the Earth as seen from the probe. If ℓ_3 is defined as the perpendicular to ℓ_1 from the Earth, the relationships indicated on Figure 6-3 follow.

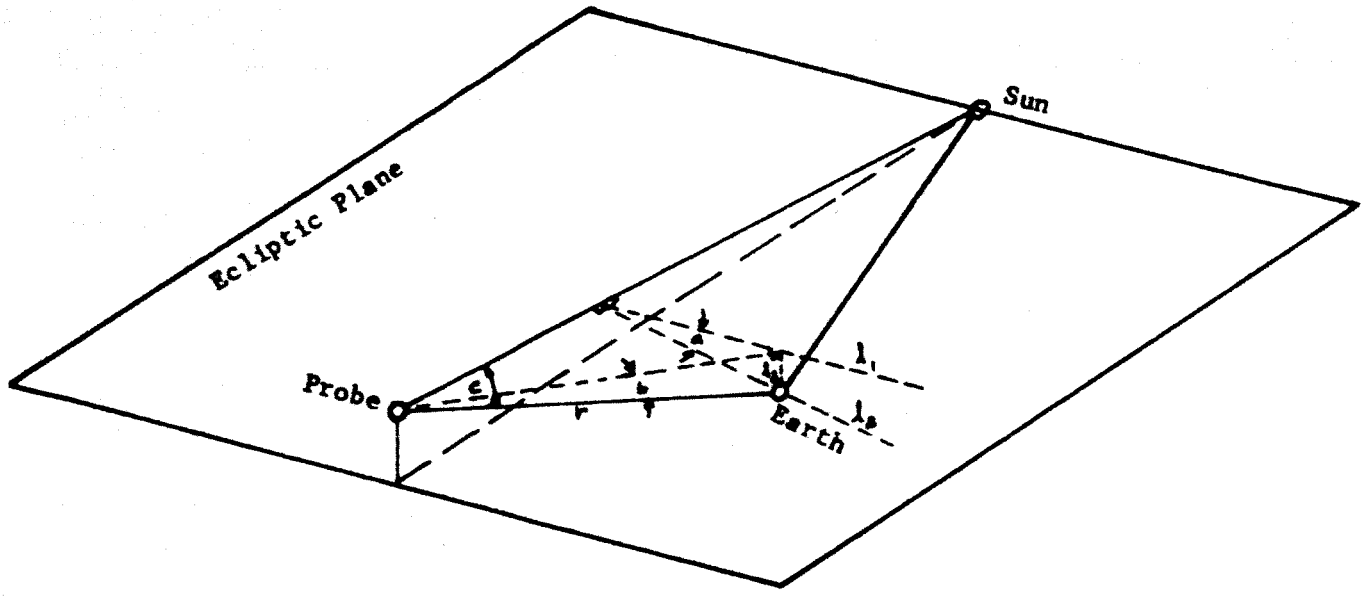

$$\ell_3 = \ell_2 \sin a = r \sin b$$

$$b = \sin^{-1}\left[\frac{\ell_2}{r} \sin a\right]$$

$$\ell_2 = r \sin (c)$$

Therefore $$b = \sin^{-1}\left[\sin c \sin a\right]$$

r = probe-Earth range

c = cone angle

FIG. 6-2. Angle b Derivation

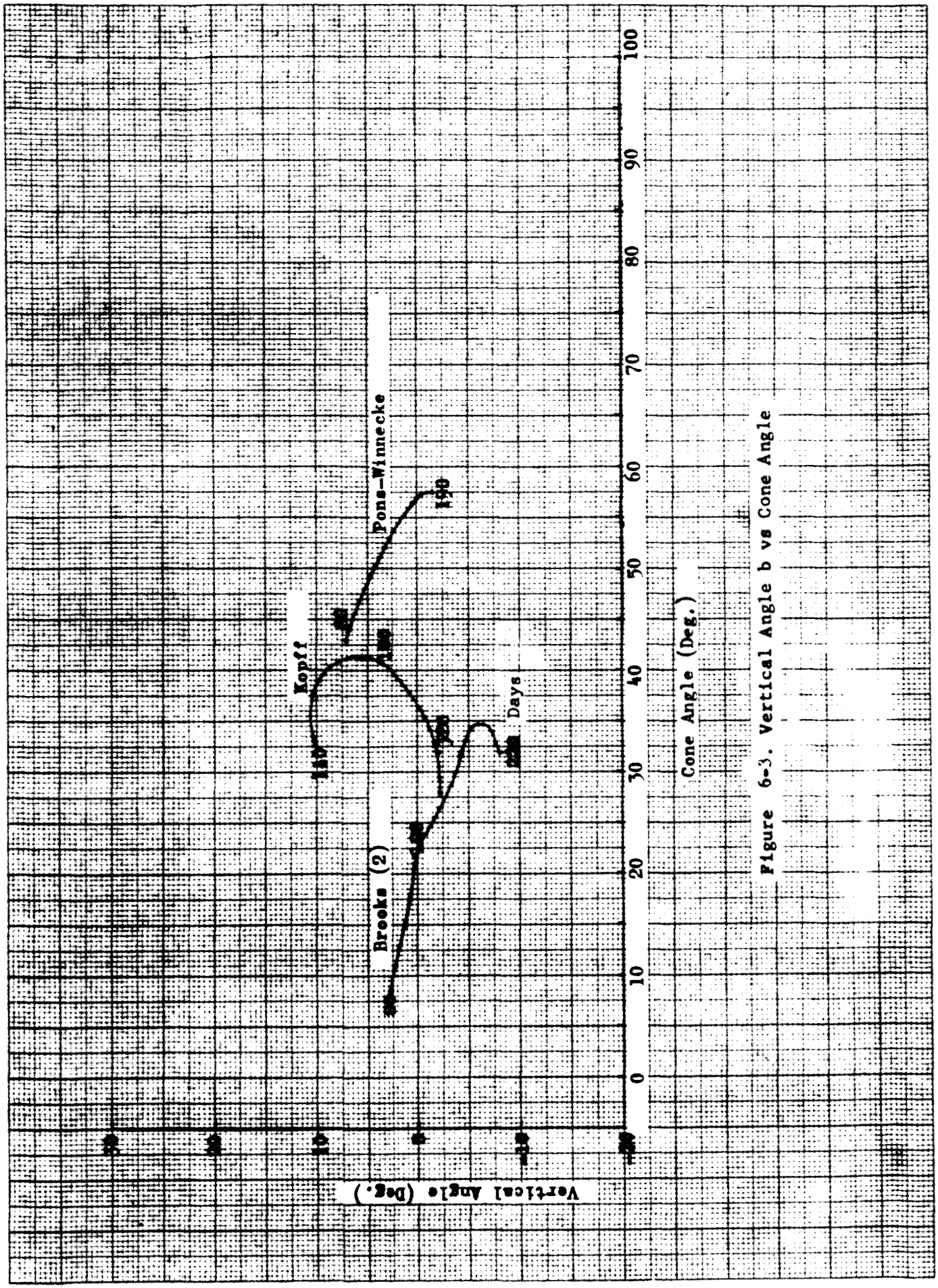

Figure 6-3. Vertical Angle b vs Cone Angle

6.5 MICROELECTRONICS AND PACKAGING

Assuming a minimum of modification is desired, the units used for the receiver, exciter, command detector, ranging module, power distribution system and telemetry subsystem building blocks are those of the Mariner. This, however, may not be the optimum system since it does not take advantage of micro-element components and the better packaging techniques now available. Whereas Mariner-C hardware is welded cordwood construction, the state-of-the-art in micro-element logic is such that all of the digital circuitry and a good portion of the analog circuitry can be converted to micro-elements presently on the market. A high percentage of the circuitry in the command detector can be digital. Only the filter circuitry, some amplifiers, and some of the chopper circuitry are not convertible immediately to off-the-shelf micro-element circuits. The savings in weight of the unit is estimated conservatively to be 35%, the cost of the detector will be cheaper and the intrinsic mean-time-to-failure of the unit will be improved.

It is recommended that only those analog circuits that can be implemented by present, well-proven techniques that provide reliability advantages should be attempted. Considering both the requirements of all the Command Detector circuits and the present state-of-the art, one would probably develop the following chart:

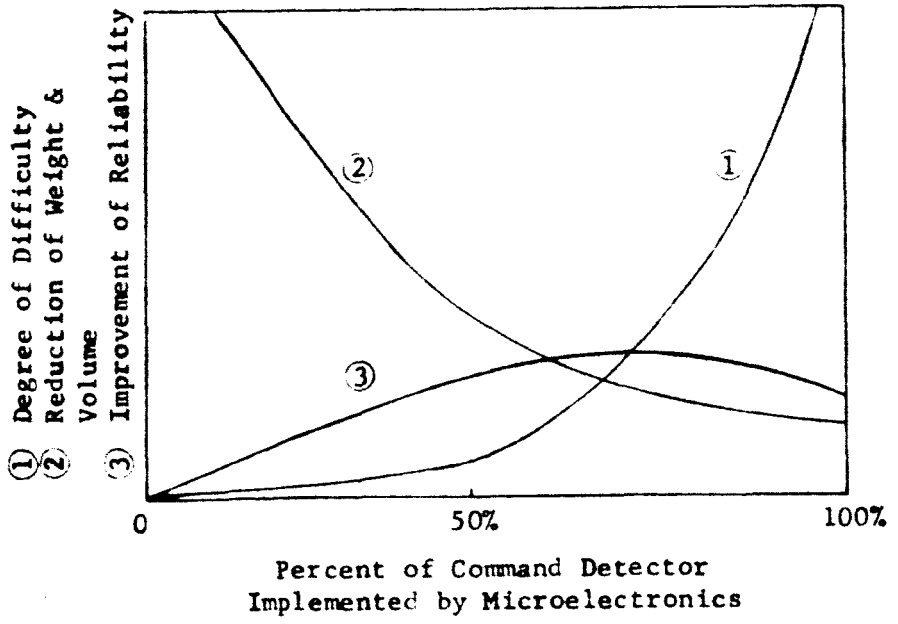

SECTION 7

POWER

7.1 OBJECTIVES

The parallel investigation of a photovoltaic and isotopic power subsystem has been carried out. A detailed conceptual design for each approach has been completed and weight, dimensional, and power trade-offs obtained as a function of comet mission. Finally, a comparison is made between the two approaches and recommendations advanced for the most desirable Comet Probe System.

7.2 PHOTOVOLTAIC SUBSYSTEM

Components for the photovoltaic power subsystem have been selected on the basis of the current state-of-the-art utilizing test evaluations and flight data. Hence, the power output figures represent readily obtainable performance, which can be upgraded by incorporating future solar-cell panel developments. Experience gained on the MACS programs, which aims at 1967-1970 flights, has been utilized. Four rectangular or trapezoidal panels with N/P silicon solar cells having 10% conversion efficiency installed over 85% of the frontal panel area have been considered for missions to six comets of interest. The design is based on a minimum-power output from the conditioning equipment of 200 watts at 28 volts after the panels have experienced a giant solar flare. The design points are the sun-probe distances at intercept. Batteries supply power during prelaunch, launch, solar panel deployment, peak loads, acquisition and maneuver. Power is augmented during peak power loads and maneuvering by a secondary silver-zinc battery system which is continuously recharged by the solar panels. The initial battery charge will supply power from prelaunch checkout to solar panel deployment.

Solar cells are installed with multi-layer transmission filters deposited on cover slides that are bonded directly to the cell surface by a transparent adhesive. A multi-layer interference filter is vacuum-deposited on the inner surface of the cover glass and an anti-reflective coating deposited on the outer surface, i.e. exposed surface. A transmission cut-on wavelength of 435 milli-microns is recommended for this filter. This cut-on can provide better protection against transmission losses in the adhesive due to ultraviolet degradation, while paying a very small penalty in power for cutting off a small portion of the cell's spectral response.

The cover glass slides provide protection from particle radiation, increase the cells's spectral emittance, and afford micrometeoroid protection. An investigation conducted during Philco's MACS design effort indicates that fused silica suffers the least reduction in transmission after exposure to electrons, protons, and ultraviolet radiation. Mission-end power output of the panels is thus a function of cover-slide thickness. With a 30 to 60-mil thickness the solar cell system can survive one giant-solar flare. Panel sizing has been based on the current-voltage characteristic temperature dependence of a N/P silicon cell with a manufacturer's conversion efficiency rating of 10%. Perihelions of the comets of interest have been used as the design position for minimum power output. The most important panel sizing parameter is the solar-cell stack temperature from panel deployment to post-intercept. The solar panel temperature profile as a function of position with respect to the sun has been determined using two control-volume boundaries. The first considers the active solar cell surface, the uncovered frontal thermal surface, and the conductive panel substrate up to, but not including, the rear panel thermal control surface.

The power loading requirements during various flight phases for 10, 25, and 50 watt power amplifiers are detailed in Table 7-1.

TABLE 7-1 Power Load Requirements

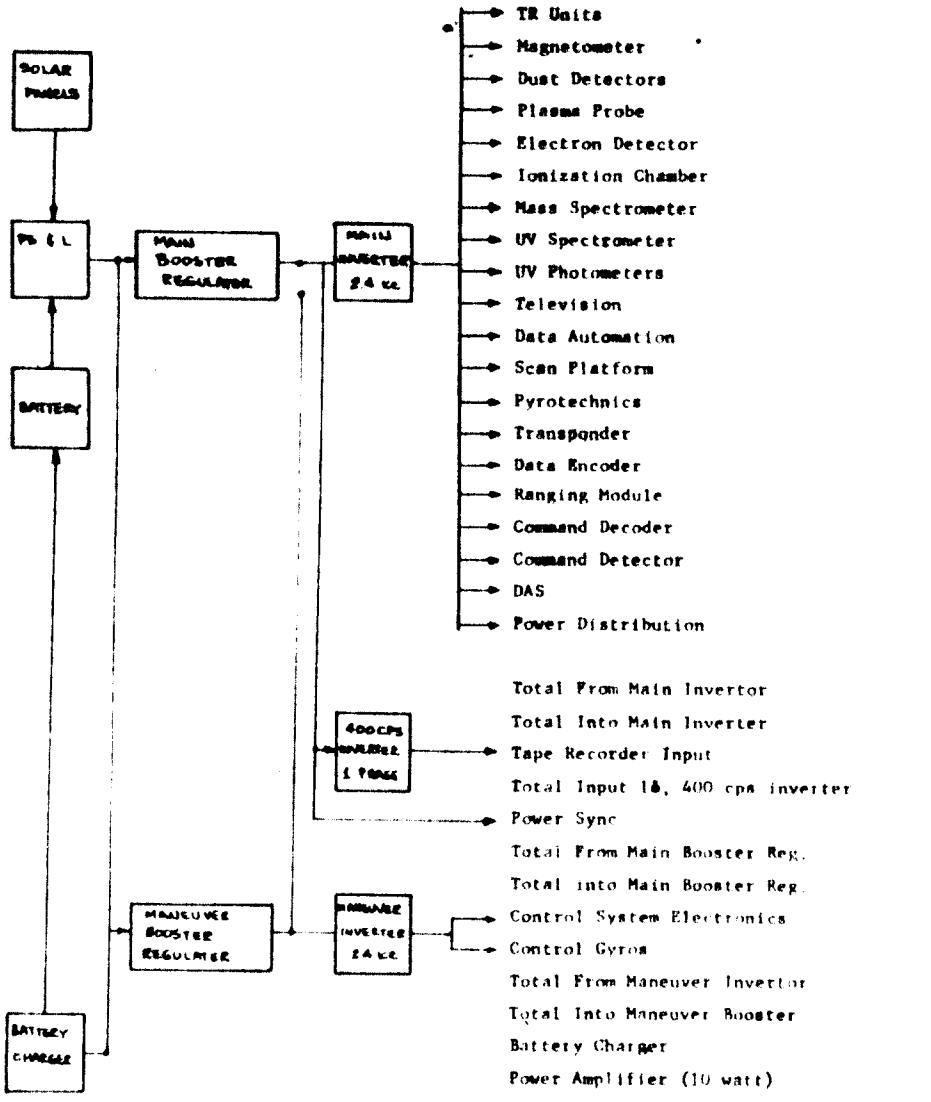

	PRE-LAUNCH	LAUNCH	ACQUI-SITION	CRUISE	MANEUVER (TWICE)	EN-COUNTER	PLAY-BACK
TR Units	16	16	16	16	16	16	16
Magnetometer	7	7	7	7	7	7	-
Dust Detectors	0.2	0.2	0.2	0.2	0.2	0.2	-
Plasma Probe	3.5	3.5	3.5	3.5	3.5	3.5	-
Electron Detector	2.0	2.0	2.0	2.0	2.0	2.0	-
Ionization Chamber	0.5	0.5	0.5	0.5	0.5	0.5	-
Mass Spectrometer	-	-	-	-	-	8.0	-
UV Spectrometer	-	-	-	-	-	12.0	-
UV Photometers	-	-	-	-	-	3.0	-
Television	-	-	-	-	-	9.0	-
Data Automation	-	-	-	-	-	8.0	-
Scan Platform	2.1	2.1	2.1	2.1	2.1	3.0	-
Pyrotechnics							
Transponder	15	15	15	15	15	15	15
Data Encoder	15	15	15	15	15	15	15
Ranging Module	3	3	3	3	-	3	3
Command Decoder	3	3	3	3	3	3	3
Command Detector	2	2	2	2	2	2	2
DAS	3.5	3.5	3.5	3.5	3.5	3.5	3.5
Power Distribution	1.85	1.85	1.85	1.85	1.85	1.85	1.85
Total From Main Invertor	74.65	74.65	74.65	74.65	71.65	115.55	59.35
Total Into Main Inverter	83.50	83.50	83.50	83.50	80.20	129.22	68.90
Tape Recorder Input	-	-	-	-	-	7	6
Total Input 1Ø, 400 cps inverter	-	-	-	-	-	9.35	8.00
Power Sync	0.69	0.69	0.69	0.69	0.69	0.69	0.69
Total From Main Booster Reg.	84.19	84.19	84.19	84.19	80.79	139.26	77.59
Total into Main Booster Reg.	105.2	105.2	105.2	105.2	101.0	176.5	97.0
Control System Electronics	10.35	10.35	13.50	6.00	13.5	6.0	6.0
Control Gyros					54.0		
Total From Maneuver Invertor	10.35	10.35	13.50	6.0	67.5	6.0	6.0
Total Into Maneuver Booster	24.9	24.9	32.6	14.48	163.3	14.48	14.48
Battery Charger	4.40	4.40	4.40	20.20	-	-	-
Power Amplifier (10 watt)	-	28.5	28.5	28.5	28.5	28.5	23.5
Total From PS & L	134.5	163.0	170.7	168.35	264.4	219.48	140.
Total Demand on Solar Panels or Battery With 10-watt Amplifier	138.2	168.0	176.0	173.8	303.5	226.2	144.3

TABLE 7-1 Power Load Requirements
(Continued)

	PRELAUNCH	LAUNCH	ACQUISITION	CRUISE	MANUEVER	ENCOUNTER	PLAYBACK
Total Demand on Solar Panels or Battery With 10-watt Amplifier	138.7	168.0	176.0	173.8	303.5	226.2	144.3
Additional Power Required for 25-watt Output Amplifier	-	46.5	46.5	46.5	46.5	46.5	46.5
Total Demand on Solar Panels or Battery With 25-watt Amplifier	138.7	214.5	222.5	220.3	350.0	272.7	190.8
Additonal Power Required for 50-watt Output Amplifier	-	75	75	75	75	75	75
Total Demand On Solar Panels or Battery for Spacecraft With 50-watt Amplifier	138.7	289.5	297.8	295.3	425.0	347.2	265.8

Figure 7-1 shows solar panel temperatures and power output per unit area (corrected for non-ideal thermal conductions) as a function of heliocentric distance. Table 7-2 presents solar panel size and weight for 200-watt minimum output for 30 and 30 mil cover-glass thickness for four comet probe missions. Figure 7-2 and 7-3 show in detail, respectively, total panel area, power and cover-glass thickness; and total panel weight and temperature versus heliocentric distance between 0.9 and 2.0 A.U.

7.3 ISOTOPIC POWER SUBSYSTEM

The design and integration of a radioactive thermoelectric generation (RTG) into an instrumented scientific probe vehicle is accomplished in three parts:

1. Design of the RTG unit
2. Determination of radiation sensitivity of instrumentation
3. Design and compatible placement of required instrument shielding.

The generator is shown in Figure 7-4 and is an all-brazed assembly in which GeSi thermoelements are metallurgically joined directly to the isotope capsule and outer-casing cold junction. The case and four radiator fins are made either of HM21A magnesium-thorium alloy or of beryllium. The outer diameter of a PuO_2 RTG producing 200 electrical watts is 6.7 inches, with each of the rectangular cross section fins extending 16 inches; thus they extend approximately one inch beyond the height of the RTG cylinder on top and bottom. There is clearance in the centaur shroud for fins up to 24 inches in length.

The output from the thermoelements, which are connected in series and parallel for optimum voltage-current characteristics, is fed into a power conditioning unit. The load can be varied from no-load to full-

Fig. 7-1 Solar Panel Temperature and Power Corrected for Non-Ideal Thermal Conduction

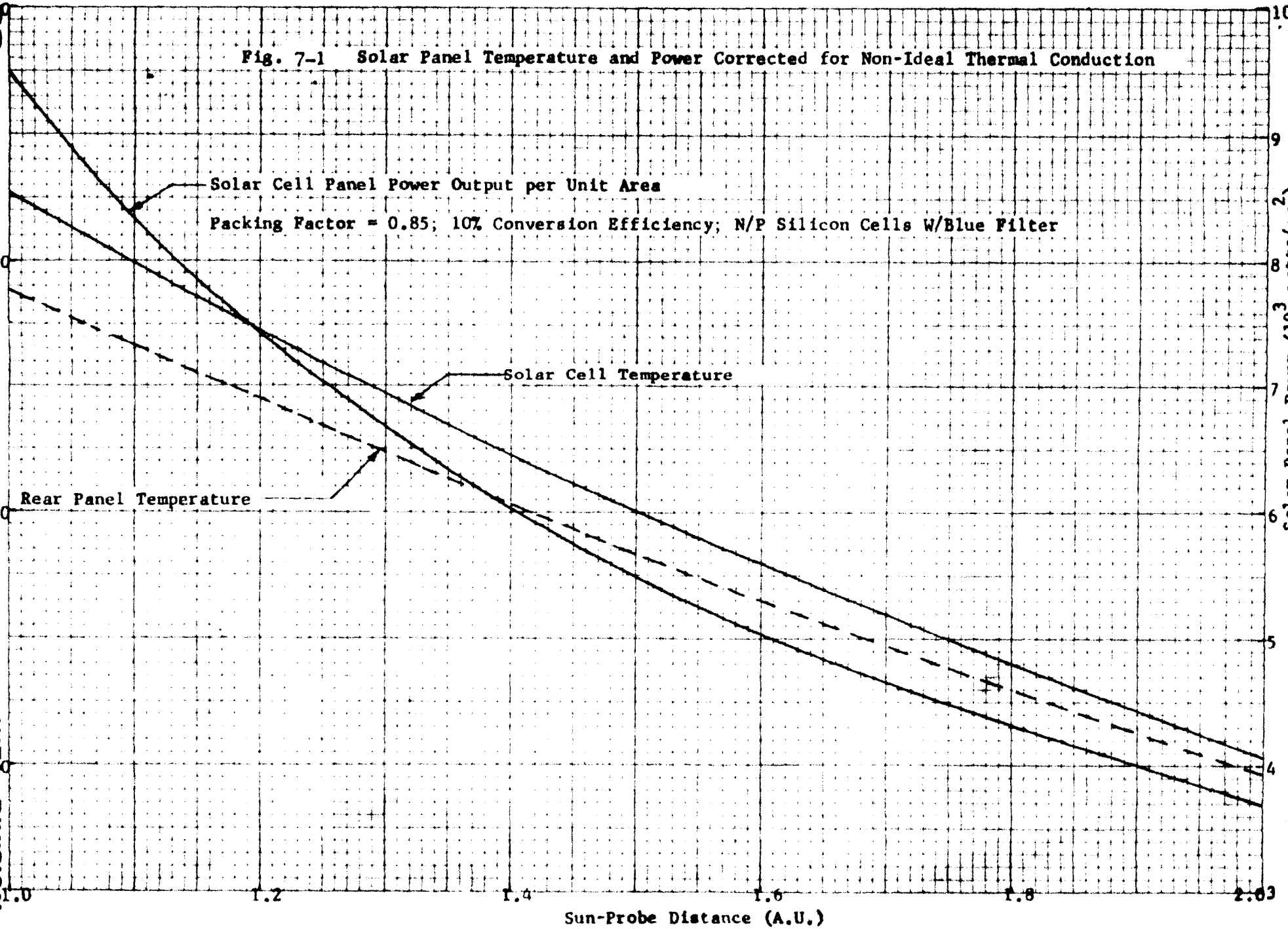

TABLE 7-2

SOLAR PANEL SIZING FOR 200-WATT MINIMUM OUTPUT FROM POWER CONDITIONING EQUIPMENT

Comet	Maximum Encounter Distance (AU)**	Cover Glass Thickness (mils)	Temp. ^{o}K	P/A 10^3 watts/cm^2	Total Panel Area* (ft^2)	Total Panel Weight (lbs)
Brooks (2)	1.80	30 60	220	4.29	90.6 80.4	113.2
Pons-Winnecke	1.26	30 60	278	6.96	54.9 49.2	68.6 78.3
Tempel (2)	1.36	30 60	266	6.60	57.9 51.9	72.3 82.6
Kopff	1.57	30 60	243	5.19	74.3 66.0	92.9 105.0

* Packing Factor = 0.85

**Heliocentric

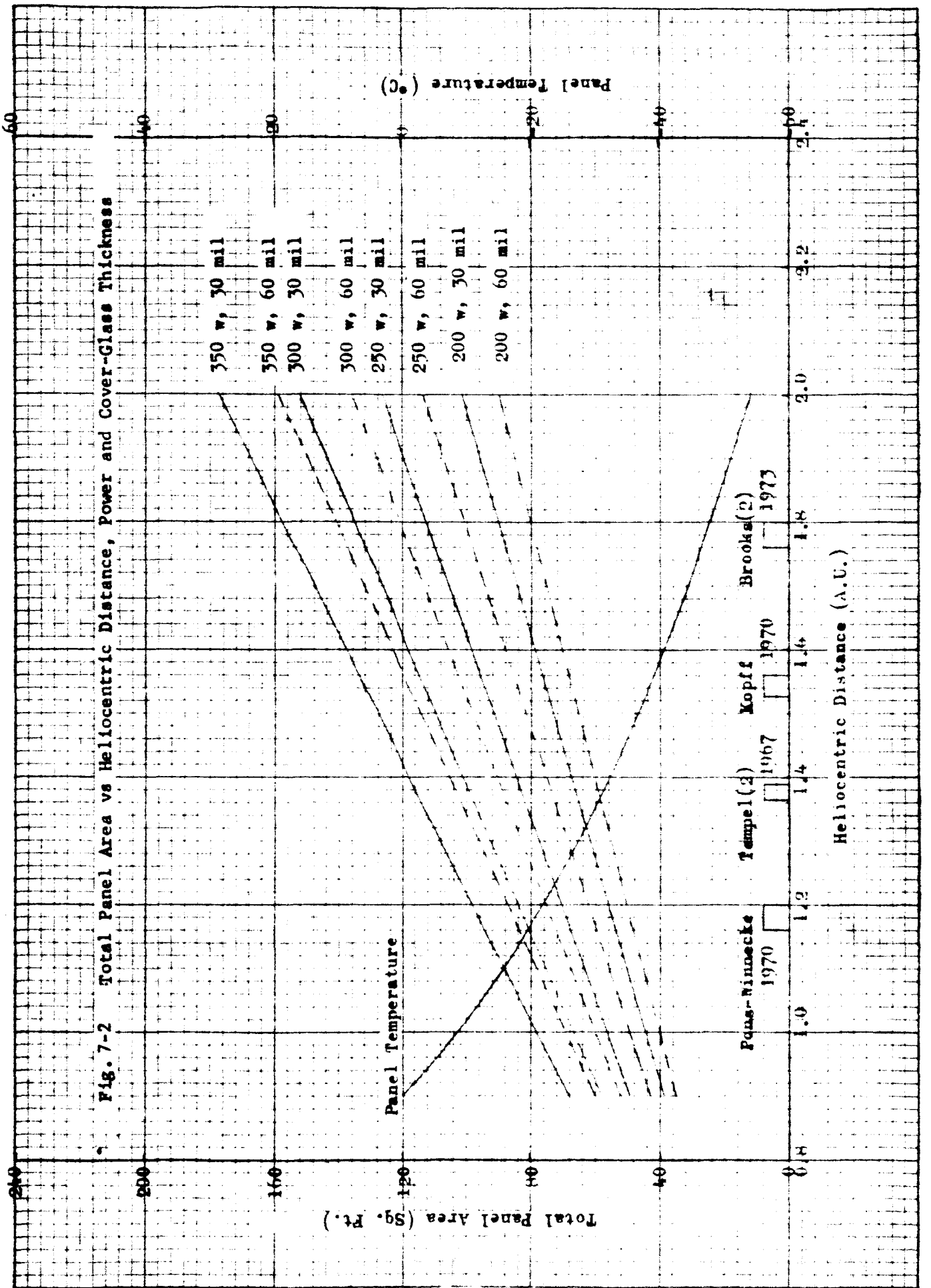

Fig. 7-2 Total Panel Area vs Heliocentric Distance, Power and Cover-Glass Thickness

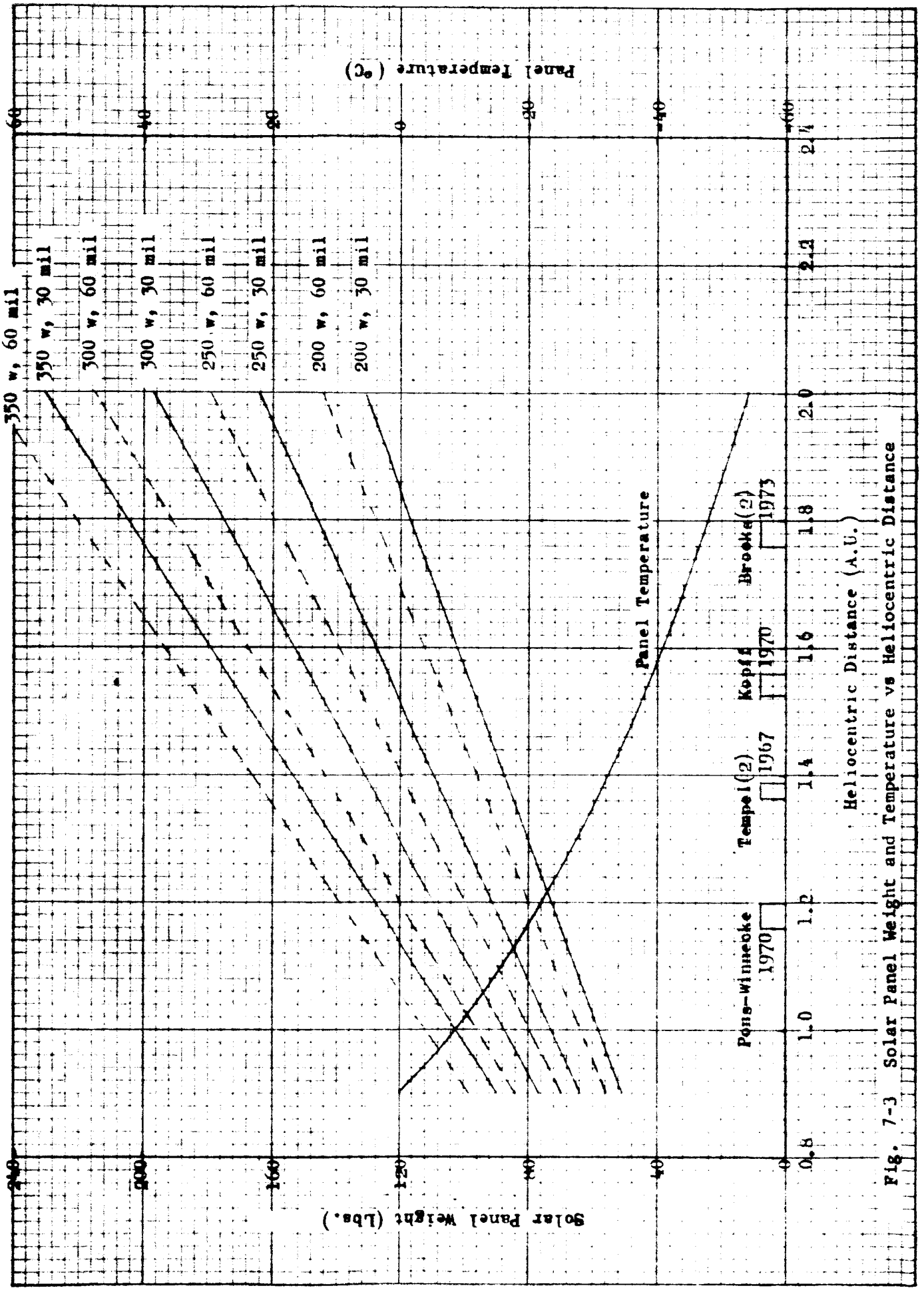

Fig. 7-3 Solar Panel Weight and Temperature vs Heliocentric Distance

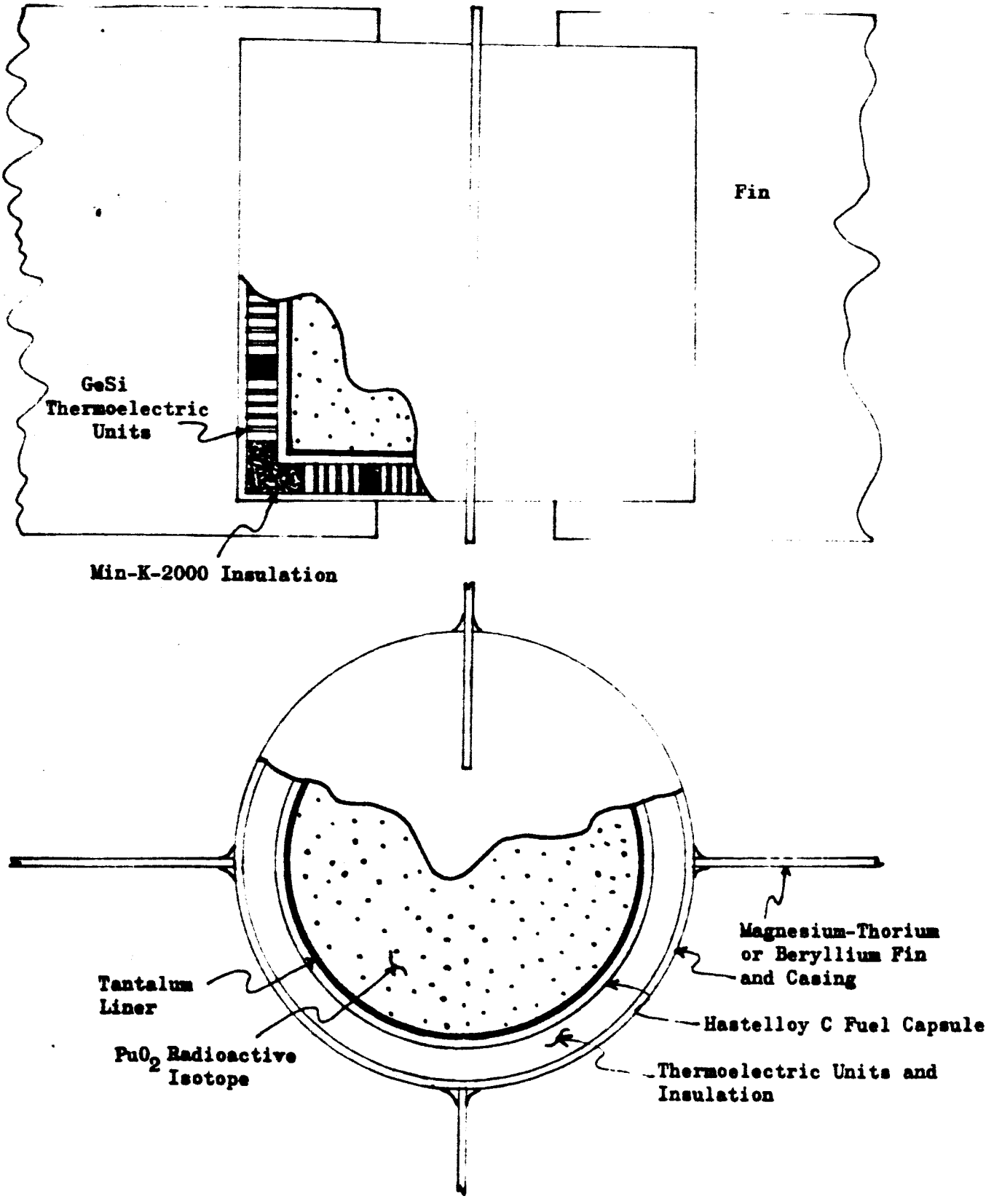

Fig. 7-4 Radioisotope Thermoelectric Generator

load as required, without regard to damaging the generator.

For a PuO_2 system, Figure 7-5 shows weight vs thermal power output for isotope, isotope cladding, thermoelectric modules, generator casing, fins, and miscellaneous construction materials. Thermal power output is converted to electrical power by multiplying it by the overall conversion efficiency of the generator, which is a variable in time between now (3%) and 1975 (10%). Figure 7-6 is a projection of RTG technology and shows power-to-weight ratios as a function of year of flight. Martin Company estimates that RTG systems generating 5 electrical watts per pound will be feasible by 1975.

A compound of plutonium for the isotopic heat source is ideal from the standpoint of radiation hazards and will require no additional shielding to protect personnel. Extremely sensitive instruments may, however, require shielding to reduce radiation-induced noise. Plutonium will be an expensive isotope to use in RTG units until wider use of nuclear reactor energy sources comes into being throughout the world. A comparison of 1968 costs, weight, and lead shielding required to provide similar gamma doses for a 200 watt system has been made for WDL by Battelle; and is tabulated below:

ISOTOPE	WEIGHT (lb)	SHIELDING (cm of lead)	COST (1968)
Pu-238 PuN	20	0	$3,600,000
Pm-147 Pm_2O_3	40	4.6	$ 465,000
Cm-244 Cm_2O_3	3.8	9.5	$1,570,000

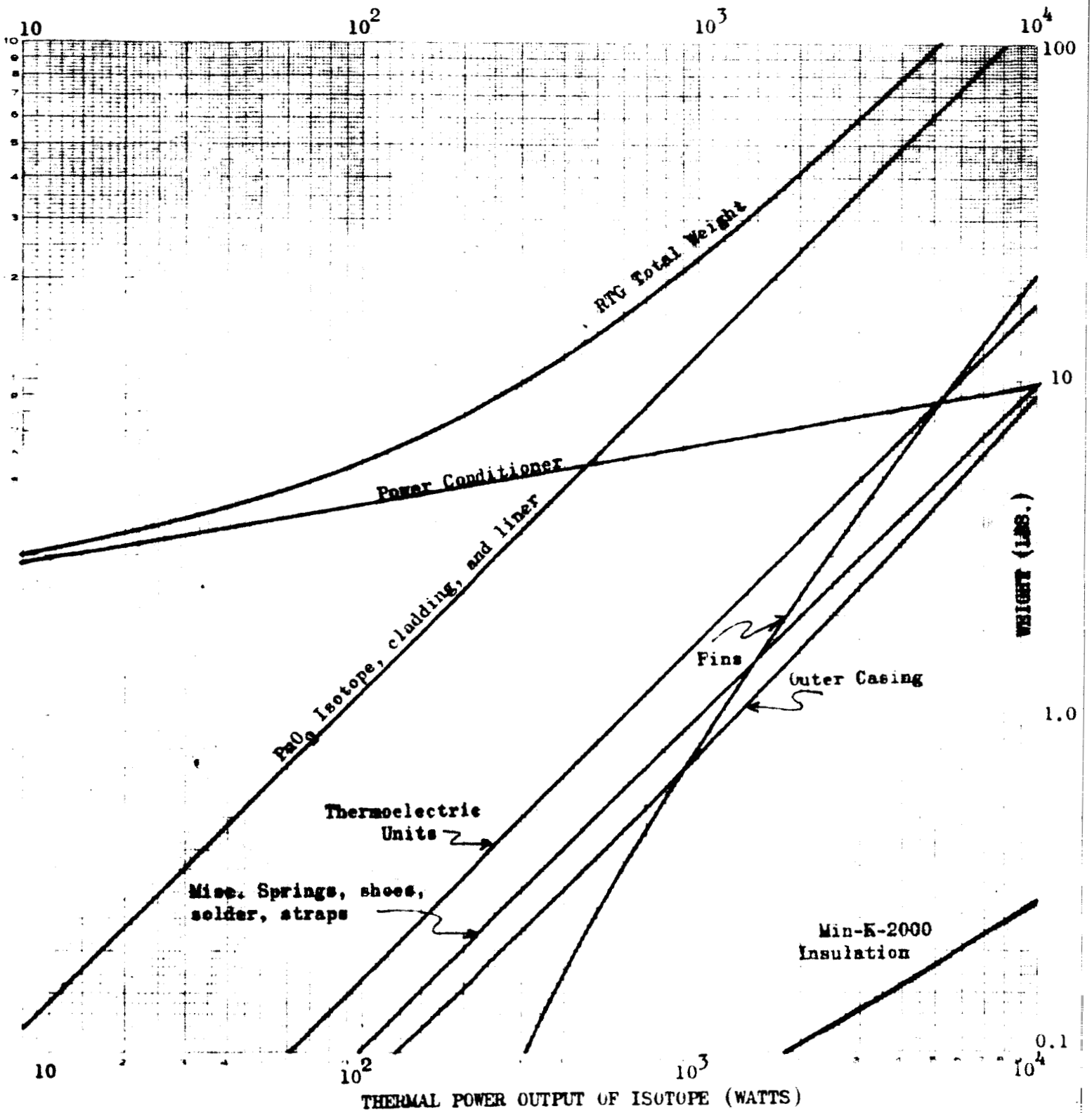

Fig. 7-5 Component Weight of RTG as a Function of Power

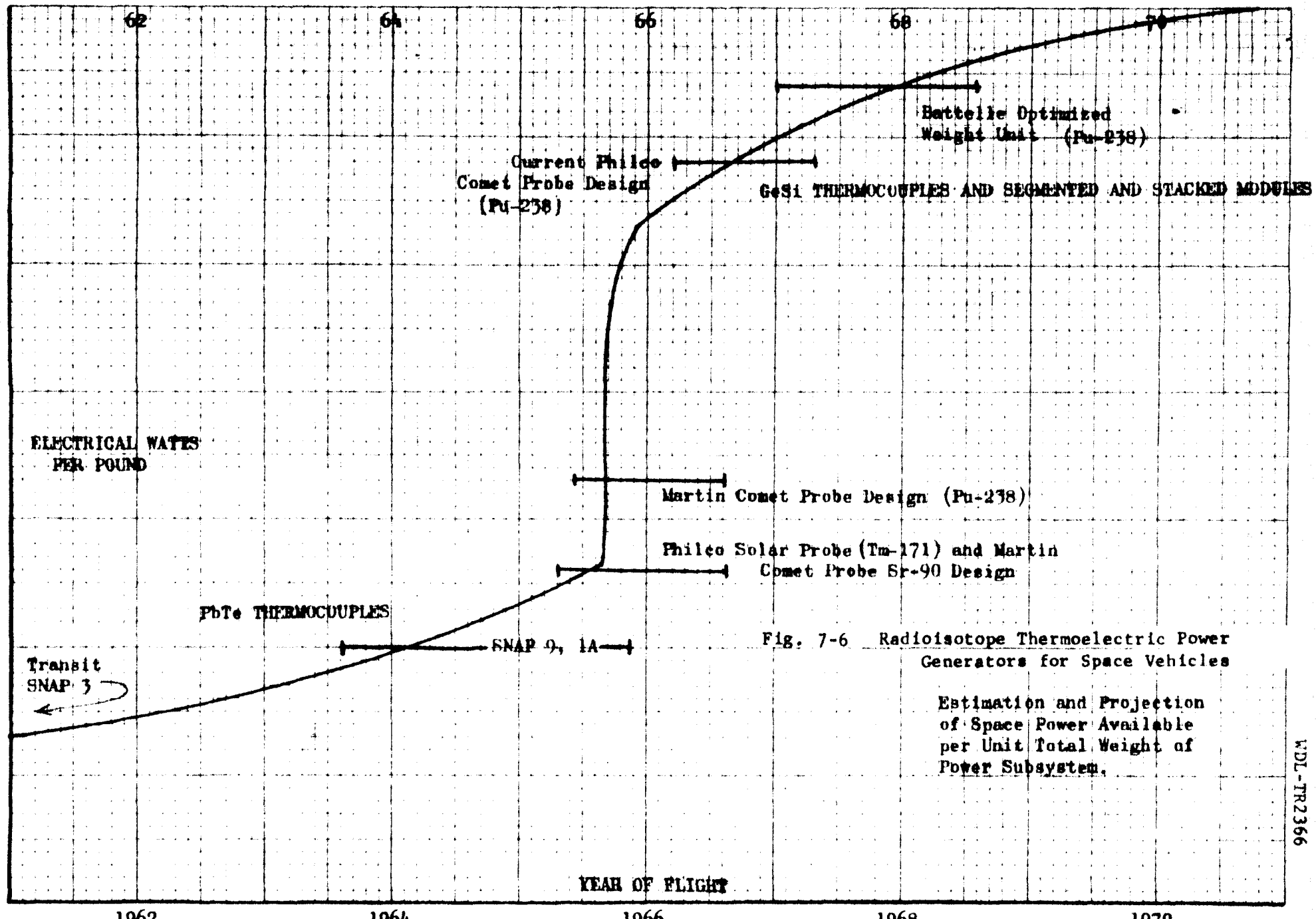

Fig. 7-6 Radioisotope Thermoelectric Power Generators for Space Vehicles

Estimation and Projection of Space Power Available per Unit Total Weight of Power Subsystem.

7.4 OPTIMUM SHIELDING CONFIGURATIONS

A study to advance the state-of-the-art in shielding techniques forms the bulk of effort. A mathematical analysis employing the calculus of variations has produced a technique to determine the minimum-weight shape and location for a radiation shadow shield. This approach is outlined in Table 7-3.

Figure 7-7 shows the change in minimum-weight shadow shields as a function of position. The optimum position has been determined to be located at the intersection of the diagonal rays. Figure 7-8 is a plot of the optimum solutions compared to conventional slab shielding for a material with and without the broad gamma beam "build-up factor".

By "rotating" the two-dimensional solutions reached in this report, it has been shown that a conventional slab shield is more than 41% heavier than the weight optimized shield.

The determination of instrument sensitivity to radiation has not been made. It was hoped to include experimental data on this subject from an external source; the promised data has not yet reached Philco.

7.5 PHOTOVOLTAIC-ISOTOPIC COMPARISON

The physical characteristics and performance capabilities of the photovoltaic and isotpic configurations are tabulated and compared in Table 7-4. On the basis of this comparison between the performance of photovoltaic and isotpic power subsystems on a comet probe requiring 200 watts or more photovoltaic panels are recommended for flights to comets out to heliocentric distances of about 7.6 A.U. Photovoltaic panels are large but nevertheless desirable because of proven technology at a 200-watt power level. For higher power (e.g., 300 watts), RTG units are recommended.

Table 7-3

RADIATION SHIELDING

MATHEMATICAL OPTIMIZATION TECHNIQUE

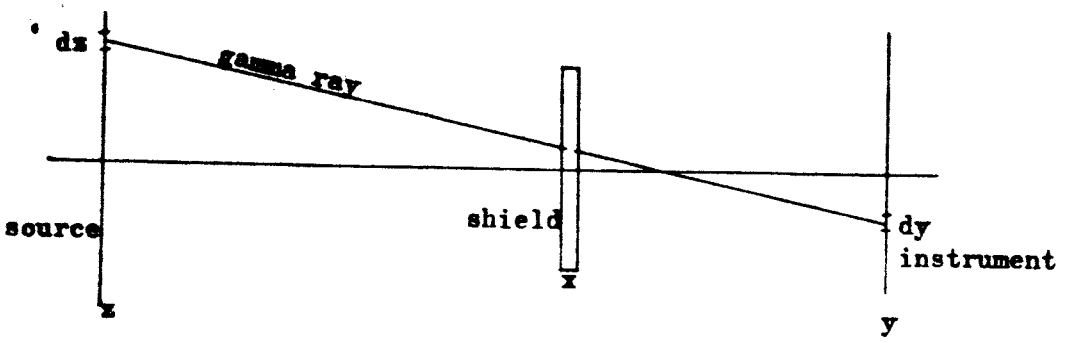

1. Shield Weight $W = \int \rho t \, dx$

2. Dose $D = \iint S \, B(t) \frac{e^{-\alpha t}}{r^2} \, dz \, dy$

3. Transformation: $D = \int f(x, t) \, dx$

4. Combine with LaGrange Multiplier Appr. to Variational Approach: $I = W + \lambda D = \int \left[\rho t + \lambda f \right] dx$

5. Take First Variation: $\delta I = \frac{\partial}{\partial t} \left[\rho t + \lambda f \right] = 0$

6. Solve for Thickness: $t = t(x)$

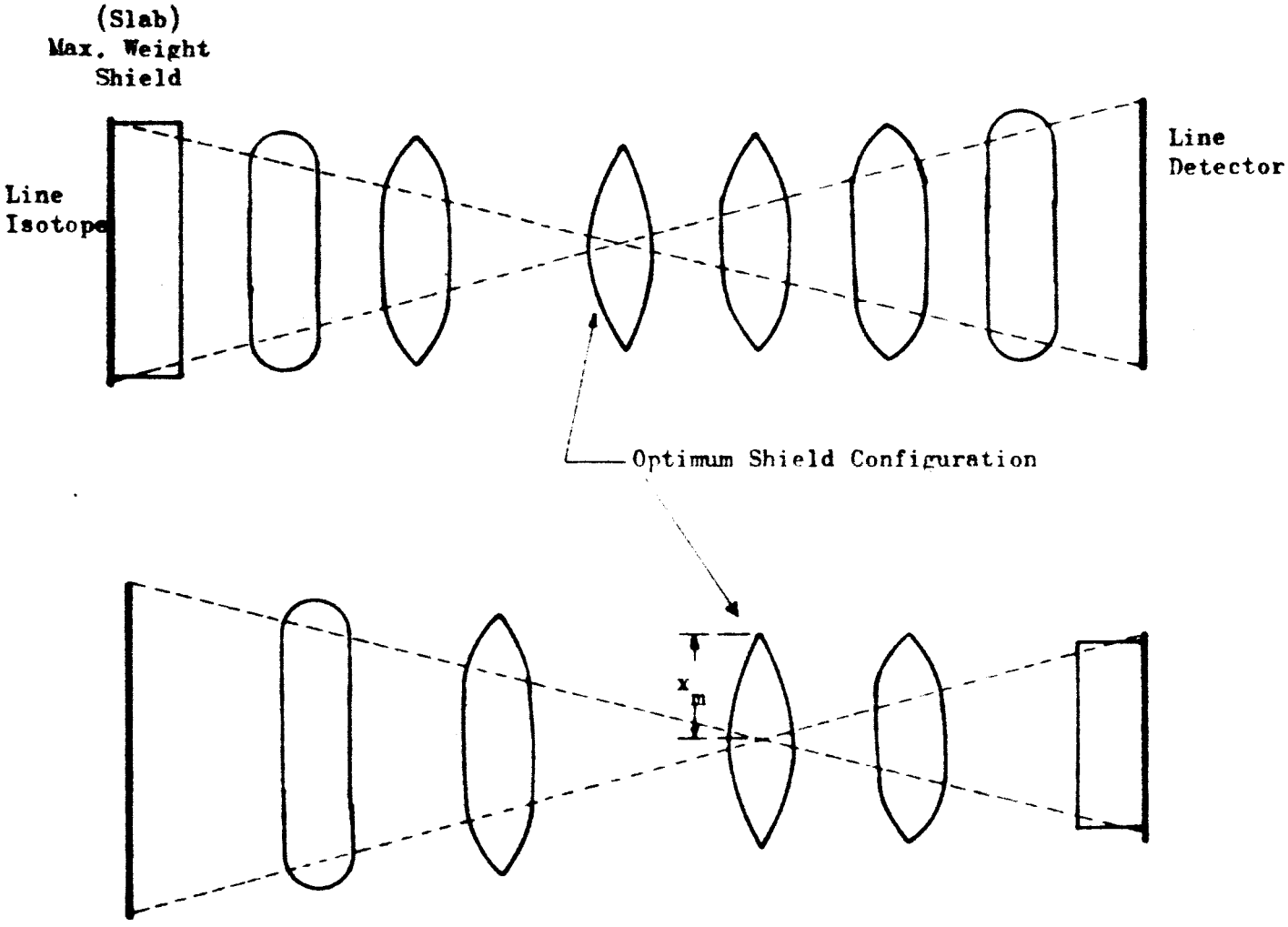

Fig. 7-7 **MINIMUM WEIGHT SHIELDS AS A FUNCTION OF POSITION**

The portion of the shield between the diagonal rays is a straight slab. Beyond this region, a logarithmic taper occurs to a maximum extent, x_m, which is a function of dose.

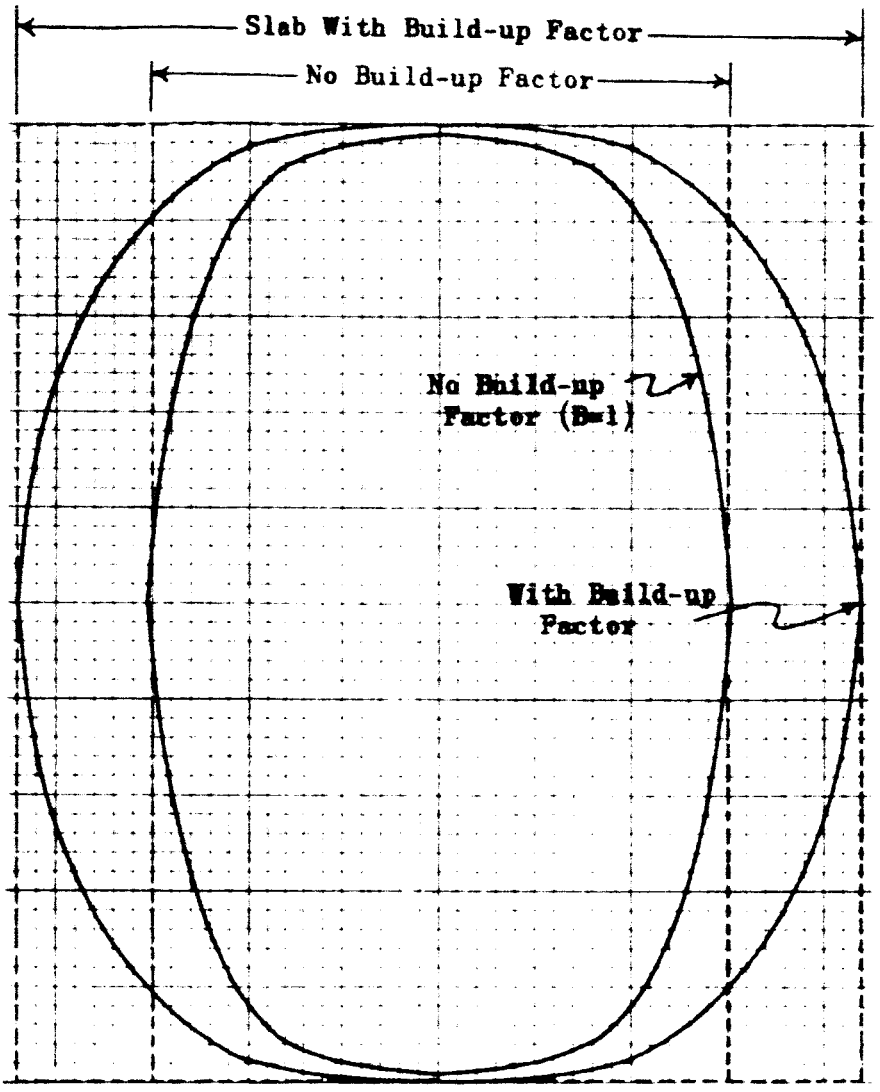

Fig. 7-8 COMPARISON OF OPTIMUM SHIELDS CALCULATED WITH AND WITHOUT BUILD-UP FACTORS

Both figures are located at the intersection of the diagonal rays. The outer shield uses the build-up factor for aluminum with 1.25 Mev gamma rays. Conventional slab shielding for both cases is indicated by the dotted line.

Table 7-4 Comparison of Photovoltaic and Isotopic Power Subsystems (200 watts)

PARAMETERS	PHOTOVOLTAIC*	ISOTOPIC
Specific Weight	1.68 - 1.24 watts (e)/lb	1.8 watts (e)/lb
Weight - Pons-Winnecke - Brooks (2)	119 lbs 162 lbs	110 lbs 110 lbs
Shroud - Pons-Winnecke - Brooks (2)	R&D envelope Surveyor envelope	R&D envelope R&D envelope
Reliability	Simple, static system Flight proven assemblies	Static system Not yet flight proven
Component Availability	Off-the-shelf components	Developmental stage
Dust Erosion	Small power degradation	No effect
Solar Flare Effects	Degrades power; can be minimized by cover glass**	No degradation
Hazards	No special ground handling No abort precautions necessary No shielding of S/C components	RTG must be cooled on the pad Abort casing required Shielding of S/C may be necessary depending on isotope***
Mission Adaptability	Panel varies with mission	Size independent of sun distance
Growth Potential	Small increase in efficiency Moderate decrease in cost	Increase in specific weight to 5 w/lb projected for 1975

* Does not include batteries
** A 30-mil cover-glass thickness is assumed in the specific weight value
*** For Plutonium-238 minimum shielding is required

SECTION 8

THERMAL CONTROL

8.1 THERMAL SHIELD

Since the distance between the spacecraft and sun changes for the missions under investigation, the variation of solar heating, as indicated in Figure 8-1, imposes the most severe condition on the temperature control subsystem. This condition is minimized by orienting a spacecraft axis at the sun and by applying a heat shield on the side that "sees" the sun. Instruments and components that require a closely controlled environment are located in a compartment protected by the shield.

Two spacecraft configurations have evolved from shroud constraints and the choices of power subsystems, i.e., solar panels and radioisotopes. The thermal control subsystem for each is illustrated in Figures 8-2 and 8-3. There is basically little difference between configurations with regard to thermal control design. It can be noted in both designs that surfaces that "see" the sun have, in most cases, coatings where the solar absorptance is equal to the emittance. This is a major constraint imposed on the thermal design to insure a design that can be thoroughly assessed by ground tests. This is directed at eliminating the problems associated with present-day solar simulation capabilities as compared with actual conditions.

8.2 INSULATION

Each design has a solar shield that combines the shading of the antenna with multiple-foil insulation. The isotopic configuration has an additional shield to reduce the energy interchange between isotope and equipment compartment. It also allows a low emissive coating on the insulation external surface, thereby increasing the protective capability of the insulation. The adequacy of these designs in preventing heat leakage into or out of the spacecraft is illustrated in Figure 8-4 and 8-5.

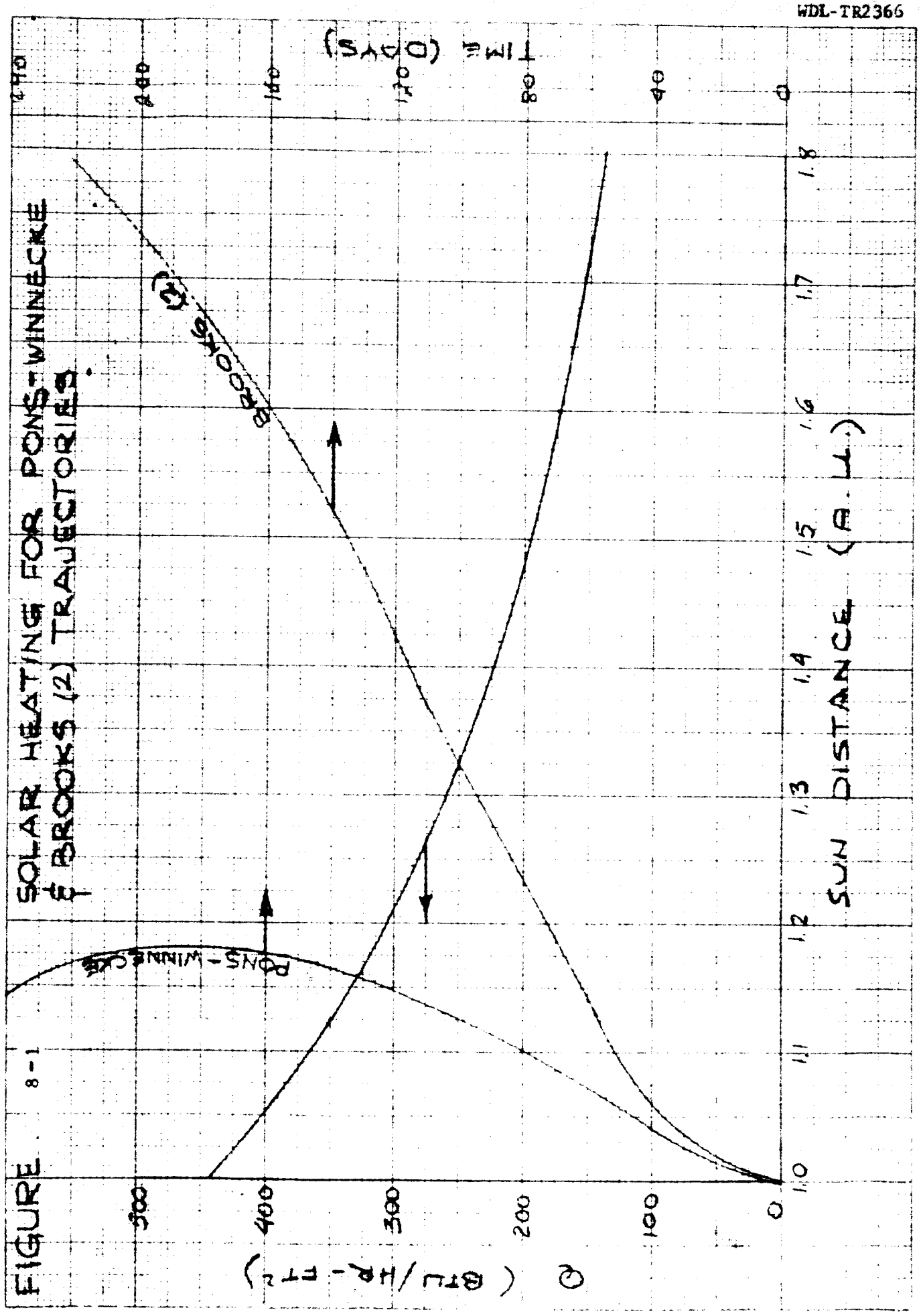
SOLAR HEATING FOR PONS-WINNECKE & BROOKS (2) TRAJECTORIES
PONS-WINNECKE
BROOKS (2)
TIME (DAYS)
Q (BTU/HR-FT²)
SUN DISTANCE (A.U.)
480
440
400
360
320
280
240
200
160
120
80
40
0
300
400
300
200
100
0
1.0
1.1
1.2
1.3
1.4
1.5
1.6
1.7
1.8

FIGURE 8-1

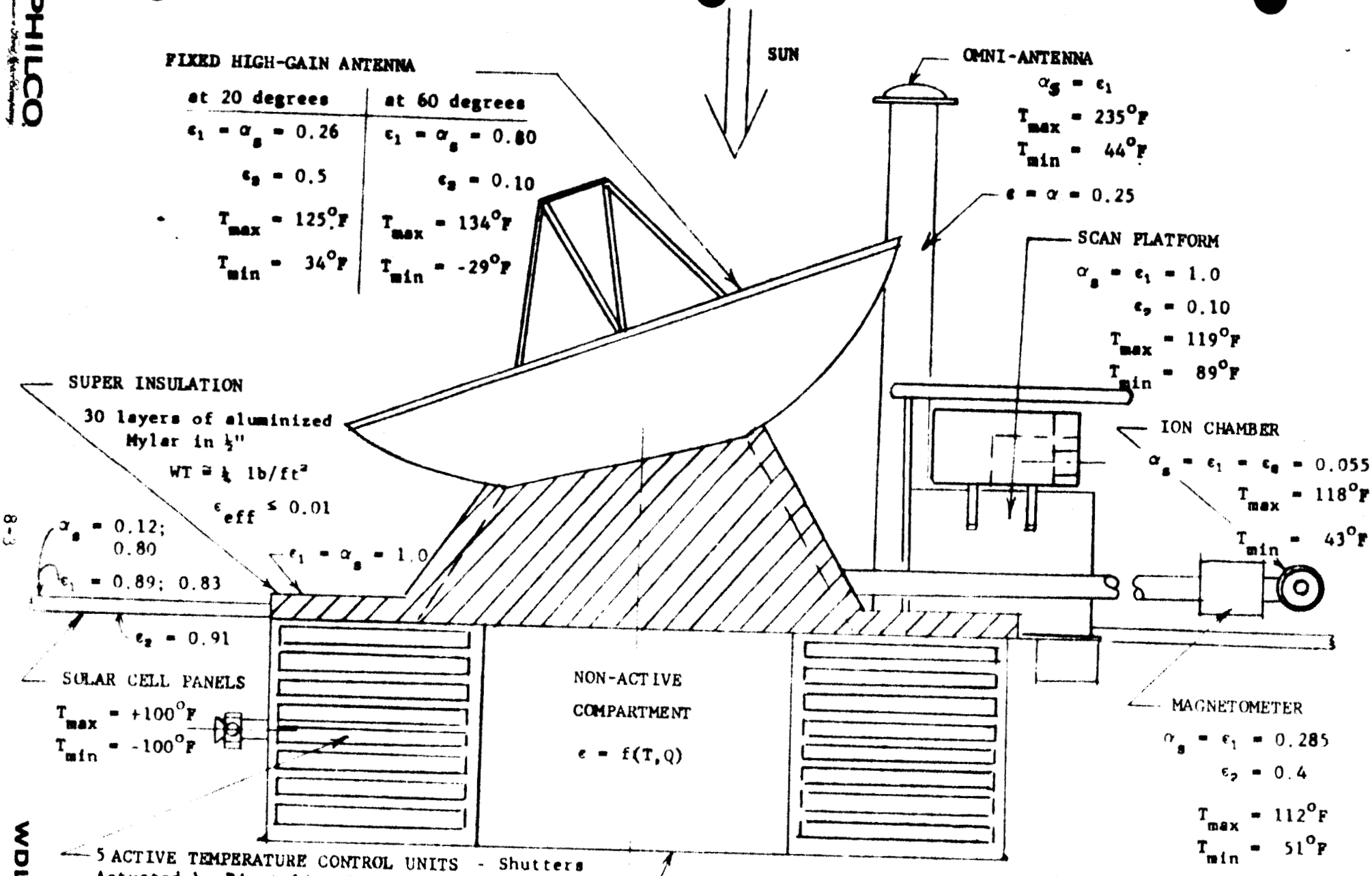

Fig. 8-2 Solar Panel Vehicle Thermal Design

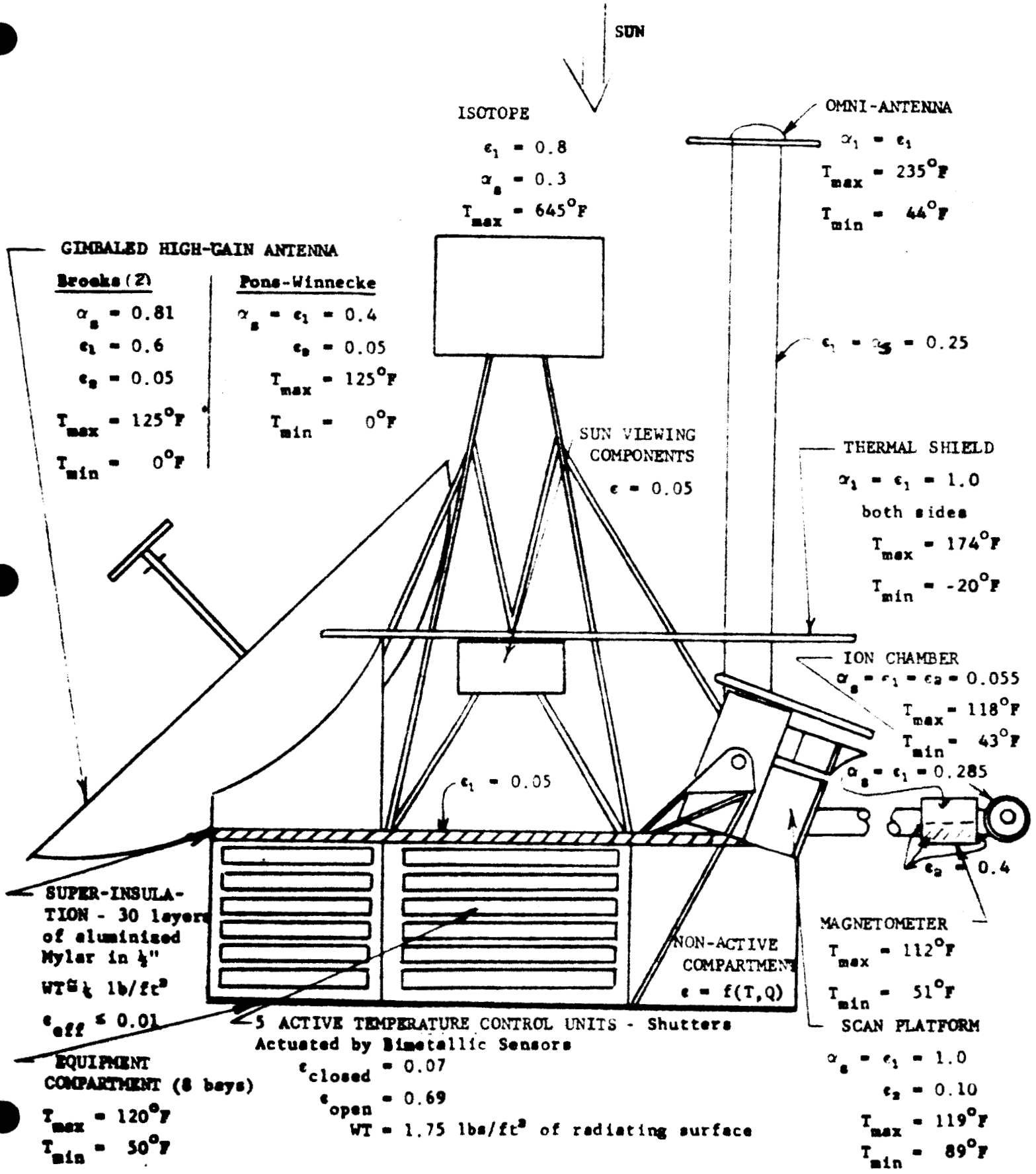

Fig. 8-3 Isotope Vehicle Thermal Design

Fig. 8-4 Comet Probe Insulation Effectiveness (Solar Panel Design)

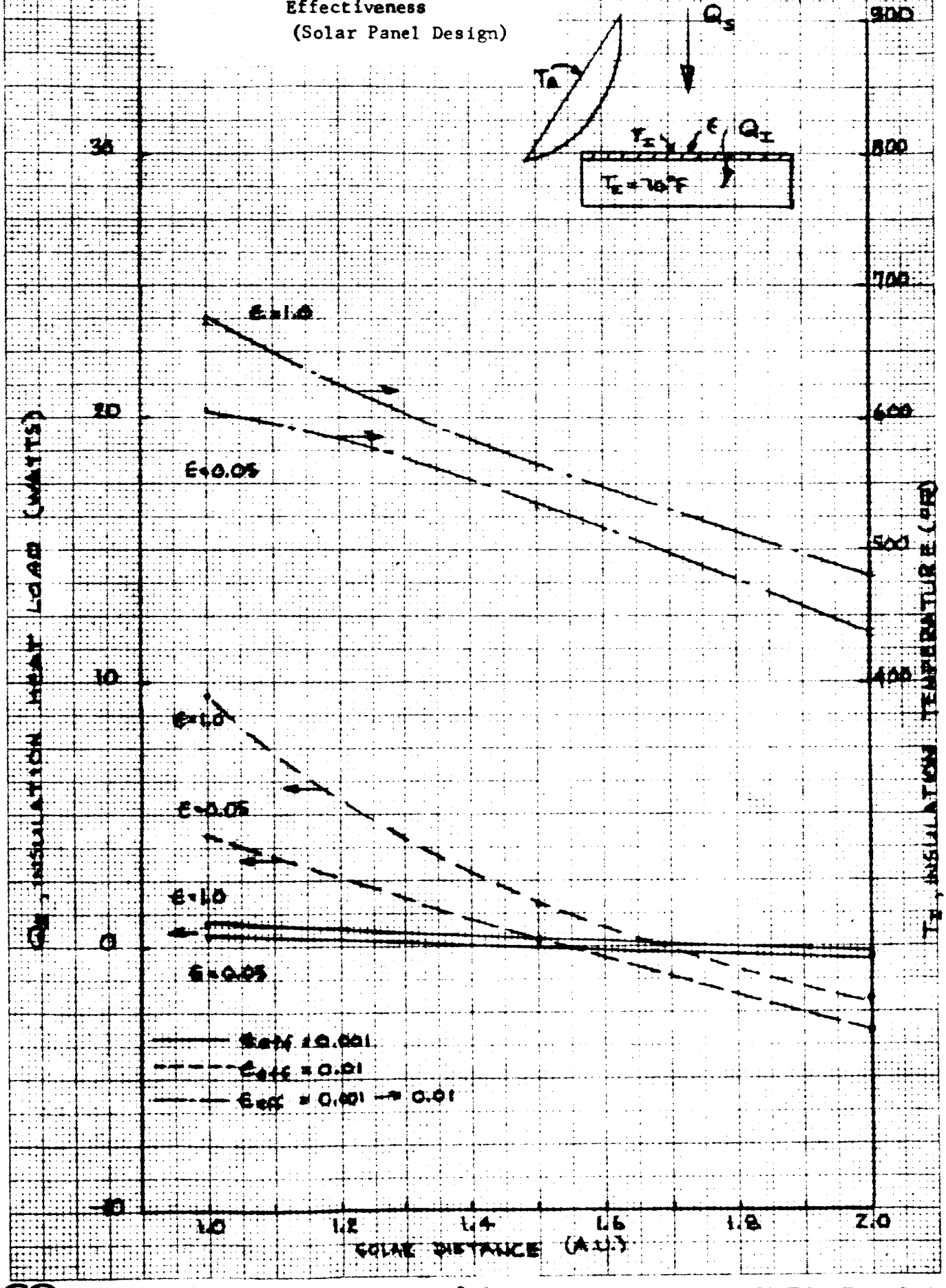

Fig. 8-5 Comet Probe Insulation Effectiveness with One Thermal Shield (Isotope Design)

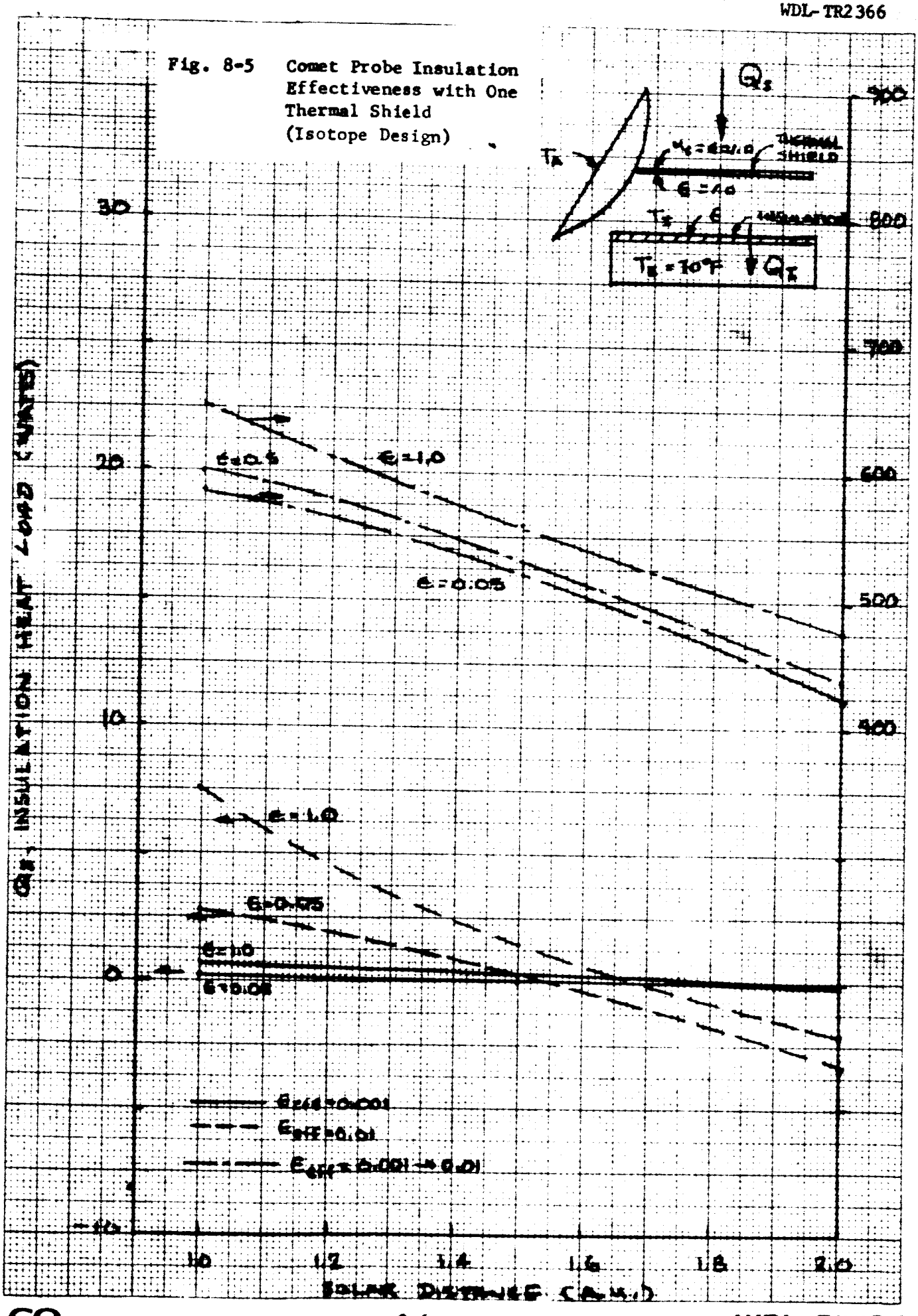

Insulation test results published by National Research Corporation [1959], General Electric [Casagrande, 1962], and Philco WDL [1963] indicate that an overall effective emissivity of 0.01 is very conservative, particularly where the fasterner and edge area is much less than the covered area. Assuming this effective emissivity, an equipment compartment temperature of 70°F (530°R) and an external insulation emissivity (aborptivity) of unity the heat input at 1 A.U. is +9.6 watts for the solar panel design. This results in a heat leak at 2 A.U. of only -1.9 watts which is well within the allowable limit of -30 watts.

The isotopic design has a heat input into the spacecraft from the sun of only +3.0 watts, assuming the shield has an absorptivity (emissivity) of 1.0 and the insulation external emissivity is 0.05. Again the effective emissivity is taken at 0.01. The insulation design recommended for the heat shield consists of 30 layers of crinkled aluminized mylar stacked to a height of 1/2 inch. The external surface material is a heat-conductor to dissipate the heat absorbed from the sun by the shield and/or antenna, over the complete insulation area and, thereby, prevent local hot spots. This material, perhaps aluminum for its low emissive characteristic, could also support a coating if required. The insulation is attached with a minimum of fasteners, preferably ceramic-type bolts, and properly overlapped to prevent edge losses. The total shield weight for the solar panel design is less than 4 lbs. while the isotpic design is less than 8 lbs.

8.3 ACTIVE CONTROL

With the effect of the external environment negated, equipment temperature control is then maintained by judiciously using thermal control surfaces in conjunction with internal heat generation. The radiating surface area of the equipment compartment on the remaining sides of the spacecraft that "see" only cold space in both designs are sufficient to dissipate the expected peak load of 375 watts. Due to the cycling of equipment during the mission, active temperature control in the form of moveable shutters is used. The design employed on the Mariner-C has sufficient performance to be applicable here. The number of active units can be minimized by carefully locating

the components. A compartment whose heat dissipation during the mission is fairly constant due to the cycling on of units when others are off can utilize the more reliable and less weighty passive technique for control. Active control can not be totally eliminated but can be optimized as the equipment and their heat-dissipation cycles become better known during a detailed design. The present design utilizes 5 active units at a total weight of less than 21 lbs. based on a unit weight of 1.75 lbs/ft^2 of radiating area.

The equipment is mounted directly to the radiating surface to minimize internal heat conduction and thereby, increase the efficiency of the radiating surface. This results in an integrated temperature control system and equipment package.

All surfaces not used for temperature control are covered either with super-insulation or a low-emissive coating, depending upon the ratio of edge and fastener area, to total areas, complexity of design and total performance required. This is to prevent sub-cooling of the equipment and to minimize energy interchange with solar panels and extended booms. Assuming an effective emissivity of 0.01, the total heat leak is 9.1 watts. The weight of this insulation is approximately 6.9 lbs. This brings the total weight of the thermal control subsystem to about 32 lbs. for the solar panel design and 36 lbs. for the isotopic design.

8.4 EXTERNAL EQUIPMENT

Serious thermal design problems associated with the variation in solar heating other than the main equipment compartment are spacecraft appendages, such as solar panels, the high-gain antenna and scientific instruments mounted directly on the spacecraft and/or booms. Steady-state temperature control of the solar panels in conjunction with the power design is discussed in detail in Volume 7 on power. However, panel temperatures can fall well below -100°F during a manuever should the panels become oriented edgewise to the sun. The severity of this problem can be noted in Figure 8-6 where the temperatures can drop as low as -224°F within two hours, assuming

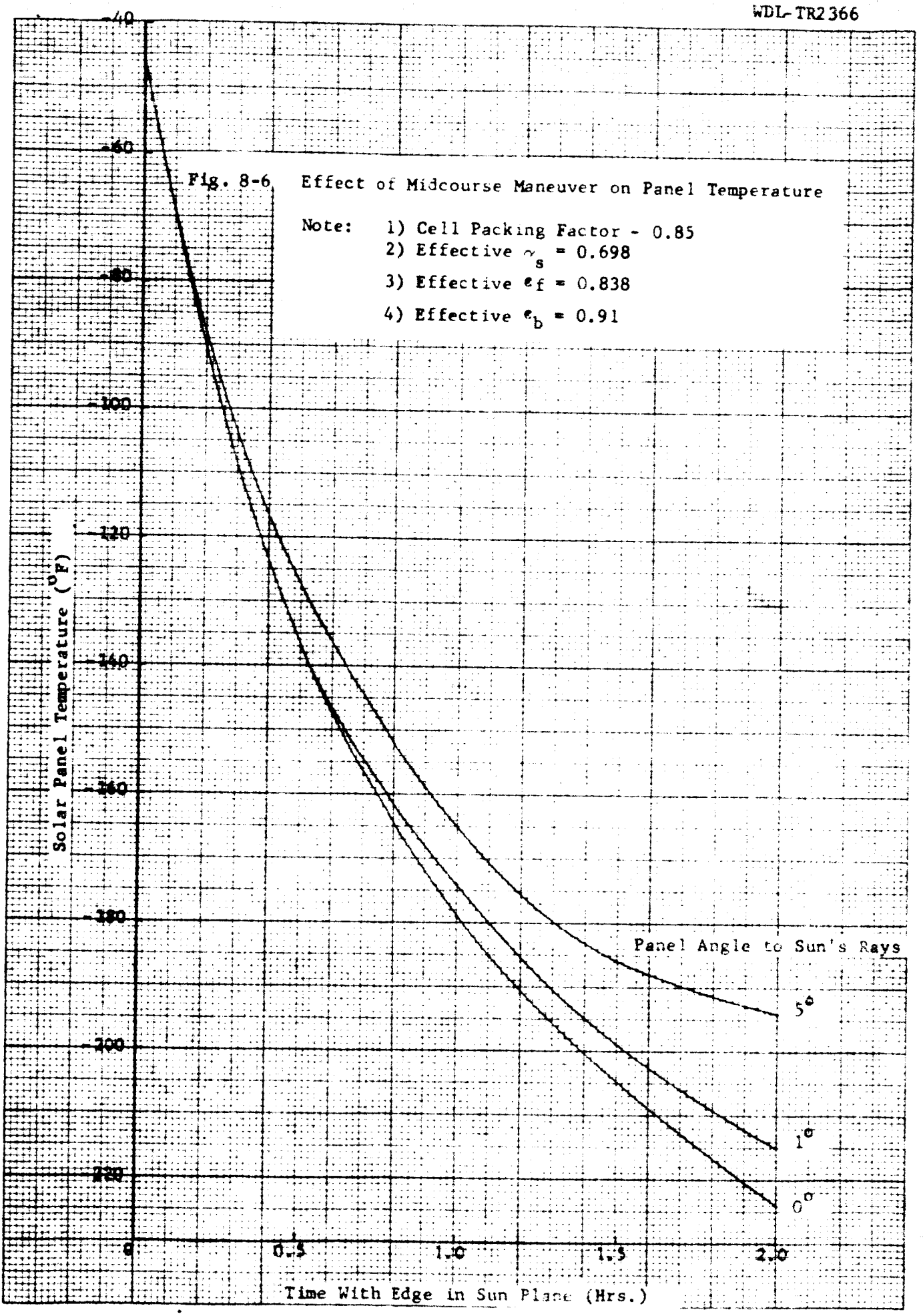

Fig. 8-6 Effect of Midcourse Maneuver on Panel Temperature

Note:
1) Cell Packing Factor - 0.85
2) Effective α_s = 0.698
3) Effective ϵ_f = 0.838
4) Effective ϵ_b = 0.91

a manuever occurs 30 days from a Brooks (2) encounter. This imposes a severe condition on the solar cell adhesive which is normally limited to a minimum temperature of -160°F. Careful consideration of panel orientation during manuevers and the limits of solar cell design must be included in any future investigations.

The temperature will range from +100° to -100°F between 1 and 2 A.U. The low temperature at 2 A.U. may impose a severe heat leak on the equipment compartment. To reduce the problem, a high thermal resistive joint is needed. The joint must also have sufficient structural integrity to support the solar panels during the boost and deployment phases. Although the two requirements are normally incompatible because a strong structural joint is inherently a good thermal conducting joint, there are a number of possible methods to achieve the desired joint characteristics.

One of these possibilities is the use of an isotope-impregnated material that would expand or vaporize due to the heat added by the isotope decay. There are some isotopes that have an increasing heat generation with time, e.g., U-232, which can be used to reach a threshold some time during the mission and, thereby, reduce the thermal continuity of the joint. This technique suggests that further exploration should be conducted.

Two possible high-gain antenna mounting techniques have been investigated: (1) a body-fixed antenna oriented to 60° off the spacecraft-sun axis; and (2) a gimbaled antenna whose axis always points toward the earth. A temperature range of -30° to +135°F can be maintained on the fixed orientation while a range from 0° to 125°F is achievable on a movable antenna. In both cases, this temperature control can be achieved by proper utilization of optical characteristics on the inside and outside surfaces. These characteristics are available in existing coatings.

In addition, three externally mounted scientific units have been examined to determine the surface optical characteristics required for temperature control. The units are the magnetometer, ion chamber, and the scan

platform which supports a UV spectro photometer, IR radiometer or UV photometers, and a slow-scan television. Parametric curves have been generated for three different shapes, viz., spherical, cylindrical and cubic, to obtain the temperature at the two extreme solar distances of 1 and 2 A.U. as a function of surface optical properties, internal heat generation and geometry. These curves indicate that a temperature range of 51 to 112°F can be obtained for the magnetometer with a solar absorptance (emittance) of 0.285 and an emissivity of 0.4 on the surfaces not having solar impingement. Further, the ion chamber can be held between 43° and 118°F with surface properties all equal to 0.055. The emissivity of the portion of the surface viewing the sun is assumed to be equal to the solar absorptance as previously discussed.

The scan platform does not fall in the same category as these instruments. Analysis indicates that fine temperature control can be obtained by utilizing a heat shield and by turning the unit on at a pre-arranged time during the flight. The maximum temperature at 1 A.U. with the units off is 119°F while the coldest with the units off at 2 A.U. is -51°F. The latter value can be raised to a respectable 89°F if the units are turned on approximately 60 days prior to recording data.

8.5 MIDCOURSE MANEUVERS

The effect of midcourse maneuvers on temperature rise rate in the equipment compartment has been evaluated assuming the following conditions:

a. Maximum misalignment of 90° from the sun-spacecraft axis.

b. Equipment compartment taken as lump mass weighing 450 lbs. and at an initial temperature of 70°F.

c. Active control shutters full open, which results in an effective emissivity of 0.69 over 12 ft^2 while the rest of the external surface is covered with super-insulation.

d. Internal heat generation at 300 watts.

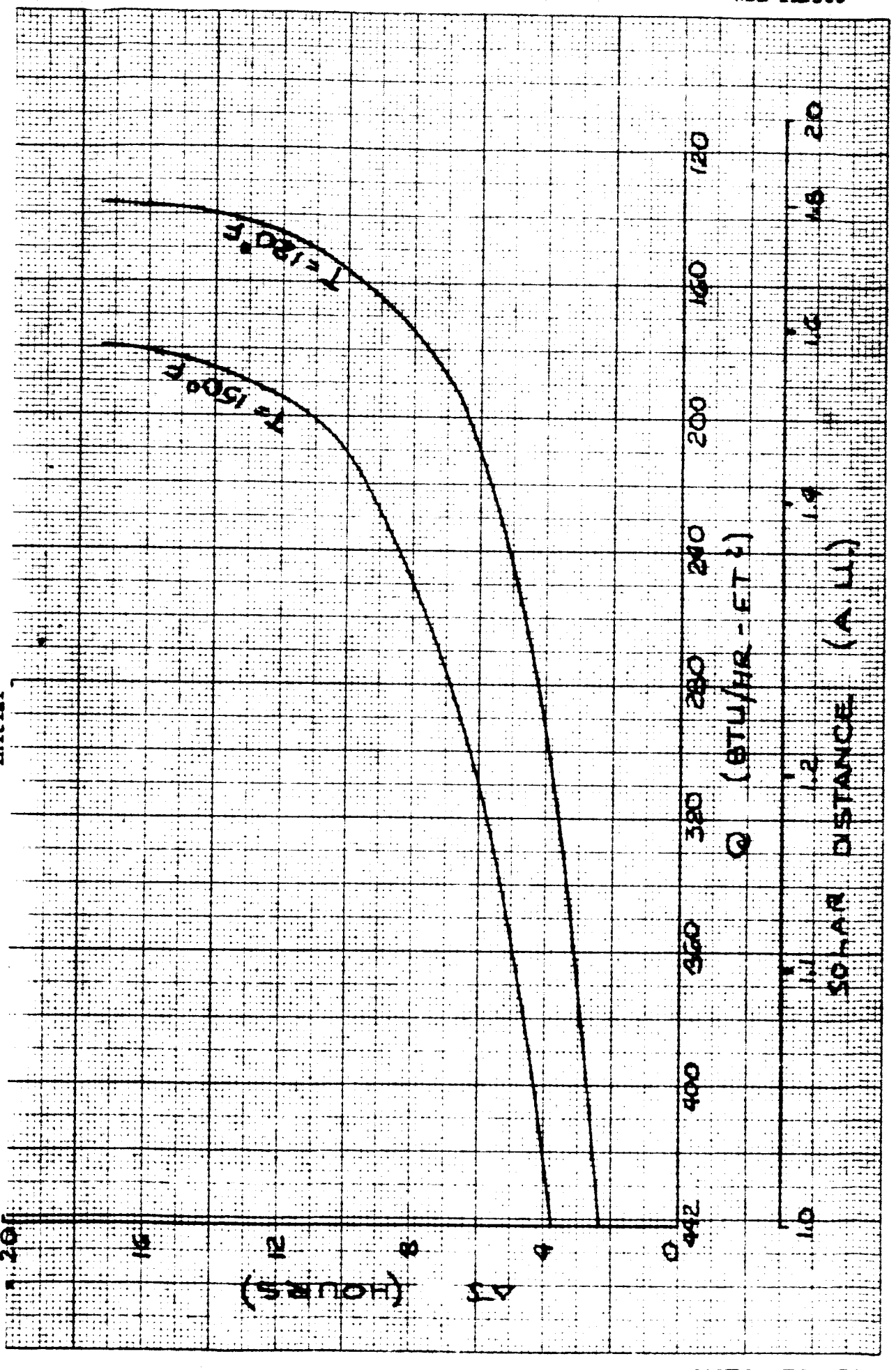

Fig. 8-7 Time to Reach 120°F and 150°F with 90° Misalignment to Sun Axis ($T_{initial}$ = 70°F)

SECTION 9

SPACECRAFT CONFIGURATIONS

9.1 DESIGN REQUIREMENTS

It is the intent of this study to indicate a desirable physical integration of operational sybsystems rather than to present a detailed spacecraft design. In this sense the configuration drawings may be considered to represent "block diagrams" of a spacecraft to satisfy the mission requirements. The following objectives and requirements have been guidelines for developing spacecraft configurations:

1. Physically integrate the subsystems by means of a rigid, lightweight structure. Objectives of this integration, or packaging, are the following:

   a. Facility with which subsystem packages may be assembled and tested prior to final assembly into the spacecraft.
   b. Facility of subsystem removal for repair, retest, or replacement.
   c. Ease with which subsystem units may be handled and shipped prior to final assembly.
   d. Use of modular construction for the basic equipment compartment to minimize fabrication cost and to maximize subsystem location flexibility.

2. Accommodate a high-gain, 28" x 48" parabolic-section antenna having a fan-beam pattern in the ecliptic plane. For this design it is assumed that the RF axis is permanently oriented with respect to the spacecraft.

3. Accommodate a low-gain antenna providing essentially uniform coverage in the forward hemisphere of the spacecraft. Forward is defined as the direction toward the sun.

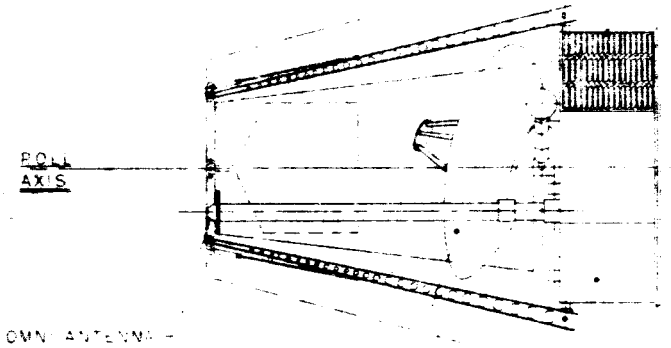

Fig. 9-1 Comet Probe Photovoltaic Power

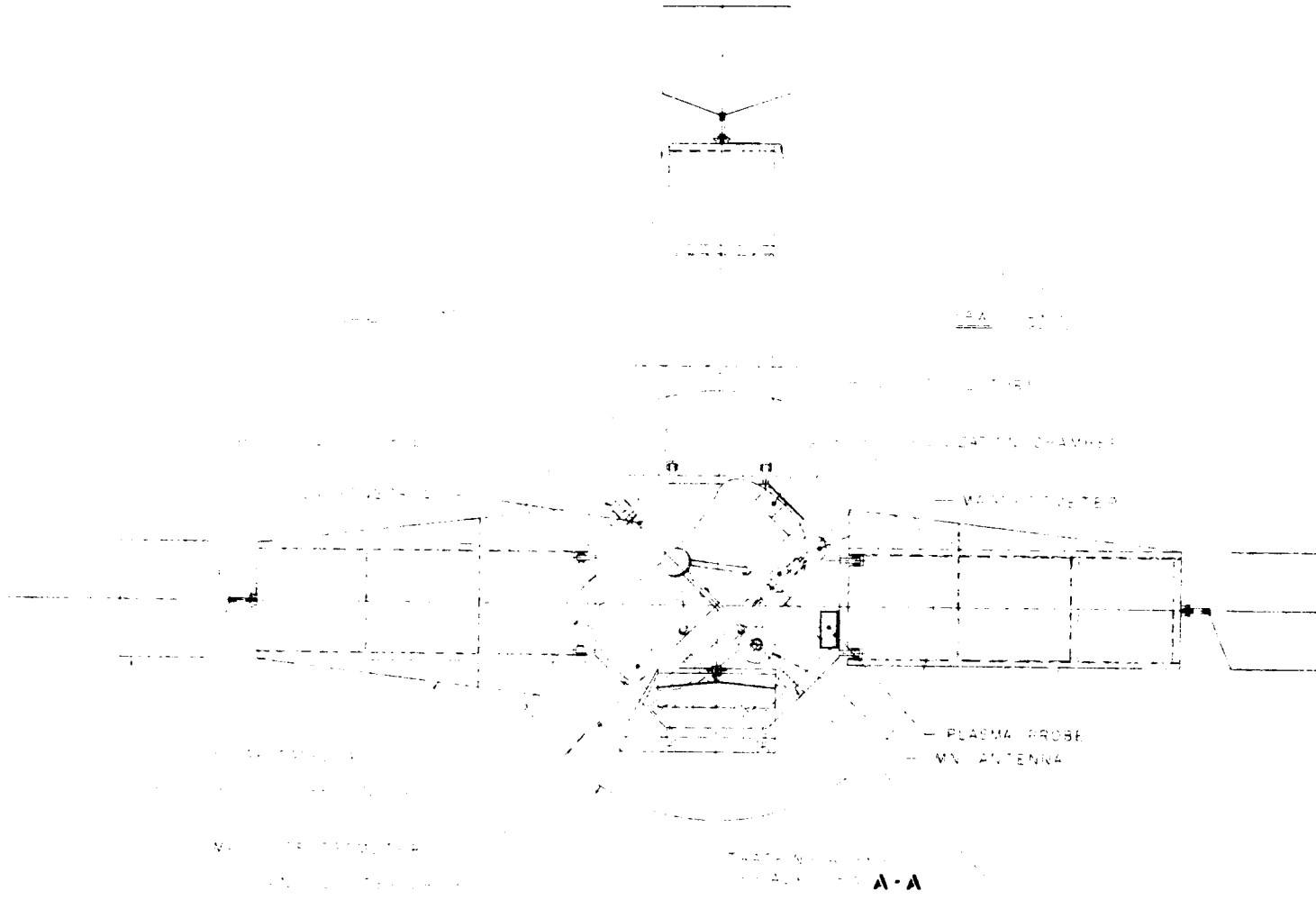

A - A

4. Accommodate a post-injection propulsion system capable of producing up to 150 meters-per-second velocity increment.

5. Utilize one of two possible on-board power supplies:

   a. A photovoltaic array having a panel area of 58 to 90 square feet.

   b. An isotopic power supply requiring a nearly omni-directional view of space.

6. Provide a large field of view for a comet-tracking assembly housing certain encounter mode scientific experiments. The design assumes that the comet passes on the anti-solar side of the spacecraft.

7. Conform to the Centaur launch vehicle interface with the R&D or Surveyor payload envelope.

Consideration of these requirements and objectives has led to the development of two basic configurations whose difference is dictated by the choice of on-board power systems. The spacecraft are referred to as the Photovoltaic Configuration and the Isotopic Configuration; a description of each follows below.

9.2 PHOTOVOLTAIC CONFIGURATION

9.2.1 Main Equipment Compartment

The main equipment compartment of this spacecraft, shown in Figure 9-1, is an octagonal structure providing eight bays in which to package equipment. The size and construction of the compartment is the same as

that of the Mariner-C spacecraft, except for the use of heavier gage material. The dimensions of the compartment can be extended somewhat should the need for more equipment volume become necessary. As in the case of Mariner-C, seven of the eight bays supply packaging volume for the majority of the electronic equipment. The eighth bay contains the propulsion subsystem with its thrust axis aligned in the ecliptic plane approximately normal to the roll axis of the spacecraft. Fuel and cold-gas supply tanks are located in the eighth bay and center compartment. Sun sensors are located on the top and bottom of the compartment. The compartment is supported during launch on a 7-inch-high interface adapter ring in order to provide space under the compartment for the comet tracking assembly and Canopus tracker. The spacecraft separation interface is at the top of this ring structure.

9.2.2 Solar Panels

Attached to the basic compartment are four erectable solar panels on which to mount the solar cells. Four solar pressure vanes are attached to the ends of the panel structures. The R&D envelope allows 75 square feet of area, while the Surveyor envelope allows the 90 square feet required on a mission to Brooks (2) at 200 watts power. The panels are supported by a hydraulically damped structure during launch and deployed into a plane normal to the spacecraft roll axis after its separation from the launch vehicle. Active damping is necessary at the solar-panel hinge points to reduce the cantilever vibration modes of the panels during operation of the spacecraft propulsion system. The trapezoidal panels shown in the drawing represent the maximum area required, except for Brooks (2). A mission to Brooks (2) requires two unsymmetrical panels in order to provide the forward field of view required by the approach geometry. For missions to Pons-Winnecke and Kopff, the smaller panel areas and the more favorable approach geometry lessen the view interference by the solar panels.

9.2.3 Antennas

A parabolic antenna, elliptical in plan view, is fixed on the forward surface of the octagonal compartment. The RF axis is permanently oriented toward the earth at the time of comet intercept. The orientation is somewhat different for each comet mission. For a maximum rigidity-to-weight ratio, aluminum honeycomb construction, such as used on Mariner-C, appears the most desirable. A rather thorough test program is necessary to determine the effect of thermal distortion (which could be quite large for this type of construction) on the RF radiation pattern. Philco-WDL is now studying a similar problem for NASA-Ames.

A 3.5-inch diameter tubular wave guide approximately 62 inches long serves as the low-gain antenna. It is mounted on top of the equipment compartment with its longitudinal axis parallel to the spacecraft roll axis. The antenna provides uniform coverage over the forward hemisphere of the spacecraft. Its length is such that it will operate in the event of solar-panel deployment failure.

9.2.4 Scientific Instruments

Scientific instrument locations are in accordance with the following schedule and are illustrated in Figure 9-1:

a. Magnetometer and Integrating Ionization Chamber. Because of their respective requirements for small spacecraft magnetic field and near-omnidirectional view of space, these instruments are loacted on a 15- to 20-foot boom extended normal to the spacecraft roll axis. One boom suffices for both instruments. The boom is a pneumatically operated telescoping type (e.g., Ranger Program, Blocks I and II), and is designed to provide adequate stiffness and damping during spacecraft velocity

corrections. Unfurlable booms (e.g., DeHavilland Aircraft, Ltd.) appear to offer no advantages until longer lengths are required. A reliable method of furling the boom during velocity corrections would then be necessary. The reliability of such an operation after a long period in space has not yet been demonstrated.

b. Dust Detector. Two detectors are located on top of the octagonal compartment. The active surface of one detector is oriented normal to the spacecraft velocity vector; the other detector's surface is oriented along the velocity vector at right angles to the first detector such as to face the nucleus at encounter.

c. Plasma Probe. This instrument is located on top of the main compartment with its axis pointed along the roll axis of the spacecraft (probe-sun line).

d. Ion Mass Spectrometer and Ion-Electron Trap. This instrument is located on top of the main compartment with its axis oriented along the velocity vector.

e. Ultraviolet Spectrophotometer, Infrared Photomultiplier Radiometer or Ultraviolet Photometers, Slow-Scan Television. These three comet viewing experiments, along with a comet tracking device, are housed together below the octagonal compartment. During the encounter mode of operation, this assembly tracks the nucleus of the comet by rotating with respect to the spacecraft about two axes. It can traverse 360° (clock angle) about an axis parallel to the spacecraft roll axis, and, when the support yoke is erected, elevate through a 210° angle (cone angle). The exact location of this package (with respect to the pitch and yaw axes) depends on

the comet mission chosen. In all cases the comet is assumed to pass on the anti-solar side of the spacecraft. Some encounter geometries require a view forward to within as little as 30^{o} of the roll axis. To meet this requirement, the assembly must be located so that its view is not obscured by the solar panels or by the main compartment. Fortunately, at the time that forward viewing is required, the clock angle is constant, and therefore the assembly can be located so as to look between the solar panels.

9.3 ISOTOPIC CONFIGURATION

The Isotopic Configuration is formed by removing the solar panels of the Photovoltaic Configuration and adding an isotopically heated thermoelectric generator. As illustrated in Figure 9-2 , the power supply is supported above the main compartment by a truss framework. This method of support provides the power supply radiator fins with the good view of space for efficient operation. Because of the high temperatures at the truss interface with the power supply, titanium is used for the main truss members. Its high strength at elevated temperatures and relatively low thermal conduction make it an ideal material for such use. Stainless steel has been rejected because of its higher magnetic permeability. The lower end of the longitudinal truss members attaches to the octagonal compartment by means of hydraulic dampers. It is anticipated that the inclusion of such damping is necessary to reduce the dynamic stresses in the trust during launch.

The removal of the solar panels alleviates the encounter viewing problems that arise when the comet is well forward of the spacecraft. A comet can now be tracked that has a trajectory parallel to the spacecraft roll axis.

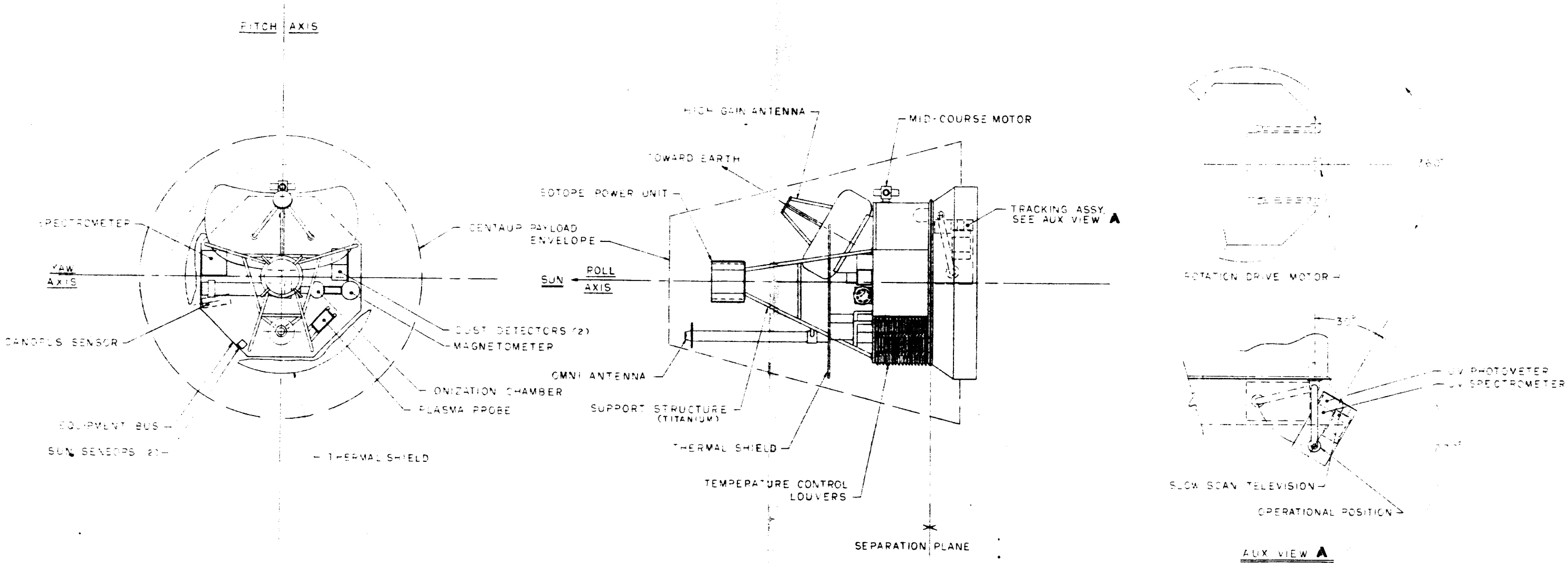

Fig. 9-2 Comet Probe Isotopic Power

The isotopic power supply presents a clear weight advantage over solar power for a mission to Brooks (2). From the standpoint of power density the advantage is far greater. The amount of payload envelope volume consumed in stowing 90 ft^2 of solar panels (even if some degree of panel articulation is allowed) presents a severe handicap to the optimization of the rest of the spacecraft. Furthermore, the isotopic configuration has a growth potential should more power be required; the photovoltaic configuration must be considered to be near the end of practicality.

9.4 ADAPTABLE SPACECRAFT

9.4.1 Comet Missions

The adaptability to several comet missions is built into the photovoltaic and isotopic spacecraft designs described in the previous section. The adaptation of either design to a particular comet necessitates changes in the following areas:

a. On-Board Power - The isotopic package is the same for all missions. The photovoltaic configuration requires different panel areas for each comet.

b. High-Gain Antenna - The antenna orientation is somewhat different for each mission.

c. Comet Tracking Assembly - The location of the comet tracking assembly is under either Bay 3 or Bay 7 of the main compartment, depending on the encounter geometry of the particular comet. The variable location is necessary because the cometary encounter trajectories are not normal to the spacecraft roll axis and hence pass to one side or the other of the spacecraft. Solar-side passage of the comet is assumed for missions requiring observations of the nucleus.

d. Post-Injection Propulsion System - It may be desirable to tailor the fuel tankage for each mission if a wide variation in velocity increments develops among comets.

With these adaptations, either configuration is amenable to any of the comet missions analyzed. The design of a configuration that can meet all mission requirements without some changes does not appear feasible.

9.4.2 Close-Approach Asteroid Missions

The comet probe configurations are adaptable to solar-side fly-by asteroid missions. The changes outlined in Section 4.1 are necessary to adapt the spacecraft to a particular asteroid mission. The comet tracking platform can be used to track the asteroid and contains the asteroid viewing experiments.

If the mission objectives go beyond those of a simple fly-by, such as firing projectiles at the asteroid, more changes must be expected in the spacecraft configurations. The exact degree of applicability of the comet probe to an asteroid mission must await a more complete definition of its mission requirements.

9.5 SUMMARY - ATLAS/CENTAUR COMET PROBE

Two configurations have been developed based upon the use of the Atlas-Centaur launch vehicle. Except for the power supplies, both configurations are identical and bear a close resemblance to the Mariner-C spacecraft. The resemblance of the configurations to the Mariner-C spacecraft means that maximum advantage can be taken of that technology and experience. An important difference from Mariner is that, by using an Atlas-Centaur, stringent weight and payload volume restrictions are not present. The use of heavier gage structural materials is permitted and recommended. Their use will alleviate the handling, testing, and analysis problems associated with very light construction. Present state-of-the-art materials and fabriaction methods are envisioned for the structure. The projected weight of either configuration is 700-800 pounds. This figure is below the payload capability of the Atlas-Centaur. A weight breakdown by principal subsystem is given in Table 9-1.

Table 9-1. Weight Breakdown
for Atlas-Centaur Comet Probes

SUBSYSTEM		PHOTOVOLTAIC CONFIGURATION	ISOTOPIC CONFIGURATION
Structure	90	110	110
Interface	20		
Science			
Tracking Platform	26	152	152
TV-Tracker	16		
Encounter Science	50		
Cruise Science	40		
Boom	10		
DAS	10		
Attitude Control		80	80
Midcourse Propulsion (150 m/s)		100	100
Telecommunication	100	110	110
Antennas	10		
Thermal Control		30	30
Power (200 w)		119-162	110
Panels or Isotopic Unit		69-112	70
Isotope Support Structure		--	10
Power Conditioning		10	--
Batteries		40	30
System Total - 200 w		701-744	692
- 300 w		737-800	742

SECTION 10
MARINER-C COMET PROBES

10.1 ADAPTATION OF MARINER-C SPACECRAFT TO A COMET MISSION

An Atlas/Agena has sufficent payload capability for a mission to Pons-Winnecke. Additional cometary opportunities may exist, but their investigation and discussion are not within the scope of this document.

Based on a 30-day launch window, payloads of 630 and 578 pounds are available for a Pons-Winnecke fly-by using Type I and Type II trajectories respectively. This capability suggests the use of a modified Mariner-C. The degree of change from the present Mariner-C configuration depends upon whether the spacecraft is optimized for the mission at the expense of utilizing present Mariner technology. It is possible, for instance, to change only the orientation of the high-gain antenna and fly an otherwise unaltered Mariner. The other end of the modification scale cannot be defined within the scope of this study. Two points on the modification scale have been chosen for discussion. They represent near-minimal and maximal cases and correspond to the Type II- and Type I- trajectory payloads respectively.

10.2 TYPE-II TRAJECTORY SPACECRAFT

The first step in the modification of the spacecraft design is the removal of unnecessary or unusable equipment. The Planet Scan Assembly has only one degree of freedom and hence is unsuitable for cometary tracking at encounter. The unit is therefore removed along with the TV subsystem which lacks sufficient sensitivity to view the nucleus at the nominal fly-by miss distance of 5,000 km. The tape recorder is

retained in order to permit a higher science data sampling rate at encounter. The solar panel area of 70 sq. ft. can be reduced by approximately 15 sq. ft. to 55 sq. ft. because of the higher solar intensity at encounter. This reduction includes designing for a giant solar flare.

In order to achieve a 5000-km nomical miss distance, a PIPS capability of 120 m/sec must be provided. Hence, increased fuel capacity must be added to the configuration. It is assumed that the present midcourse motor design is adequate for the resulting increased burn time.

In addition to these required modifications, additions to the scientific payload are desirable. With the high data capacity of the tape recorder now available at encounter, an Ion-Mass Spectrometer can be accommodated. In addition, a gimbaled Comet Tracking Assembly can be designed to replace the removed Planet Scan Assembly. Integrated with the tracking unit are UV photometers. At encounter, the spacecraft-referenced comet trajectory is nearly perpendicular to the spacecraft roll-axis. Hence, it does not appear necessary to extend the Comet Tracking Assembly from the main compartment of the spacecraft as in the configurations (Figures 9-1 and 9-2) designed to accommodate the comet tracking requirements of several comet encounters.

An estimated weight summary for the Type-II trajectory Mariner-C modifications is given in Table 10-1 No weight penalty is incurred in reorienting the high-gain antenna. Electronic assembly changes (such as those to the DAS to permit a high data rate at encounter) are assumed to require no weight increase within the accuracy of the estimate.

Table 10-1 Weight Summary

Type-II Trajectory Modifications to Mariner-C Spacecraft (1969)

Basic Mariner-C Spacecraft Weight		565 lb
Remove		
Planet Scan Assembly	15	
TV Electronics	8	
Scan Electronics	4	
15 sq. ft. from Solar Panels	15	
Total Removed Weight		42
Reduced Spacecraft Weight		523
Add		
Increase PIPS Capability to 120 m/sec	16	
Ion-Mass Spectrometer	8	
Gimbaled Comet Tracker, UV Photometers, and Electronics	25	
Installation Allowance	1	
Total Added Weight		50
Modified Spacecraft Weight		573 lb
Type-II Trajectory Capability		578 lb
Margin		5 lb

10.3 TYPE-I TRAJECTORY SPACECRAFT

This configuration differs from the former by its accommodation of a higher sensitivity TV subsystem (Advanced Mariner type). Integrating the TV electronics modifies the input to one of the communications assemblies. The TV camera is located along with UV photometers on a large comet tracking assembly mounted below the center of the octagonal compartment. The height of the Agena/spacecraft adapter is increased to provide the volume needed to stow the assembly. Resizing the solar panels down to 55 sq. ft. permits the octagonal structure to be raised. The midcourse motor must be repositioned to accommodate the change in center of gravity.

Table 10-2 outlines the weight summary for this configuration.

10.4 SUMMARY

Two configurations have been discussed for an Atlas-Agena mission to Pons-Winnecke. The spacecraft are modified versions of the Mariner-C design and represent minimal and extended modification cases. The weight breakdowns for these two cases and for the launched Mariner-C are given in Table 10-3.

10.5 CHOICE OF SPACECRAFT CONFIGURATION

The Atlas-Centaur Photovoltaic configuration is recommended for most missions (e.g. Kopff 1970) except Pons-Winnecke and Brooks (2). The use

Table 10-2 Weight Summary

Type I - Trajectory Modifications to Mariner-C Spacecraft (1970)

Basic Mariner-C Spacecraft Weight		565 lb
Total Removed Weight (Table 5-1)		42
Reduced Spacecraft Weight		523 lb
Add:		
Increase PIPS Capability to 80 M/sec for 640 lb spacecraft	2 lb	
Ion-Mass Spectrometer	8	
Comet Tracking Platform Assembly Electronics	20	
Comet Tracker	10	
Advanced-Mariner TV System	35	
(or UV Spectrometer and	(22)	
Ion-Electron Trap*)	(8)	
UV Photometers	6	
Increase Height of Spacecraft/Agena Adapter by 6 in.	16	
Installation Allowance	3	
Total Added Weight		100 lb (or 95)
Modified Spacecraft Weight		623 lb (or 618)
Type-I Trajectory Capability		630 lb
Margin		7 lb (or 12)

*Ion-Electron Trap Not On Tracking Assembly

Table 10-3. Mariner-C Comet Probe

Weight Breakdowns

MARINER-C SUBSYSTEM	TRAJECTORY-II MODIFICATION (late 1969)	MARINER-C (1964)	TRAJECTORY-I MODIFICATION (Early 1970)
SCIENCE			
Comet Tracker & Experiments	25	15	71
Independently Mounted Experiments	16	8	16
Electronics & DAS	36	48	36
GUIDANCE AND CONTROL			
Attitude Control; CC & S	39	39	39
Gas System	29	29	29
Sensors	7	7	7
PROPULSION			
Midcourse Motor	66	50	52
TELECOMMUNICATION			
Data Encoder & Command	42	42	42
RF & Tape Recorder	64	64	64
Antennas	10	10	10
POWER			
Panels	63	78	63
Regulator	16	16	16
Conditioning	32	32	32
Battery	33	33	33
THERMAL CONTROL			
Thermal Control Assemblies	13	13	13
STRUCTURE			
Pyro & Actuators	6	6	7
Structure	59	58	76
Cabling	17	17	17
	573 lb	565 lb	623 lb

of the proven Mariner spacecraft design, even though modifications are necessary, is recommended for Pons-Winnecke missions in late 1969 and early 1970. The minimal modification configuration is recommended unless the inclusion of a high-resolution, highly sensitive TV system becomes a high-priority scientific objective. In that case, an extended redesign of the Mariner-C is recommended.

The RTG Configuration appears attractive for the Brooks (2) 1973 mission because of the large solar panel area required. On the other hand, because of the larger volume Surveyor payload envelope and the payload weight available with the Atlas-Centaur, such panels can be accommodated in the interest of using proven technology.

SECTION 11

SPACECRAFT SYSTEM EVALUATION

11.1 PERFORMANCE MODEL

The criteria established for evaluating system capability are the following key system parameters:

1. Weight of science. The weight of the instrument payload is a measure of the number and sophistication of experiments that can be performed to satisfy the mission objectives.

2. Aiming error. The 3-sigma aiming-point error is a measure of the results of an early, pre-acquisition orbital determination investigation for determining the uncertainty in time of perihelion passage; the guidance system, injection, and DSIF tracking errors; and the velocity-correction fuel capability to control a given spacecraft weight.

3. Bit rate. The telemetered bit rate is a measure of the total data registered by the instruments; the effective radiated power of the telemetry subsystem: the capacities of the data compression and storage subsystems; and, after the second maneuver, the number of compressed pictures that can be analyzed to confirm the detection of the comet, to measure its intensity, and to determine the direction of the comet tracker relative to the optical centroid of the comet. A higher value is assigned to real-time transmission of data during intercept than to post-intercept playback only.

Table 11-1 System Capabilities of Atlas-Centaur and Atlas-Agena Comet Probes

MISSION	W_{sci}	$3\sigma/dm$	ΔV	B	$W_{s/c}$	M
Atlas/Centaur Pons-Winnecke 1969	152	0.5	200	2840	737	2470
Atlas-Agena Mariner Mod. '69 (Pons-Winnecke)	77	0.5	120	1135	573	232
Atlas-Agena Mariner Mod. '70 (Pons-Winnecke)	123	0.5	80	1135	623	270
Atlas-Centaur Kopff 1970	152	0.5	200	248	750	221
Atlas-Centaur Brooks (2)	152	0.5	200	284	800	270
Mariner-C 1964	71	0.6	80	10	565	1

and science platform pointing.

2. The conduct of a thorough analysis of comet observational data reduces cometary orbital uncertainties and thus increases the probability of intercept and reduces the velocity-correction requirements.

3. Midcourse propulsion reliability to execute velocity corrections accurately affects the miss distance and probability of intercept.

4. The biasing of the miss-distance for the spacecraft to pass on the sunlit side of the nuclear condensation determines science platform pointing, science resolution, and the ability to observe the nucleus from a given position on the spacecraft.

5. Comet observability after the second maneuver determines the accuracy with which encounter instruments can be pointed at the nucleus, and determines the required sensitivity of the comet tracker and science TV.

6. Comet tracker reliability to acquire and track the optical centroid of the comet determines whether television and spectrophotometric data on the nucleus can be collected.

Partial success can still be realized with the spectrophotometric instruments aboard the tracking assembly, especially if the pointing angle relative to the spacecraft and comet centroid is known. DSIF spacecraft tracking and Earth-based comet tracking data can be used in conjunction with either the preset tracker position (in the event the comet tracker does not acquire and lock onto the moving target) or the last telemetered comet tracker position (in the event of control failure).

7. Shock loading on spacecraft during entry into the cometary atmosphere at the high relative velocities is negligible.

8. Dust damage to solar cells and optical trackers during flight through the coma is unknown.

9. Communication blackout of command, ranging and telemetry signals due to electrons in the coma is absent at frequencies above the HF range.

11.3 PAYLOAD CAPACITY

The comet probe system weight now totals 700 to 800 lbs. Since the Atlas-Centaur payload capability for comet missions is 900 to 1300 lbs., it is advisable that the weight difference be appropriated in ways that will enhance the scientific value of the mission, assure a high probability of success, and introduce higher performance components. Thus, heavier components including structural materials can be used; redundant components and assemblies can be accommodated.

For example, on some missions another tracking assembly could be accommodated, and on others added spectrophotometric or television subsystems could be added to the one tracking assembly now specified. In thermal control, change-of-phase passive control techniques for battery temperature can be used rather than active shutters, redundant active control assemblies can be incorporated, and solid-slab insulation can be used rather than multifoil insulation for ease of fabrication and simplicity of attachment. In telecommunication, redundancy in the telemetry and command assemblies can be accommodated, and high-power amplifiers (e.g., 50 watts) can be supported to increase the data transmission rate during intercept (e.g., 300 bps)

In power, higher power demands mean fitting increased solar panel area within the Surveyor shroud (e.g., 90 sq. ft.). In guidance and control, higher performance components (e.g., gyros) that weigh more than those presently used can be mounted.

to permit an accurate projection of spacecraft system costs to the 1970's to be made. However, in several cases a reasonable extrapolation of subsystem or assembly costs could be performed.

The knowledge and experience of Philco WDL in spacecraft (and associated hardware) design, development, fabrication, testing, and support was utilized in generation of the cost and schedule data. The benefits derived from similar study programs also aided this effort.

Basic ground rules included costing the launch of two spacecraft by use of Atlas-Centaur launch vehicles. Fabrication and test of two additional flight-ready spacecraft were also costed. Also, costs for two sets of flight-qualified spare assemblies and two sets of GSE (including D & D) were included in the total program cost. Items requiring a completely new development and flight qualification program were not considered unless unavailable through present NASA/JPL programs.

12.2 MISSION COST

The mission cost was broken down into five major categories:

Program Management
System Engineering
Spacecraft System
Field Support
Launch-Booster

Each of these categories is further expanded to show the activities taking place under each. Figure 12-1, "Atlas-Centaur Comet Probe Program Costs", provides an illustration in block diagram form of the program cost elements down to the subsystem level. Table 12-7, "Comet Probe Cost Matrix", depicts the subsystem costs in terms of D & D (design and development), QUAL (qualification model fabrication and test), and FLT (flight model fabrication and test). The total costs are also summarized in this matrix.

SECTION 12

MISSION COST AND SCHEDULE

12.1 OBJECTIVES AND COSTING RULES

The major objective of the costing effort was to estimate the cost of the Comet Probe Mission during the 1967-1975 time period. This task was accomplished by first analyzing the scope of the program and the goals to be attained. Next, a review of Mariner-C technology and hardware, and estimates of cost, provided a baseline for subsequent costing exercises. The major cost elements of the program were then identified and separation of spacecraft, launch and support costs accomplished.

One of the objectives of the costing phase of the study was to determine the savings in program cost by judicious use of Mariner-C subsystems, assemblies, and components. In several instances, substantial savings in design, development, and qualification costs can be foreseen. Similarly, re-design of, and/or modification to, existing Mariner-C assemblies (as opposed to completely new developments) to meet the requirements of the Comet Probe Mission would result in additional savings. Approximately 60% of the subsystem assemblies were costed on this basis. Thus, less than 40% of the required assemblies for the proposed Comet Probe would require new development or major revision of NASA flight-proven hardware.

An Industrial Solicitation was conducted by means of letters and specifications sent to over 100 major spacecraft system, subsystem, and component manufacturers. Requests were made for information concerning not only products presently available, but those which would be available in the 1967-1975 time period. Manufacturers were asked to identify trends in cost and schedules as improved materials and devices are made available through advances in state-of-the-art. Insufficient information was received

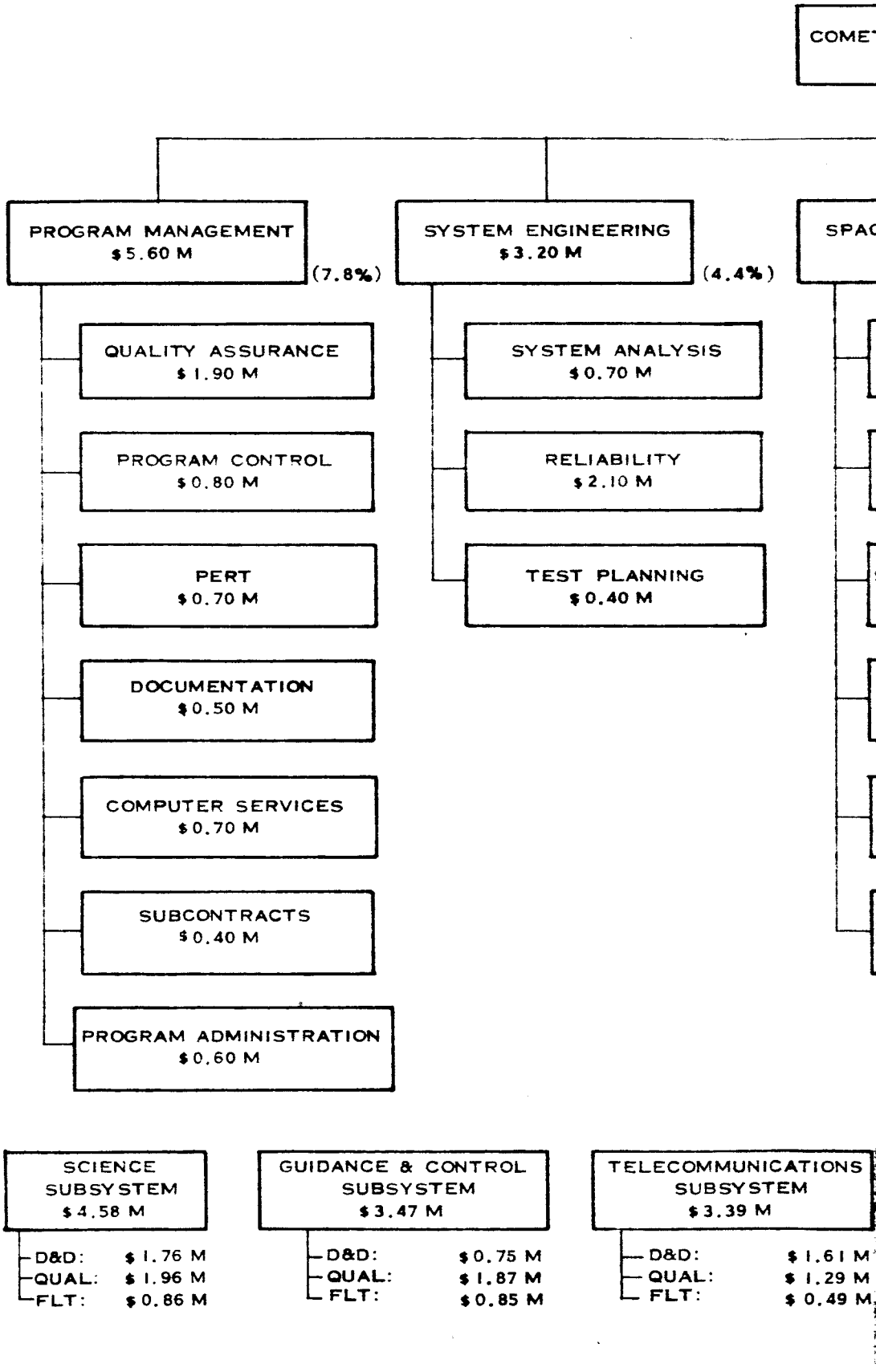
COMET
PROGRAM MANAGEMENT
$5.60 M
(7.8%)
SYSTEM ENGINEERING
$3.20 M
(4.4%)
SPAC
QUALITY ASSURANCE
$1.90 M
PROGRAM CONTROL
$0.80 M
PERT
$0.70 M
DOCUMENTATION
$0.50 M
COMPUTER SERVICES
$0.70 M
SUBCONTRACTS
$0.40 M
PROGRAM ADMINISTRATION
$0.60 M
SYSTEM ANALYSIS
$0.70 M
RELIABILITY
$2.10 M
TEST PLANNING
$0.40 M
SCIENCE SUBSYSTEM
$4.58 M
D&D: $1.76 M
QUAL: $1.96 M
FLT: $0.86 M
GUIDANCE & CONTROL SUBSYSTEM
$3.47 M
D&D: $0.75 M
QUAL: $1.87 M
FLT: $0.85 M
TELECOMMUNICATIONS SUBSYSTEM
$3.39 M
D&D: $1.61 M
QUAL: $1.29 M
FLT: $0.49 M

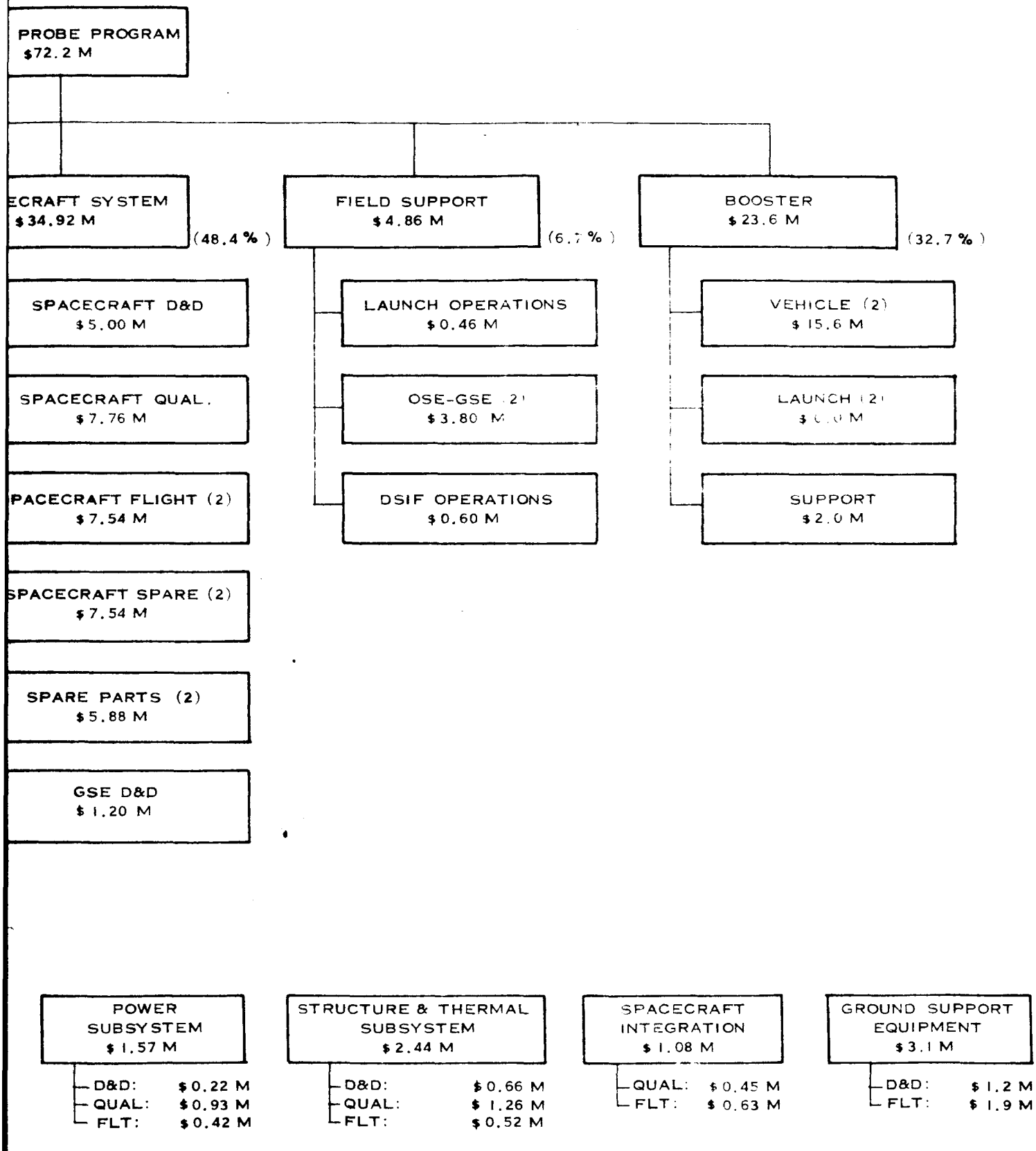

Figure 12-1 Atlas-Centaur Comet Probe Program Costs

Tables 12-1 through 12-6 show the D & D, QUAL, and FLT costs of the major assemblies of each subsystem. The totals of these costs are summarized in the cost matrix, Table 12-7.

The QUAL model spacecraft is equivalent to the PTM (proof-test-model) of JPL. QUAL costs reflect two assemblies, one to qualify the subsystem and the other to qualify the spacecraft.

The Program Management costs include all of the elements of management which past experience has shown to be necessary for effective decision-making on major aerospace programs. This includes both PERT and configuration management as well as complete program documentation. The costs have been estimated on a level of effort basis, as determined by actual experience on programs with similar complexity, schedule and overall size. The percentage of total program costs (7.8%) is at the lower end of the range generally accepted by industry and the government. This lower than average estimate is based upon the use of large amounts of already developed hardware for which extensive documentation is available.

System Engineering costs include System Analysis, System Reliability and Test Planning. The system analysis task includes the use of computer simulation techniques for trajectory analysis, for thermal and stress analysis and for optimization of system parameter tradeoffs. A level of engineering effort is provided to establish system and subsystem requirements, prepare specifications and to evaluate performance against the mission objectives. A preliminary estimate of system reliability based upon the use of Mariner-C component parts and system redundancy provides a calculated probability of .08 of accomplishing all primary and secondary mission objectives. The reliability program has been designed and costed to provide approximately a five times improvement in reliability prior to launch. This program includes upgrading of parts failure rates through improvement in specification and materials application as well as optimization of circuit redundancy.

Table 12-1 Science Assembly Costs

Instruments	D/D	1238 K	Television	D/D	225 K
	QUAL	1430 K		QUAL	234 K
	FLT	619 K		FLT	90 K
DAS	D/D	225 K	Platform Assembly	D/D	68 K
	QUAL	240 K		QUAL	56 K
	FLT	90 K		FLT	22 K

Table 12-2 Spacecraft Integration Costs

Assembly	QUAL	125 K	Flight Proof Test	QUAL	295 K
	FLT	175 K		FLT	400 K
Delivery	QUAL	30 K			
	FLT	55 K			

Table 12-3 Guidance and Control Assembly Costs

Sun Sensors	D/D	11.3 K	Canopus Tracker	D/D	22.5 K
	QUAL	14 K		QUAL	376 K
	FLT	2.25 K		FLT	169 K
Comet Tracker	D/D	225 K	Gyros (3) and Electronics	D/D	22.5 K
	QUAL	214 K		QUAL	293 K
	FLT	90 K		FLT	124 K
Pneumatic System	D/D	22.5 K	CC&S	D/D	360 K
	QUAL	157 K		QUAL	249 K
	FLT	124 K		FLT	103 K
Monopropellant System	D/D	45 K	Autopilot	D/D	45 K
	QUAL	113 K		QUAL	101 K
	FLT	45 K		FLT	68 K
Integration	QUAL	350 K			
	FLT	225 K			

Table 12-4 Telecommunication Assembly Costs

Lo-Gain Antenna	D/D	24 K	Pre-Amplifier	D/D	48 K
	QUAL	18 K		QUAL	30 K
	FLT	6 K		FLT	6 K
Transponder	D/D	390 K	Command Detector	D/D	240 K
	QUAL	166 K		QUAL	221 K
	FLT	46 K		FLT	84 K
Command Decoder	D/D	216 K	Ranging Module	D/D	96 K
	QUAL	173 K		QUAL	72 K
	FLT	72 K		FLT	34 K
Telemetry Logic	D/D	66 K	Multiplexers (2)	D/D	120 K
	QUAL	42 K		QUAL	75 K
	FLT	18 K		FLT	27 K
Buffer	D/D	30 K	Tape Recorder	D/D	120 K
	QUAL	30 K		QUAL	102 K
	FLT	12 K		FLT	42 K
Telemetry Encoder	D/D	48 K	Power Amplifiers (2)	D/D	120 K
	QUAL	30 K		QUAL	102 K
	FLT	12 K		FLT	42 K
Hi-Gain Antenna	D/D	96 K	Integration	QUAL	150 K
	QUAL	78 K		FLT	60 K
	FLT	30 K			

Table 12-5 Power Assembly Costs

Panel Assembiles (4)	D/D	96 K	Power Synchronizer	D/D	7.2 K
	QUAL	696 K		QUAL	20 K
	FLT	324 K		FLT	6.6 K
Regulator Assembly	D/D	30 K	Inverter Assembly	D/D	39.6 K
	QUAL	36 K		QUAL	62 K
	FLT	13.2 K		FLT	22.8 K
Battery Charger	D/D	16.8 K	Battery Assembly	D/D	32.4 K
	QUAL	21 K		QUAL	27 K
	FLT	7.2 K		FLT	11.4 K
Integration	QUAL	68 K			
	FLT	30 K			

Table 12-6 Structure and Thermal Assembly Costs

Thermal Shields	D/D	36 K	Insulation	D/D	22.5 K
	QUAL	5 K		QUAL	20 K
	FLT	2.25 K		FLT	9 K
Louver Assembly	D/D	81 K	Coatings	D/D	36 K
	QUAL	40 K		QUAL	11 K
	FLT	18 K		FLT	4.50 K
Pyrotechnics	D/D	11.3 K	Boom, Actuators	D/D	67.5 K
	QUAL	23 K		QUAL	79 K
	FLT	11.3 K		FLT	33.8 K
Booster Adapter	D/D	45 K	Structural Damper	D/D	45 K
	QUAL	124 K		QUAL	56 K
	FLT	56.3 K		FLT	22.5 K
Structure and Configuration	D/D	180 K	Vehicle Heat Balance	D/D	135 K
	QUAL	810 K			
	FLT	360 K			
Thermal Balance Tests	QUAL	90 K			

Table 12-7 Comet Probe Cost Matrix

Subsystem Cost

ITEM	DESIGN & DEVELOPMENT	QUALIFICATION	FLIGHT	TOTAL
Science	$ 1.76 M	$ 1.96 M	$ 0.86 M	$ 4.58 M
Guidance & Control	0.75 M	1.87 M	0.85 M	3.47 M
Telecommunications	1.61 M	1.29 M	0.49 M	3.39 M
Power	0.22 M	0.93 M	0.42 M	1.57 M
Structure & Thermal	0.66 M	1.26 M	0.52 M	2.44 M
S/C Integration		0.45 M	0.63 M	1.08 M
GSE	1.20 M			1.20 M
S/C System Sub-Total	$ 6.20 M	$ 7.76 M	$ 3.77 M	$ 17.73 M

Program Costs

Flight Spacecraft (2)			$ 7.54 M	
Space Spacecraft (2)			7.54 M	
Spare Parts (2)			5.88 M	
Program Management				$ 5.60 M
System Engineering				3.20 M
Spacecraft System	$ 6.20 M	$ 7.76 M	$ 20.96 M	34.92 M
Field Support				4.86 M
Booster/Launch (2)				23.60 M
TOTAL PROGRAM COST				$ 72.18 M

The cost of a test program for planetary exploration vehicles poses some difficult management questions. Previous space vehicle test programs have been based upon statistical techniques which take advantage of the fabrication of multiple components, subsystems and spacecraft. So far as can be determined, the criteria for launch of lunar and planetary spacecraft has been largely determined by availability of launch windows rather than any achieved confidence in survival. The costs contained in this report have been derived by establishing the elapsed time available for test and estimating the probable number of performance failures which may occur during the test cycle. Improvements in "inherent" reliability can be expected to reduce the number of system failures and increase confidence in mission success. A trade-off study is required to determine the optimum test time to insure confidence without wearing out the equipment before launch. Because of the factors discussed above, Philco's confidence in the cost of the reliability and test program is approximately $\pm 50\%$.

Cost of operating the SFOF is not included, since information regarding this item was not available. Similarly, the DSIF Operations cost does not represent the total cost throughout the entire mission since it is believed this cost would be shared among several programs.

12.3 MISSION SCHEDULE

Simplified cost and manpower schedules are shown in Tables 12-8 and 12-9 respectively. The cost schedule does not include launch and booster costs, but does include the cost of a pre-design phase study.

Both cost and manpower schedules are based on a three-year program, with adequate allowances for contingencies and re-direction of effort. It is believed that this time interval could be appreciably shortened to meet the scientific goals and objectives of a specially selected comet or asteroid. The schedule is also dependent on the degree of utilization of Mariner-C assemblies or subsystems, being shortened by increasing use of these items.

Table 12-8 Cost Schedule

COST CATEGORIES	1966						1967						1968											
	1	2	3	4	5	6	7	8	9	10	11	12	13	14	15	16	17	18	19	20	21	22	23	24
DEVELOPMENT																								
Design	0.3		0.3		0.5		0.5		0.3		0.3													
Breadboard & Prototype			0.3		0.5		0.5																	
Spacecraft Models			0.3		0.7		0.8		0.5															
Proof Test Model			0.5		1.0		1.0		0.5		0.3		0.3		0.5		0.5		0.5					
Type Approval			0.6		1.0		1.0		0.5		0.3		0.3											
Special Equipment					0.5		0.5		0.4		0.3													
GSE					0.4		0.5		0.4		0.2													
FLIGHT HARDWARE																								
Spacecraft Launched (2)							0.5		1.0		1.0		0.6		0.6		0.4		0.4		11.8			
Spacecraft Spare (2)							0.5		1.0		1.0		0.7		0.5		0.5		0.3					
Spare Parts (2)							1.2		2.0		1.4		1.0		0.4									
GSE (2)							0.7		0.7		0.6		0.2											

Note: Cost in $ millions
Cost of launch vehicle not included

Table 12-9 Manpower Schedule